RICE UNIVERSITY

**Development of Osteoinductive Tissue Engineering Scaffolds with a Bioreactor**

by
**Richard A. Thibault**

A THESIS SUBMITTED
IN PARTIAL FULFILLMENT OF THE
REQUIREMENTS FOR THE DEGREE

**Doctor of Philosophy**

APPROVED, THESIS COMMITTEE:

Antonios G. Mikos, Ph.D. (Committee Chair)
Louis Calder Professor
Departments of Bioengineering and Chemical and Biomolecular Engineering
Rice University

K. Jane Grande-Allen, Ph.D.
Associate Professor
Department of Bioengineering
Rice University

Rebekah A. Drezek, Ph.D.
Professor
Departments of Bioengineering and Electrical and Computer Engineering
Rice University

Kyriacos Zygourakis, Ph.D.
A.J. Hartsook Professor
Department of Chemical and Biomolecular Engineering
Rice University

F. Kurtis Kasper, Ph.D.
Faculty Fellow
Department of Bioengineering
Rice University

John A. Jansen, D.D.S., Ph.D.
Professor and Head College of Dental Sciences
Department of Biomaterials
Radboud University, Nijmegen Medical Center

Houston, Texas
December 2012

# ABSTRACT


**Development of Osteoinductive Tissue Engineering Scaffolds with a Bioreactor**

by

**Richard A. Thibault**

The conventional treatments for craniofacial bone defects currently are unsatisfactory due to several drawbacks. Replacement of lost bone by autografts typically causes donor site morbidity while allografts, xenografts, and demineralized bone matrix have a chance of disease transmission. Current synthetic implants placed within the defect site generally lack osteogenicity and biodegradability.

There are several methods of generating an extracellular matrix (ECM) and synthetic material hybrid construct. These include coating a scaffold with collagen and calcium phosphate, incorporating acellular biological tissue within scaffolding material, and using cells to generate an ECM coating on the scaffold. The research performed in this thesis developed and characterized mesenchymal stem cell (MSC)-generated ECM poly(ε-caprolactone) constructs (PCL/ECM) for the replacement of bone.

The osteogenic potential of the PCL/ECM constructs was explored by culturing MSCs or whole marrow cells combined with MSCs onto the construct with or without the osteogenic differentiation supplement, dexamethasone. It was established that the osteogenic differentiation of MSCs seeded onto ECM-containing constructs was maintained even in the absence of dexamethasone and that the co-culture of MSCs and

whole bone marrow cells without dexamethasone and ECM enhances the proliferation of a cell population (or populations) present in the whole bone marrow.

The osteogenicity of the constructs encouraged the characterization of the protein and mineral composition of the ECM coating on the PCL/ECM constructs. Characterization revealed that at short culture durations the MSCs used to generate the ECM deposited cellular adhesion proteins that are a prerequisite protein network for further bone formation. At the later culture durations, it was determined that the ECM was composed of collagen 1, hydroxyapatite, matrix remodeling proteins, and regulatory proteins.

The prior studies on the PCL/ECM constructs persuaded exploration of the effect of devitalization and demineralization processes on the retention of the ECM components within and the osteogenicity of the PCL/ECM constructs. Analysis demonstrated that the freeze-thaw technique is a milder method of devitalization of cell-generated ECM constructs as compared to other methods. In addition, it was elucidated that void spaces in the surface of the constructs were important for allowing access of MSCs into the interior of the constructs.

## ACKNOWLEDGEMENTS

*Donny (Richard), you are out of your element! – The Big Lebowski*
*Oh Richard, hold me! – Tommy Boy*

Quite often as a graduate student here at Rice, I've heard these words from many of my friends. I know it's just teasing, but I did feel several times that I was out of my element and that only time and hugs from friends and family would help. I think many graduate students feel this way, so I would like to thank everyone that was able to help me successfully complete my Ph.D..

To my advisor, Dr. Antonios Mikos and my thesis committee members, Dr. Grande-Allen, Dr. Drezek, Dr. Zygourakis, Dr. Kasper, and Dr. Jansen:

Thank you for all of your assistance and guidance in my many experiments. Without this, I would not have been able to learn how to design rigorous scientific experiments or write clear and logical manuscripts describing my results.

To Dr. Yasuhiko Tabata:

I really appreciate the opportunity to study at your laboratory and spend 3 months in Japan. It allowed me to explore and observe other methods of guiding students in achieving their Ph.D. and scientific experimentations.

To Mike Starbuck and Dr. Grande-Allen:

I would like to thank both of you for assisting me in figuring out my issues with histology. Without you, I would still be pondering a solution.

To Quynh Pham:

Thank you for all the time you spent training me in the proper cell culture techniques, rat euthanizations, and sterile assembly of the flow perfusion bioreactor. Your words of advice will remain with me for life.

To the Mikos research group:

Thanks for all your advice on my manuscripts, presentations, and overall encouragement in our everyday pursuit of our Ph.D.s. The time we spent together in lab made coming into lab exciting.

To my friends:

Ryan Schweller, Emily Day, Mike Cuchiara, Maude Rowland, Kelsey Rosbach, Noah Bedard, Ying Hu, Clark Needham, Erica Levorson, Allan Henslee, Brendan Watson, Matt Kyrish, Brian McCall, Hubert Tseng, Elizabeth Figueroa and the many others who I can't include here. Thank you for all the fun times we had together. You guys made my time here exciting and enjoyable and helped to keep me sane. Time with you guys validated that pursuing my Ph.D. at Rice was the right choice.

To my best friend, Shoichi Okada:

Thanks for checking in with me even when you were busy with ‘med skool’ and letting me escape Houston to chill with you up in St. Louis. Even if we couldn’t see each other, our video game sessions reminded me of the wonderful times we had at JHU.

To Mom, Dad, Matt, and Marie:

Thank you for all your encouragements, presents, cards, and time spent with me. I know without all your help, accomplishing all I have would have not been possible. I love you all.

Lastly, thanks to AGEP and the NIH for their financial support over my years here.

## TABLE OF CONTENTS

## LIST OF TABLES

## LIST OF FIGURES

# CHAPTER 1

## THESIS OVERVIEW

Reconstructive surgeons face a significant challenge when repairing craniofacial bony defects caused by traumatic injury or tumor resection. Currently, autogeneic bone grafts from the tibia, ribs, and iliac crest are the current gold standard graft material for bone defect repair in clinical settings. However, treatments of these defects are may also be addressed by using synthetic graft materials such as ceramics and metals or allogeneic and xenogeneic tissues. There are inherent drawbacks to using each of these materials, with the main concerns being necrosis at the donor site for autogeneic tissues, the lack of degradation and osteointegration for many synthetic materials, and the potential for disease transmission in the case of allogeneic and xenogeneic tissues. To address these pitfalls, tissue engineering seeks to develop an osteogenic construct that can reduce or replace the need for synthetic, autogeneic, allogeneic, and xenogeneic graft materials.

The goal of the research presented within this thesis was to develop a biodegradable osteogenic extracellular matrix (ECM) and polymer construct for bone regeneration and identify the components within the ECM that encourage the osteogenic differentiation of mesenchymal stem cells (MSC). Osteogenic differentiation of MSCs *in vivo* is dependent on ECM composition and signaling molecules as well as the mechanical forces that the cells experience. Thus, MSCs were cultured on electrospun poly(ε-caprolactone) (PCL) and exposed to

shear stress in the form of fluid flow and to an osteogenic differentiation supplement, dexamethasone to generate an osteogenic ECM coating on a PCL scaffold (PCL/ECM). In order to elucidate the properties of this PCL/ECM construct, the following specific aims were proposed and investigated:

1. *Evaluate the osteogenicity of a statically generated PCL/ECM construct by culturing MSCs or MSCs and whole marrow cells onto the constructs under static conditions with or without the osteogenic differentiation supplement, dexamethasone*

2. *Determine the temporal change in protein and mineral composition of PCL/ECM constructs generated within a flow perfusion bioreactor*

3. *Determine the effect of various devitalization and demineralization processes on the ECM composition and osteogenicity of the treated PCL/ECM constructs*

This thesis starts with a review on the various methods of creating a hybrid ECM and scaffold construct for bone tissue engineering, which includes scaffolds coated with collagen and calcium phosphate, scaffolds incorporating decellularized biological tissue, and scaffolds with a cell-generated ECM coating. In Chapter 3, MSCs or MSCs and whole marrow cells were seeded onto the PCL/ECM constructs and cultured with or without dexamethasone to explore the osteogenicity of the constructs. This study validated the osteogenicity of the PCL/ECM constructs and encouraged further research into the PCL/ECM constructs. Chapter 4 investigates the composition of the PCL/ECM constructs to determine what components are important to the osteogenicity of the constructs. Temporal differences in the protein and mineral composition of the PCL/ECM construct was observed and warranted additional investigation into the compositional changes in the MSC-generated ECM due to construct processing.

Chapter 5 elucidates the effect of the devitalization and demineralization processing on the ECM composition and osteogenicity of the PCL/ECM constructs. This study demonstrated that processing causes visible void spaces in the outer ECM coating of the PCL/ECM constructs allowing access to the interior. Lastly, the conclusions of this thesis and future directions of exploration into PCL/ECM constructs are presented in Chapter 6.

# CHAPTER 2

## Scaffold/Extracellular Matrix Hybrid Constructs for Bone Tissue Engineering


### Abstract

The limited natural ability of the body to fully repair large bone defects often necessitates the implantation of a replacement material to promote healing. While the current clinical strategies to address such bone defects generally carry associated limitations, bone tissue engineering approaches seek to minimize any adverse effects and facilitate complete regeneration of the lost tissue. Of particular interest are hybrid constructs that incorporate multiple components found within native bone matrix to enhance the osteogenicity of biocompatible materials, which might otherwise be non-osteogenic. This review will focus on such hybrid constructs that incorporate multiple components from native bone matrix for bone tissue engineering and will highlight the synthesis and characterization of the hybrid constructs, cellular attachment and proliferation within the constructs, *in vitro* osteogenicity of the constructs, and the biological response to *in vivo* implantation of the constructs at ectopic and orthotopic sites.


---

* This manuscript was prepared as presented for submission to Advanced Healthcare Materials

## 2.1 Introduction

Reconstructive surgeons often face significant challenges when repairing craniofacial bony defects arising from traumatic injury and tumor resection among other causes. Currently, these defects are addressed clinically by using synthetic graft materials such as ceramics, polymers, and metals; autologous bone tissue; or allogeneic and xenogeneic demineralized bone matrix.[1-4] However, there are various inherent drawbacks associated with the use of these including a lack of biodegradability for most metals and for some ceramics, limited supply and donor site morbidity with autologous bone tissue, and the potential for disease transmission with allogeneic and xenogeneic tissue.[3,5,6]

Tissue engineers seek to overcome these drawbacks by developing osteogenic materials that support the capacity of the body to regenerate bone and integrate with the surrounding bone tissue. Prior approaches have focused on mimicking isolated components of native bone, such as the nanoscale extracellular matrix (ECM) architecture by using nanofibrous materials; the bioactive moieties by coating surfaces with cell-adhesive peptide sequences; the inorganic matrix elements by incorporating hydroxyapatite (HAp); and the signaling molecules by releasing growth factors from the materials.[7-10] However, natural bone ECM is a composite material consisting of fibrous collagen, hydroxyapatite, proteoglycans, and growth factors.[11] Recent approaches have evolved to generate scaffold/extracellular matrix hybrid constructs integrating the multiple components found in native bone matrix with synthetic biomaterials. These

approaches typically include the use of porous scaffolds or polymeric carriers combined with various ECM components. The synthesis and characterization, cellular attachment and proliferation, *in vitro* osteogenicity, and the biological response to *in vivo* implantation at ectopic and orthotopic sites of hybrid constructs incorporating multiple components of native bone matrix will be discussed in this review.

## 2.2 Synthesis of Scaffold/ECM Hybrid Constructs

Natural bone consists of collagen, HAp, and noncollagenous proteins such as proteoglycans, matrix metalloproteinases, and growth factors.[11] The collagen present within bone is organized into fibers approximately 300 nm in length and 1.5 nm in diameter.[11,12] The fibers are mineralized with biological HAp, a calcium-deficient apatite with carbonate ion substitutions. The plate-like HAp crystals grow preferentially along the collagen fibers and have very small crystallite sizes with a lower crystallinity than synthetic HAp.[12] They are nucleated in the 40 nm gaps present between the collagen fibers and initiated by trace proteins bound to the collagenous ECM. In addition to initiating HAp crystals, trace proteins are important for binding growth factors, remodeling the ECM, promoting angiogenesis, and inducing new bone formation.[11]

There are many approaches for generating hybrid constructs for bone tissue engineering that can incorporate the key aspects of the composition of bone **(Table 2.1)**. One method includes coating a polymeric scaffold of micro- or

nano-scaled architecture with collagen and calcium phosphate.[13,14] This type of construct is beneficial because of its simplicity and resemblance to bone ECM. The coating of both collagen and calcium phosphate may provide stem cells cultured within the construct an environment that encourages osteogenic differentiation and bone-like ECM deposition. On the other hand, such constructs may lack the complex organization and composition needed to provide cells with the biological cues to form bone. The fibrillar structure of collagen or the inclusion of growth factors may be necessary to form bone correctly. Another approach is to incorporate components of decellularized tissues within a polymeric carrier or scaffolding material.[15,16] The use of decellularized tissue may allow for the inclusion of many of the proteins and minerals found in the biological tissue. These decellularized tissues also retain much of their original structure and may provide cells with the correct template for tissue regeneration. Nevertheless, some devitalization processes may irreversibly damage the proteases and growth factors found in the native tissue, rendering them inactive. In addition, this approach requires donor tissue, although at lower amounts with respect to autologous, allogeneic, and xenogeneic bone grafts. The same disadvantages observed with these grafts are also found in hybrid constructs incorporating biological tissues. The last method covered in this review is the creation of a cell-generated ECM coating on the surfaces of the scaffold that mimics the composition of native bone.[17,18] Osteoblasts or osteogenically differentiated stem cells are typically used to generate the ECM coating. This cell-generated ECM coating may potentially have all the components that can

regulate the composition and organization of the ECM similar to that of native bone. However, disadvantages to this method are that the biological components of this construct are difficult to characterize and the optimal cell culture time to generate an osteogenic ECM coating must be elucidated. In addition, it is difficult to provide the cells with the correct distribution and environment to evenly deposit the osteogenic ECM coating throughout the scaffold.

### 2.2.1 Polymeric Constructs Incorporating Collagen and Calcium Phosphate

These hybrid constructs seek to mimic bone ECM by combining porous polymeric scaffolds that have nano- and micro-sized features with collagen and calcium phosphate **(Figure 2.1)**. Also under consideration are hybrid constructs incorporating gelatin instead of collagen. Although, gelatin is a hydrolyzed form of collagen, it has a similar composition, allows for cell adhesion, and is biodegradable *in vivo*.[19-21]

Three major methods of construct synthesis have been reported in the literature. The first method involves a polymer scaffold coated initially with collagen and subsequently with hydroxyapatite. The second method uses a combination of polymer, collagen, and calcium phosphate in suspension to generate a hybrid construct after the removal of the solvent. The third method combines the two prior methods by incorporating either the collagen or the calcium phosphate into

the polymer solution, removing the solvent, and then coating the surface of the composite scaffold with the other component.

In the first method, the generation of the synthetic portions of several hybrid constructs was accomplished in several ways, including electrospinning, 3D printing, and freeze-drying of polymer solutions.[13,14,22] Electrospinning creates a non-woven fiber mesh mat with controllable fiber diameter, porosity, and thickness.[23] With 3D printing, it is possible to generate a scaffold with a pre-determined macrostructure and microstructure.[24] Freeze-drying of polymer solutions can create a porous sponge with a controlled pore structure.[25] Each of these methods is capable of creating a highly porous scaffold that allows for the penetration of the coating solutions throughout the scaffold.

Following fabrication, the scaffold may be submerged within a collagen or gelatin solution and subsequently in simulated body fluid (SBF) solution to generate a coating of collagen or gelatin and HAp on the polymer surface. A layer-by-layer method may be used to control the thickness of the coating.[26] As an example, Li et al. coated a poly(ε-caprolactone) (PCL) scaffold several times, first with gelatin followed by a number of layers of poly(styrene sulfonate) and finally with gelatin.[13] The amount of HAp present on the scaffold may also be controlled by varying the incubation time within the SBF solution. SBF has nearly the same ionic concentration as human plasma but is highly supersaturated with respect to apatite.[27] As a result, SBF forms bone-like HAp crystals on bioactive surfaces

such as collagen or gelatin.[27] However, SBF with the same concentration as human plasma (1X SBF) may take more than 16 days to fully coat a surface with HAp.[28] Therefore, in order to decrease the mineralization time, SBF with up to 10 times the concentration of ions found in 1X SBF may be used. To further decrease the construct preparation time, it is possible to soak scaffolds in a combined collagen and SBF solution. Yun et al. used this combined method and were able to remove a fully coated construct after 24 hours.[14]

The second method uses electrospinning, lyophilization, or vacuum evaporation to remove the solvent from a polymer, collagen, and calcium phosphate suspension. As an example, Zhang et al. dispersed chitosan, bovine collagen, and HAp nanoparticles in dimethyl sulfoxide and acetic acid and created a nanofibrous scaffold by electrospinning.[29] Lyophilization was used to generate sponges from a suspension of micro-sized HAp with chitosan and gelatin or a suspension of alginate, porcine gelatin, and β-tricalcium phosphate (TCP).[30,31] In another method, a porous sponge was generated via lyophilization using ice microparticles as a porogen.[32] Specifically, Li et al. created ice microparticles from a solution of bovine collagen with dispersed 500 nm sized HAp particles frozen in liquid nitrogen. The ice microparticles were combined with poly(L-lactic acid) (PLLA) dissolved in dioxane at -5$^{o}$C, kept in liquid nitrogen for 12 hours, and lyophilized to remove the solvents. Li et al. also created porous scaffolds through vacuum evaporation. They combined HAp nanoparticles with bovine collagen and paraffin microspheres in water and malonic acid, allowed the

mixture to air dry, and followed by cross-linking of the collagen using formaldehyde. Subsequently, poly(lactic-co-glycolic acid) (PLGA) dissolved in pyridine was drop-cast into the interspace between the paraffin microspheres. The pyridine solvent was allowed to evaporate under low vacuum and then the paraffin microspheres were dissolved with cyclohexane, resulting in composite scaffolds.[33]

In the third method, constructs are typically fabricated by electrospinning or 3D printing of a polymer and either collagen or calcium phosphate solution followed by the coating of the scaffold with calcium phosphate or collagen, respectively. A nanofibrous polymer scaffold was generated by electrospinning a combination of PLLA, poly(benzyl-L-glutamate) (PBLG), and collagen dissolved in 1,1,1,3,3,3-hexafluoro-2-propanol (HFIP).[34] The nanofibrous scaffold was then coated with nano-sized crystals of HAp using 3 cycles of dipping in calcium chloride followed by dipping in sodium pyrophosphate. Another hybrid construct was generated by electrospinning PLGA combined with amorphous calcium phosphate and collagen I.[35] The collagen within the scaffolds was cross-linked with glutaraldehyde and then incubated in SBF to create a HAp coating. 3D printing was used to generate a PLGA and TCP composite thumb-shaped scaffold, with multiple 1 mm by 1 mm channels present throughout.[36] The scaffold was subsequently coated with a collagen-based hydrogel containing human mesenchymal stem cells (MSCs).

### 2.2.2 Biological Tissue ECM-based Construct

Biological tissue ECM-based constructs generally consist of a polymeric carrier material and acellular biological tissue **(Figure 2.2)**. Most of these hybrid constructs incorporate demineralized bone matrix (DBM) because of the osteogenic factors known to be present within DBM.[16,37,38] However, some constructs use acellular bone matrix (ABM) or acellular urinary bladder submucosa (UBS).[15,39]

DBM is an osteoinductive material that is generated by decellularizing and demineralizing cortical bone.[40] A typical method of generating powdered DBM involves first cleaning of cortical bone to remove any remaining soft tissue followed by rinsing with a saline solution.[40,41] The bone is subsequently cut into small fragments and defatted and dehydrated using a 1:1 chloroform-methanol solution. The resulting fragments are frozen and pulverized into particles of sizes in the sub-millimeter range using a mill or mortar and pestle. The particles are then demineralized using hydrochloric acid ranging from 0.1 – 0.6 N at 4$^{o}$C and sterilized using ethylene oxide.[41] ABM is generated in a similar manner as DBM, but there is no demineralization step. Instead it is generated by sterilizing the bone particulates with ethylene oxide immediately following the pulverization step.[39]

UBS is generated from the submucosal layer of the smooth muscle layer of the bladder. One method of creating UBS is by mechanical delamination of the

submucosa from the smooth muscle followed by a treatment with dilute peracetic acid and deionized water to render the tissue acellular.[15] The acellular tissue is subsequently lyophilized and pulverized using a mortar and pestle to create a powder of particulates in the range of 100 to 500 μm.[15]

Each of these decellularized tissues provides many of the native components of the tissue. UBS is composed mainly of collagen, but also retains fibroblast growth factor (FGF) and vascular endothelial growth factor (VEGF).[42] ABM contains both the organic matrix and the mineral components of bone whereas DBM only retains the organic matrix. However, it has been shown that demineralization of bone matrix increases access to the bone morphogenic proteins (BMP) bound to the organic matrix.[43] The presence of BMPs have been shown to induce bone formation at an ectopic site.[44] Thus, DBM should provide any seeded cells with access to BMPs. Nevertheless, it is possible to excessively demineralize the tissue and deplete the BMPs from DBM.[45] In addition, it has been shown that particulate size can affect the osteogenicity of DBM.[46-48]

The formed particulates from different tissues are combined with either a liquid polymeric carrier that later solidifies to form a gel or combined with a polymer to form a film. In the liquid polymeric carrier case, there are several types of polymers used and different methods of solidification employed. For example, poly(ethylene glycol)-PCL-poly(ethylene glycol) (PEG-PCL-PEG) co-polymer

was dissolved in water at 60$^{o}$C, mixed with ABM, and cooled to form a composite gel.[39] As another example, Kurkalli et al. combined rat DBM with Pluronic F-127, a reverse thermo-responsive polymer, and placed the solution *in vivo* to gel.[38] Reverse thermo-responsive polymers display low viscosity at room temperature, but form a gel at body temperature.[49] In another study, porcine UBS and a sucrose polymer were combined with PLGA in solution, polymerized, and the sucrose polymer was dissolved away to form a porous structure.[15]

In order to generate a film, a polymer and the acellular tissue particulates are combined and placed at the bottom of a well to generate a 2D surface that is a composite of the two materials. Thomas et al. combined DBM particles with PLLA beads ranging from 0.52 mm to 1.91 mm in size at varying ratios to generate a 2D substrate.[16] A film was generated by combining human ABM or human DBM with PLGA in chloroform. The suspension was then cast as a thin layer in a petri dish and subsequently dried under air flow for 24 hours to create a composite thin film.[37]

### 2.2.3 Cell-generated ECM-based Construct

Cell-generated ECM-based constructs are generated by culturing stem cells, osteoblasts, or pre-osteoblastic cells on porous scaffolds. The goal of this approach is to create a cell-generated ECM coating on the surfaces of the scaffold that mimics the composition of native bone **(Figure 2.3)**. The cell culture

to generate the ECM has been performed under static conditions, flow conditions, electromagnetic stimulation, or dynamic strain.

Static culture has been used to generate ECM coatings on scaffolds because of the ease of culture. This method of culture works well for small scaffolds, where diffusional limitations of nutrients are less significant.[50] The varieties of scaffolds that have been used in static culture include mineral pellets, porous polymer scaffolds, gelatin cryogels, and fiber mesh scaffolds ranging in thicknesses from 0.8 mm to 5 mm.[17,18,51-57] Osteoblast-like cell lines such as SaOS-2 cells, bone marrow stromal cells (BMSCs) from human and rat sources, and primary rat osteoblasts have been cultured on these scaffolds from a minimum of 16 days up to 6 weeks to generate the bone mimetic ECM.

However, in large constructs, portions of the scaffold may encounter a lack in nutrients due to diffusional limitations, causing cells present in these areas to become less active.[58] Bioreactor culture addresses the diffusional limitations by enhancing the mass transfer of nutrients and oxygen and the removal of metabolic waste products using fluid flow around or through the scaffold.[58] In addition, fluid flow through the pores of constructs stimulates seeded cells in the form of shear stress, which has been shown to enhance osteogenic differentiation of stem and progenitor cells.[59,60]

Bioreactors involving flow culture conditions include a flow perfusion bioreactor, a rotational oxygen-permeable bioreactor, and a spinner flask bioreactor. A flow perfusion bioreactor consists of a pump that perfuses constructs with media through a confined fluid path at a controlled flow rate.[61,62] A variety of porous scaffold types have been placed within a flow perfusion bioreactor including foam and fiber mesh scaffolds.[63-77] The cells cultured under flow perfusion conditions are similar to those cultured under static conditions and include SaOS-2 cells and BMSCs from human, rat, and goat sources and have been cultured from 15 days up to 40 days. A rotational oxygen-permeable bioreactor consists of a rotating apparatus and a chamber which allows for gas exchange.[78] Cell seeded constructs and media are placed within the chamber and rotated at a controllable rate, which causes the constructs to be continuously in free fall and thus subjected to constant fluid flow.[58] Electrospun polymer fiber mesh scaffolds and polymer foam scaffolds have been cultured with rat BMSCs, rabbit amniotic MSCs, and porcine bone marrow progenitor cells using the rotational oxygen-permeable bioreactor for durations ranging from 10 days to 34 weeks.[79-82] The spinner flask bioreactor generates fluid flow by suspending constructs within a media reservoir and placing a stir bar at the bottom to stir the media at a controlled rate.[83] A cell-generated ECM construct was created from silk fibroin scaffolds seeded with human BMSCs and cultured within a spinner flask that was stirred for 5 weeks.[84]

Analogous to shear stress, pulsed electromagnetic fields (PEMF) have been shown to stimulate osteogenic differentiation of stem cells and ECM mineralization.[85,86] Additionally, dynamic loading has been shown to enhance matrix production and osteogenic differentiation.[87,88] Both PEMF and dynamic loading have been used to generate an ECM coating on constructs without the addition of any osteogenic cell culture supplements.[88-94] Polymer foams, gelatin cryogels, and titanium disks were used as scaffolds and cultured with such cells as the SaOS-2 cell line and human BMSCs.[89-93] These cell-seeded constructs were statically cultured for 22 days or 6 weeks in the presence of an electromagnetic field and, in some cases, with additional ultrasonic stimulation. Investigators have also cultured polymer foam scaffolds with cells such as human MSCs and an osteoblastic cell line, MLO-A5, under 5% strain for 19 or 20 days to enhance ECM production.[88,94]

Also of note, several of the cell-generated ECM-based constructs were decellularized prior to analysis. Most hybrid constructs underwent 3 cycles of freezing in liquid nitrogen and thawing in 37$^{o}$C water followed by ultrasonication for 10 minutes.[18,51,64,73,74,76] An alternate method of decellularization was accomplished by treating the constructs with 0.5% Triton X-100 and 20 mM ammonium hydroxide for 3 minutes at 37$^{o}$C.[57]

### 2.2.4 Compositional and Physical Characterization of Hybrid Constructs

While the method of synthesis for these various hybrid constructs drastically differs, the manner of characterization is quite similar. Construct characterization has been approached using i) visualization of the distribution of cells, proteins, and minerals through the construct, ii) analysis of the protein and mineral composition, and iii) determination of physical characteristics.

Scanning electron microscopy (SEM) allows for the visualization of micro- and nano-scaled features on the surface of the construct. However, SEM does not allow for ready observation of the distribution or identification of the cellular, protein, and mineral components within the interior of hybrid constructs. A combination of fluorescent staining and confocal microscopy has been used to demonstrate the distribution of cells throughout the construct.[52,66] For further characterization of the biological factor distribution within the construct, several histological stains have been used, including methylene blue and hematoxylin & eosin for cells, alcian blue and Safranin O for proteins and glycosaminoglycans (GAGs), and alizarin red and von Kossa for minerals, while immunohistochemistry has been used to visualize the distribution of specific biological components.[17,30,82,84]

In order to determine more precisely the composition of the hybrid constructs, the amount of proteins and GAGs have been determined using colorimetric assays and their identification has been established using enzyme-linked

immunosorbent assay (ELISA), western blotting, and mass spectrometry. Typically, to determine the amount of proteins and GAGs in the construct, a detergent or chaotropic solution has been used to solubilize the proteins.[17,55,92] Once the proteins are in solution, colorimetric assays such as the bicinchoninic acid (BCA) assay, coomassie blue assay, 1,9-dimethylmethylene blue (DMMB) assay, and chloramine T assay have been used to determine protein and GAG amounts.[14,57,92] Precise identification of the proteins and GAGs present within the protein solution can be performed via ELISA and western blotting using antibodies.[95,96] Another method for precise identification of proteins in the solution combines a liquid chromatography column along with a tandem mass spectrometer (LC-MS/MS) and a protein database search engine.[97] The protein solution first undergoes trypsinization and is then run through the liquid chromatography column, followed by injection into a tandem mass spectrometer. The resulting spectrum is analyzed by a protein database search engine and matched to specific proteins.[97] If known amounts of the specific protein are analyzed in a similar manner, a standard curve can be created from the LC-MS/MS spectra and the amount of the specific protein can be calculated.[98]

However, each of these methods has a threshold necessary to correctly identify and determine the amount of a protein and a GAG. The chloramine T, DMMB, and BCA assays are typically able to detect molecular concentrations in the micromolar ranges, although submicromolar ranges have been reached using various modifications.[99-101] The coomassie blue staining typically can only detect

greater than 10 ng of protein, but has been recently improved to detect greater than 2 ng of protein.[102] Meanwhile, the techniques that use antibodies allow for the detection of proteins at much lower levels. Conventional ELISA has a detection limit in the picomolar range, but using a modified technique, detection in the subfemtomolar range has been accomplished.[103] Western blotting can detect greater than 100 pg of protein while LC-MS/MS permits detection of proteins on the order of subpicograms.[104,105]

When determining the mineral amount and composition within the hybrid constructs, colorimetric and spectroscopic assays have been applied. Quantifying the amount of calcium phosphate mineral present within the construct has been accomplished by the colorimetric calcium and phosphate assays.[51,76] However, these assays cannot accurately determine what form of calcium phosphate is present. This issue is addressed with several techniques including X-ray diffraction (XRD), Fourier transform infrared spectroscopy (FTIR), NMR, energy dispersive X-ray spectroscopy (EDX), or X-ray photoelectron spectroscopy (XPS) to determine the chemical composition and crystallinity of the minerals **(Figure 2.4)**.[13,22,39] Each type of mineral presents a unique spectrum or diffractogram in each of these analyses, thus allowing for identification of the specific minerals present.[106]

Several methods have been used to determine the physical characteristics of the constructs. Contact angle measurements can be used to quantitatively

demonstrate that the surface has been altered. Water placed onto the surface of a construct forms a droplet, and the hydrophobicity of the surface can be predicted based on the angle that the droplet of water makes with the surface. This is especially useful when a hydrophobic scaffold material is coated with a hydrophilic substance such as HAp or collagen. Micro-computed tomography (μCT) and fluid replacement methodologies have been used to determine the porosity of the constructs.[14,54,65] μCT uses X-rays to visualize sections of radio-opaque materials and uses a computer to reassemble the sections into a 3-D rendering of the construct.[107] Using this representation, the interconnectivity of the pores, pore size, and porosity can be calculated.[107] The fluid replacement methodologies, such as mercury porosimetry, gas pycnometry, and liquid intrusion, measure the change in initial fluid volume when the pores of the constructs are filled by the various fluids, which in turn is used to calculate the construct pore size and porosity.[108]

## 2.3 *In Vitro* Cell Culture on Hybrid Constructs

Following the synthesis and characterization of a hybrid construct, the assessment of its bone repair potential is an important step in establishing the cytocompatibility and osteogenicity of the material. Typically, the initial characterization is through *in vitro* cell culture, since it is a less intensive method of determining the bone repairing potential as compared to *in vivo* implantation. Through the attachment and proliferation of cells onto the hybrid constructs, the cytocompatibility of the material can be elucidated. Increased cellular attachment

and proliferation may suggest that if the hybrid construct is implanted, osteoblasts and stem cells will be able to successfully invade and colonize it. Furthermore, an increase in osteoblastic gene expression, protein secretion, and construct mineralization can demonstrate its osteogenicity. The osteogenic differentiation of the cells within the hybrid construct *in vitro* suggests that once it is implanted, stem cells migrating from the surrounding tissue may be able to differentiate down an osteogenic pathway and contribute to bone regeneration *in vivo*.

### 2.3.1 Cellular Attachment and Viability on Hybrid Constructs

Several cell types have been cultured on hybrid constructs to determine their overall cytocompatibility. These cell types include cell lines such as MC3T3-E1, mouse marrow stromal cells (D1 cell line), human fetal osteoblasts (hFOBs), and SaOS-2 or stem cells such as adipose derived stem cells (ADSCs) and MSCs from human, rat, and mouse sources. An advantage of cell lines is that they are easily procured and cultured. However, with the exception of MC3T3-E1 and D1 cells, the cell lines are already differentiated into osteoblasts and thus can only provide limited information regarding the osteoinductivity of the hybrid construct. Notwithstanding, certain stem cell populations present the potential to differentiate down the osteoblastic lineage and may be useful in assessing the osteogenicity of a hybrid construct.

The viability and proliferation of the cultured cells can be determined by a variety of assays. For instance, the lactate dehydrogenase assay quantifies the number of dead cells, while the PicoGreen assay determines the total amount of dsDNA which then can be used to calculate the number of cells if the amount of dsDNA has been measured for a known number of cells. In addition, the 3-(4,5-dimethylthiazol-2-yl)-5-(3-carboxymethoxyphenyl)-2-(4-sulfophenyl)-2H-tetrazolium (MTS), 3-(4,5-dimethylthiazol-2-yl)-2,5-diphenyltetrazolium bromide (MTT), and glucose consumption assays measure the metabolic activity of the viable cells.

Cell lines cultured on hybrid constructs generally demonstrate a higher attachment and proliferation as compared to cell lines cultured on the corresponding scaffold material in the absence of an ECM component.[13,14,16,29,32] Li et al. determined that MC3T3-E1 cells cultured on electrospun PCL coated with collagen and calcium phosphate demonstrated significant enhancement in proliferation at day 7 when compared to cells seeded onto unmodified electrospun PCL fiber meshes.[13] Additionally, the surface of the construct was covered with multiple layers of cells due to proliferation. MC3T3-E1 cells were also shown to have faster attachment, higher degree of cell extension, and flattened morphology after 30 minutes of incubation and a higher increase in cell number after 7 days of culture when seeded onto a mesoporous bioactive glass (MBG)-PCL-ECM coated construct as compared to a plain PCL scaffold.[14]

Similarly, stem cells are generally able to attach and proliferate on hybrid constructs.[18,30,31,34,35,37,51,64] Human MSCs seeded onto hybrid chitosan/gelatin/HAp constructs displayed high cell proliferation and deep cell penetration under flow perfusion conditions.[31] When mouse MSCs were cultured on films of PLGA/DBM or PLGA/ABM, they expressed a higher level of attachment than that of cells cultured on PLGA film alone.[37] Also, rat MSCs seeded onto hybrid titanium and cell-generated ECM constructs and hybrid PCL and cell-generated ECM constructs exhibited cell proliferation until day 18 or day 8, respectively, with a subsequent drop at later timepoints.[18,51,64] The investigators explained both drops at the later timepoints as being caused by the MSCs encasing themselves in matrix, preventing the DNA from being released into the analysis solution and being detected.

The information gleaned from the cell attachment and viability studies can be used to guide hybrid construct composition. For example, low cell viability may suggest that a component of the construct is cytotoxic and should be excluded, whereas cell attachment, maintenance of viability, and proliferation generally indicate cytocompatibility. Each type of hybrid construct reviewed herein has been observed generally to demonstrate cellular attachment, viability, and proliferation. Accordingly, these hybrid constructs demonstrate cytocompatibility and may support cell infiltration and survival *in vivo*.

### 2.3.2 Osteogenic Differentiation of Stem and Pre-osteoblastic Cells on Hybrid Constructs

The differentiation of stem cells such as ADSCs and MSCs from human and rat sources and pre-osteoblastic cells such as MC3T3-E1 cells cultured on the constructs can be used to determine their osteogenicity. Use of media containing osteogenic supplements has been shown to cause osteogenic differentiation of the stem and pre-osteoblastic cells.[109] Thus, the true test of the osteogenicity of the construct is through culture in media without osteogenic supplements, such as dexamethasone. This can be measured by the alkaline phosphatase (ALP) activity, an early stage marker of osteoblastic differentiation; gene expression of osteoblastic markers of the seeded cells; and the amount of osteocalcin, osteopontin, as well as mineral deposition present in the construct, all of which are late stage markers of osteoblastic differentiation.[110-112]

The alkaline phosphatase activity of cells seeded onto several hybrid constructs were seen to be increased when compared to cells seeded on the base material lacking the biological components.[14,18,31,34,51,64] However, even with osteogenic supplementation, Thomas et al. demonstrated that D1 cells cultured on the mixture of PLLA beads and DBM particles had a significantly lower ALP activity as compared to the cells cultured on PLLA beads alone.[16] Additionally, Hild et al. showed that human MSCs cultured on composite calcium phosphate/collagen/PLGA films displayed no significant difference in ALP activity when compared to PLGA films.[35]

The upregulation in the production of osteopontin has also been observed in MSCs cultured onto chitosan/gelatin/HAp constructs.[31] Similarly, MSCs cultured onto hybrid TCP/alginate/gelatin constructs exhibited enhanced osteopontin and osteocalcin production, and this was observed in both the presence and absence of the osteogenic supplement, dexamethasone.[30]

Significantly higher gene expression of osteogenic markers such as runt-related transcription factor 2 (RUNX2), Collagen I, ALP, osteopontin, BMP-2, VEGF, FGF, aggrecan, and matrix metalloproteinase 9 (MMP-9) was observed for MC3T3-E1 cells and MSCs cultured on hybrid constructs in media with or without dexamethasone as compared to cells cultured on their respective base materials alone.[14,74] However, in the case of a construct composed of PLLA beads and DBM particles, there was significantly lower gene expression by the seeded D1 cells for bone sialoprotein (BSP), RUNX2 and osteocalcin as compared to the cells cultured on PLLA beads alone.[16]

Many of the hybrid constructs also demonstrated a significantly higher amount of calcium mineralization than their base material counterparts.[18,30,34,35,51,64] In particular, the TCP/alginate/gelatin constructs showed an increase in calcium mineralization even in the absence of the osteogenic supplement dexamethasone.[30] The presence or lack of osteogenic differentiation of stem cells observed for the varying hybrid constructs does not seem to implicate any

specific combination of components. Interestingly, even the presence of the osteogenic supplement dexamethasone does not guarantee differentiation. However, the one study that resulted in lower gene expression of osteogenic markers and ALP activity did not contain any form of calcium phosphate.[16] The existence of a form of calcium phosphate may be necessary for proper osteogenic differentiation of the stem cells.

The implications from the osteogenic differentiation studies can also be used to improve hybrid construct composition for bone repair. A decrease in activity and amount of early and late osteogenic markers may signify that the construct components are not osteogenic, while an increase might suggest the potential of the constructs to promote bone repair *in vivo*. Evaluation of the hybrid constructs reviewed herein demonstrates that all of the cell-generated ECM-based hybrid constructs have an increase in osteogenic markers as compared to their base material. Meanwhile a few of the polymeric constructs incorporating collagen and calcium phosphate and the biological tissue ECM hybrid constructs demonstrate decreased osteogenic markers compared to their respective base materials. The results of the *in vitro* studies indicate that the cell-generated ECM-based hybrid constructs may enhance bone formation and osteointegration, while those with decreased osteogenic markers may perform less favorably.

## 2.4 *In Vivo* Implantation of Hybrid Constructs

Although an *in vitro* evaluation reveals important information regarding the cytocompatibility and osteogenicity of the constructs, the *in vivo* implantation of the hybrid constructs allows for the evaluation of their performance in the ultimately desired environment. Implantation of these hybrid constructs can take place at an ectopic site, such as in muscle or under the skin, or at an orthotopic site, including sites in the cranium or on the femur. Ectopic implantation occurs at a site where the tissue is not normally found and can be used to evaluate cytotoxic and inflammatory responses as well as the osteoinductivity of the construct.[113] Orthotopic implantation occurs at a site where the tissue is normally found and provides information regarding the integration of the construct with surrounding tissue along with how well it assists in the union of an otherwise non-healing bone defect.[114]

### 2.4.1 Ectopic Implantation

Analysis of a construct implanted at an ectopic site provides insight regarding the response of the body to the foreign object. Implants are typically excised, fixed, sectioned, and stained for the identification and quantification of inflammatory cells. Bone formation within the constructs has also been visualized using radiological imaging, by histology, and by immunohistochemistry for bone markers.[36,69,81] Hybrid constructs incorporating biological tissue ECM and constructs containing cell-generated ECM have been implanted ectopically and analyzed for bone formation and inflammatory response.[15,36,39,69,70,79,81]

#### ***2.4.1.1 Acellular Hybrid Constructs***

Biological tissue ECM hybrid constructs have tended to exhibit a high initial inflammatory response that drops at later timepoints.[15,39] ABM and PEG-PCL-PEG hybrid constructs were injected subcutaneously into the back of mice and excised at 1, 2 and 4 weeks.[39] The number of inflammatory cells was high in both PEG-PCL-PEG scaffolds and ABM/PEG-PCL-PEG constructs at weeks 1 and 2, but by week 4, the number had dropped significantly. Similarly, composite UBS and PLGA constructs were placed into a subcutaneous pocket on the backs of mice for 7, 14, 28, and 56 days.[15] The implants showed an inflammatory response with mixed cell populations at day 7, but by days 28 and 56, the inflammatory response was much less, with only the presence of mononuclear cells detected. By the end of the implantation period, the PLGA portion of the construct was retained, although the UBS component was not identifiable.

#### ***2.4.1.2 Cellular Hybrid Constructs***

Meanwhile, constructs containing cell-generated ECM have been typically analyzed for bone formation.[69,70,79,81] Cell-generated ECM coated biphasic calcium phosphate constructs containing human BMSCs were implanted in subcutaneous pockets on the backs of mice for 6 weeks.[69,70] The constructs demonstrated *de novo* bone formation with areas of mineralized bone and osteoids as well as the presence of osteocytes, osteoblasts, blood vessels, bone marrow, and fat cells in close proximity to newly formed bone.

Another study investigated the implantation of composite tooth and bone constructs composed of porcine cell-generated ECM-coated PLGA onto the omentum of rats for 8 weeks.[81] The implants consisted mainly of alveolar bone-like tissue found near the tooth portion, precursor osteoid tissue, and compact bone found at a distance from the tooth portion. Collagen I, BSP, and osteocalcin were detected throughout the compact bone-like tissue, while only collagen I was found in the alveolar bone-like tissue, similar to that found in native porcine alveolar bone tissue.

The hybrid construct incorporating tricalcium phosphate, PLGA, and gelled collagen was investigated for bone formation in a subcutaneous implantation model.[36] The channels present in the construct were found to contain fibrous tissue, but the constructs were also surrounded and penetrated by new cortical bone.

### 2.4.2 Orthotopic Implantation

Analysis of a construct implanted at an orthotopic site allows for investigation of the integration of the implant material with the surrounding bone tissue and the ability of the construct to promote healing of the defect.[114] Similar to ectopic implantations, orthotopic implants are typically excised, fixed, sectioned, and analyzed for the presence of inflammatory cells and bone formation. The presence of inflammatory cells and bone formation within hybrid constructs has also been visualized by histology and immunohistochemistry.[38,57] Additionally,

bone formation within hybrid constructs has been determined by staining with fluorescent dyes and X-rays of the implant.[80,82,115] Cell-generated ECM constructs and constructs incorporating biological tissue ECM have been implanted orthotopically and analyzed for inflammatory response and bone formation in both small and large animals.[38,57,80,82,115,116]

#### ***2.4.2.1 Acellular Hybrid Constructs***

Tour et al. investigated the bone formation and inflammatory response of acellular cell-generated ECM constructs. HAp and rat calvarial osteoblast-generated ECM constructs were implanted in critical-sized calvarial defects in rats for 12 weeks.[57] The composite HAp and ECM constructs contained more new bone formation than HAp scaffolds alone, with the bone forming at the margins and in the central portion of the scaffold on the dural side. However, no construct had completely restored the defect. Each construct had similar staining patterns for BSP, osteopontin, and periostin, a cell-adhesion molecule for pre-osteoblasts.[117] BSP and osteopontin were found in HAp particles incorporated within the newly formed bone, whereas the periostin was found between the non-integrated particles. There was still a large active inflammatory response at 12 weeks, but the composite HAp and ECM constructs demonstrated larger amounts of macrophages present near the non-integrated HAp particles than in the HAp scaffold alone.

In another study, biological tissue ECM hybrid constructs were examined by Kurikalli et al. for their orthotopic bone formation and inflammatory response.[38] A hybrid construct composed of Pluronic F-127, DBM, and rat MSCs was implanted into a critical-sized cranial defect in rats for 1 month. At the study endpoint, the implants displayed a continuous layer of bone throughout the defect and integration with the defect edges. The shape of the newly formed bone also showed exact conformity with the missing bone fragment, suggesting that the implanted MSCs remodeled the scaffolding. There was no visible sign of inflammatory cells reported within the implant.

#### ***2.4.2.2 Cellular Hybrid Constructs***

Titanium constructs containing rat MSCs along with their ECM coating were implanted in a critical-sized cranial defect in rats for periods of 1 week and 1 month.[116] After excision of the1 week implants, a thin fibrous capsule was seen surrounding the implant and exhibited no macroscopic sign of bone formation. Mineralized matrix was observed at the implant edges and at the periosteal side. Additionally, fibrous tissue with capillary infiltration was seen to be present throughout the implant. In the 1 month implants, there were osteocytes embedded within a mineralized matrix that had osteoids, osteoblasts covering the surface, and bone marrow present within the titanium fiber mesh. Some of the implants were seen to have a connection of bone across the defect, but a large variability in the amount of bone formation was found in each implant.

Implantation in animals larger than rats was explored by Steigman et al. through the implantation of electrospun PLLA constructs containing rabbit amniotic MSCs and their ECM coating into sternal defects of rabbits.[80] X-ray images of the implant at 8 weeks showed that there was radio-opaque material covering the constructs with complete closure of the defect. The constructs demonstrated substantial engraftment and typical bone morphology, with very little inflammatory cells present. The implants demonstrated similar amounts of mineralization before implantation and after the 8 week implantation period, but there was an increase in ALP activity in the 8 week post-implantation constructs when compared to pre-implantation constructs.

Even larger animals than rabbits have received hybrid construct implants. Zhang et al. implanted composite tooth and bone constructs comprised of porcine cell-generated ECM coated PLGA into the mandible of pigs for 12 weeks or 20 weeks.[82] Radiographs and ultra high-resolution volume computed tomography (VCT) images of the excised implants were taken to determine the density of the regenerated tissue. Radiographs and VCT images demonstrated that the 20 week implants had denser bone than the 12 week implants. They also demonstrated that the scaffolds without the cell-generated ECM or cells did not exhibit any mineralization. Histology showed complete bony bridge formation on both the buccal and lingual sides of the implant after 12 weeks. Nevertheless, there was disorganized bone formation within the centers of the implants.

Immunohistochemistry demonstrated that the bony portion of the construct contained BSP and osteocalcin.

Similar to the *in vitro* studies, a varying biological response was observed for the hybrid constructs in both small and large animals. Nonetheless, the incorporation of MSCs within the hybrid constructs displayed greater bone defect closure than the hybrid constructs lacking cells. Accordingly, these studies warrant further investigation into the use of hybrid constructs as a cell transportation vehicle for enhanced repair of bone defects.

## 2.5 Conclusions

The human body presents a limited natural ability to fully repair large bony tissue defects. To improve current clinical treatments of non-healing bone defects, tissue engineers have been researching materials that can successfully integrate with the native bone and promote tissue repair. This review discussed current approaches that have included the incorporation of several components found in native bone matrix in conjunction with a biomaterial that might otherwise be non-osteogenic. Methods of combining these components into a hybrid construct include coating a scaffold with collagen and a form of calcium phosphate, combining acellular biological tissue with a polymer, and creating a cell-generated ECM coating on a scaffold. These hybrid constructs have demonstrated an increase in overall performance in cell viability and proliferation, *in vitro* differentiation, and *in vivo* bone formation over synthetic materials alone.

Yet, the studies on hybrid constructs suggest that additional investigation into the essential components of a construct and the potential inclusion of cells within a construct will be necessary to improve their biocompatibility, osteogenicity, and repair potential.

## 2.6 Acknowledgements

This work was supported by a grant from the National Institutes of Health (R01 AR057083). R.A.T. also acknowledges the Ruth L. Kirschstein National Research Service Award (F31 AR055874) from the National Institute of Arthritis and Musculoskeletal and Skin Diseases. The content is solely the responsibility of the authors and does not necessarily represent the official views of the National Institute of Arthritis and Musculoskeletal and Skin Diseases or the National Institutes of Health.

| Construct Type | Methods of Synthesis | References |
|---|---|---|
| Polymeric constructs incorporating collagen and calcium phosphate | **Sequential deposition of collagen/gelatin and hydroxyapatite onto scaffold**<br>1. Generate polymer scaffold<br>a) Electrospinning<br>b) 3D printing<br>c) Lyophilization<br>2. Coat scaffold with collagen or gelatin<br>3. Coat scaffold with hydroxyapatite | 13, 14, 22, 26, 27 |
| | **Simultaneous incorporation of collagen/gelatin and calcium phosphate within scaffold**<br>1. Combine polymer, collagen or gelatin, and calcium phosphate<br>2. Remove solvent | 29-33 |
| | **Incorporation of collagen/gelatin within scaffold followed by deposition of calcium phosphate**<br>1. Combine polymer with collagen or gelatin<br>2. Remove solvent<br>3. Coat scaffold with calcium phosphate | 34-36 |
| | **Incorporation of calcium phosphate within scaffold followed by deposition of collagen/gelatin**<br>1. Combine polymer with calcium phosphate<br>2. Remove solvent<br>3. Coat scaffold with collagen or gelatin | |
| Biological tissue ECM-based construct | 1. Decellularize biological tissue<br>a) Bone matrix<br>b) Urinary bladder submucosa<br>2. Pulverize the acellular tissue<br>3. Combine polymer and acellular tissue particles<br>4. Solidify | 15, 16, 37-39 |
| Cell-generated ECM-based construct | 1. Seed cells on porous scaffolds<br>a) Stem cells<br>b) Pre-osteoblastic cells<br>c) Osteoblasts<br>2. Culture cell-seeded scaffolds<br>a) Static culture<br>b) Flow culture<br>c) Electromagnetic stimulation culture<br>d) Dynamic strain culture | 17, 18, 51-57, 63-77, 79-82, 84, 88-94, 115, 116 |

**Table 2.1:** Methods of synthesis for the three different types of hybrid constructs discussed within this manuscript, including polymeric constructs incorporating collagen and calcium phosphate, biological tissue ECM-based constructs, and cell-generated ECM-based constructs.

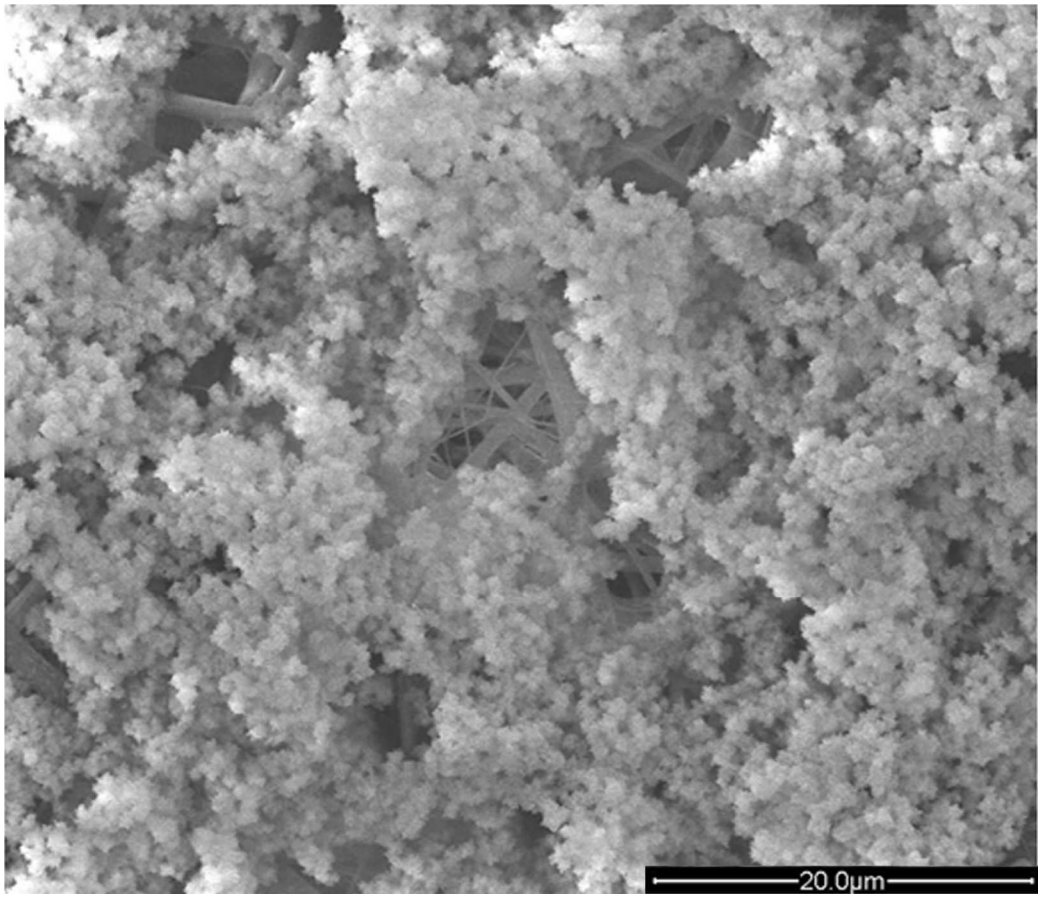


**Figure 2.1:** Scanning electron micrograph of a hybrid construct combining a synthetic material with collagen and nanohydroxyapatite. The construct was generated by initially electrospinning a PLLA/PBLG/collagen solution followed by 3 cycles of soaking in a calcium chloride solution then in sodium phosphate dibasic solution. The result was hydroxyapatite crystals covering collagen-like fibers. Reproduced with permission.[34] 2012, Elsevier.

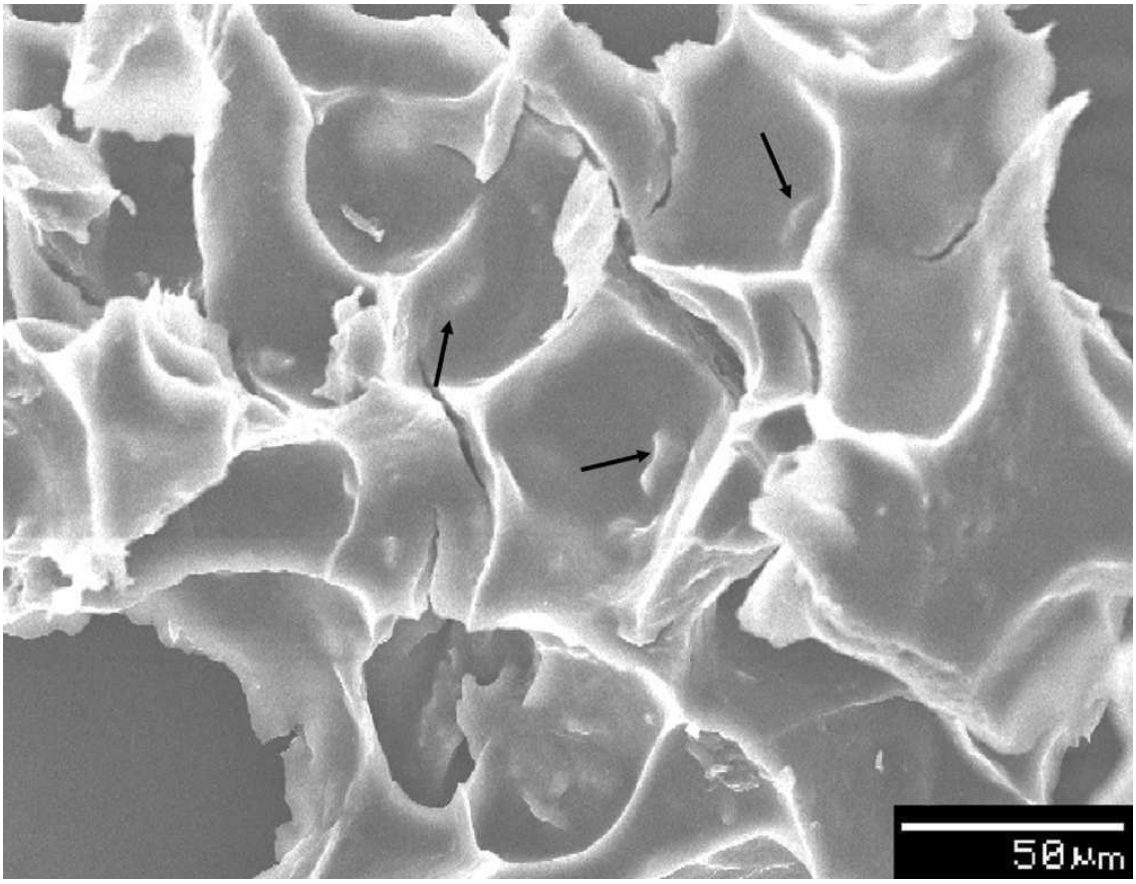


**Figure 2.2:** Scanning electron micrograph of a hybrid construct composed of biological tissue ECM and a polymer, which incorporates ABM with PEG-PCL-PEG at 20 wt%. The arrows indicate a few of the ABM particles present within the construct. Reproduced with permission.[39] 2011, John Wiley and Sons.

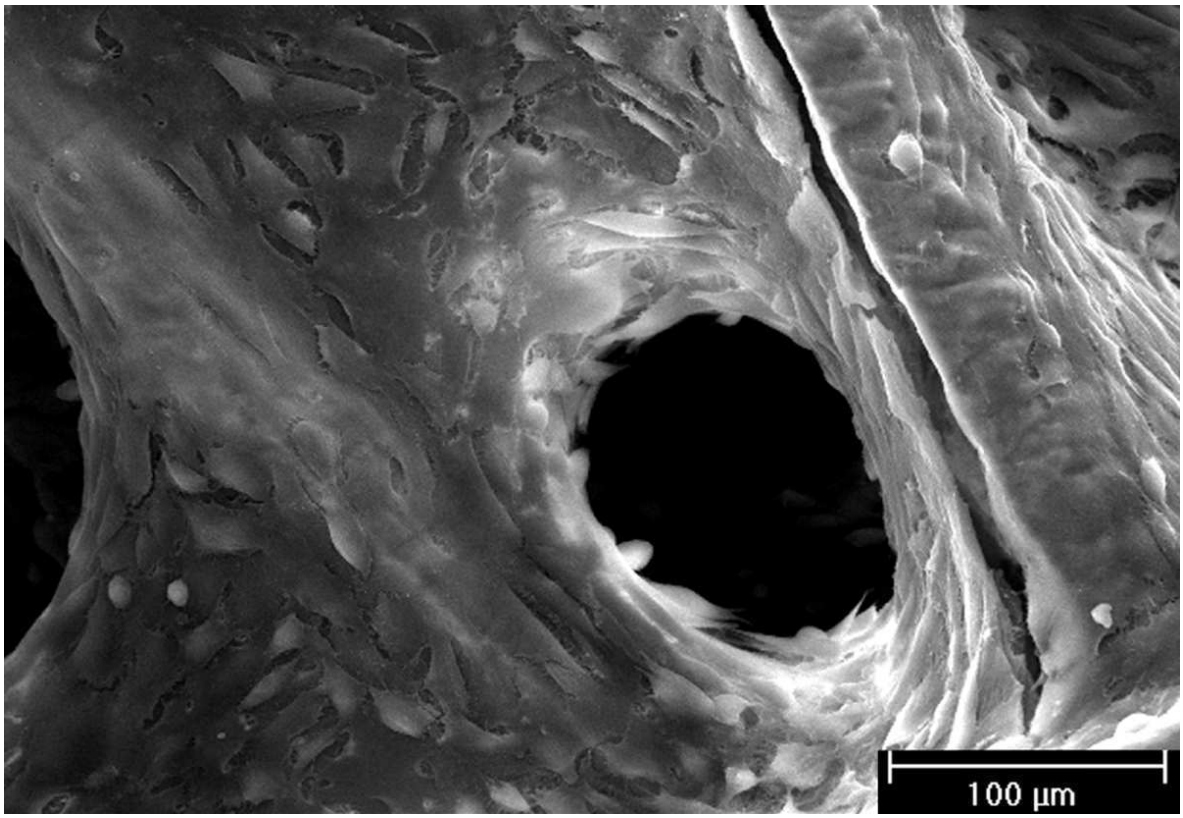


**Figure 2.3:** Scanning electron micrograph of a hybrid construct which has a cell-generated ECM coating on a fiber mesh scaffold. Rat MSCs were seeded onto titanium fiber mesh scaffolds and cultured in osteogenic media for 16 days to generate the ECM visibly coating the fibers and filling the space in between. Reproduced with permission.[68] 2005, John Wiley and Sons.

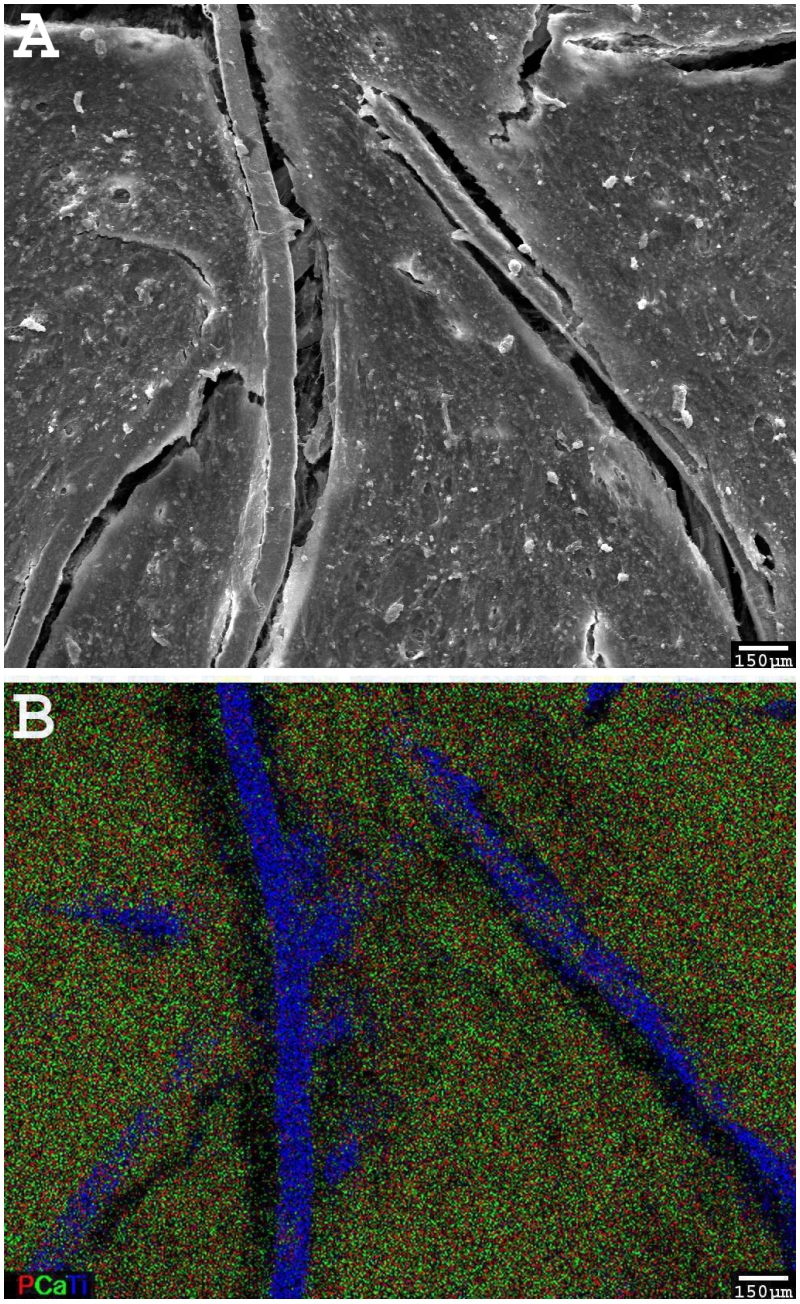


**Figure 2.4:** A SEM micrograph (A) of the surface of a cell-generated ECM-based construct and its corresponding EDX elemental mapping (B). The overlay of calcium (green), phosphorous (red), and titanium (blue) demonstrates that the calcium and phosphorous are co-localized on the titanium construct. Reproduced with permission.[73] 2009, John Wiley and Sons.

# CHAPTER 3

## Osteogenic Differentiation of Mesenchymal Stem Cells on Pre-Generated Extracellular Matrix Scaffolds in the Absence of Osteogenic Cell Culture Supplements


### Abstract

This study utilized a full factorial design to investigate the effect of four factors: presence of whole bone marrow cells, presence of in vitro-generated mineralized extracellular matrix, presence of dexamethasone, and variations in culture duration, on the proliferation and osteogenic differentiation of mesenchymal stem cells (MSCs) cultured on a polymer scaffold. Electrospun poly(ε-caprolactone) (PCL) fiber mesh scaffolds were seeded with rat MSCs and cultured in complete osteogenic medium for 12 days to generate constructs containing mineralized extracellular matrix (ECM). MSCs or MSCs and whole bone marrow cells were seeded onto decellularized extracellular matrix constructs (PCL/ECM) or plain PCL scaffolds, and cultured statically for 4, 8, and 16 days in medium either containing or lacking dexamethasone. After each culture period, the cell number was determined by DNA analysis, while the osteogenic differentiation state of the cells was determined by alkaline phosphatase activity assay and calcium assay. MSCs seeded onto PCL/ECM constructs and cultured in medium either containing or lacking dexamethasone demonstrated similar amounts of calcium deposition after 16 days. A significant increase in cell number over time compared to all other groups was observed when whole bone marrow cells were co-cultured with MSCs on PCL scaffolds in medium lacking dexamethasone.


---

* This manuscript was prepared as presented for submission to Tissue Engineering: Part A

This study establishes that the osteogenic differentiation of MSCs seeded onto ECM-containing constructs is maintained even in the absence of dexamethasone and that the co-culture of MSCs and whole bone marrow cells without dexamethasone and ECM enhances the proliferation of a cell population (or populations) present in the whole bone marrow.

## 3.1 Introduction

Replacement of diseased or compromised bone tissue is often accomplished clinically with autologous bone grafts due to its osteogenic, osteoconductive, and osteoinductive capabilties.[118-122] However, such drawbacks as donor site morbidity, persistent severe pain, and limited availability are commonly associated with autograft bone.[119,121,123,124] Alternatives to autologous bone grafts are being investigated, including polymers, collagen sponges, ceramics, and metals.[1,4,6,125] To investigate the osteogenicity of these potential bone graft materials, osteoprogenitor cells are cultured *in vitro* on scaffolds generated from the graft material and are analyzed for their effect on the osteogenic differentiation and proliferation of the seeded osteoprogenitor cells.[126-129] Research in our laboratory has previously demonstrated that a titanium mesh and extracellular matrix (ECM) composite scaffold was conducive to the osteogenic differentiation and proliferation of mesenchymal stem cells (MSCs), an osteoprogenitor cell population.[51,64]

In the bone marrow cavity, osteoprogenitor cells are in contact with other bone marrow cell populations, mineralized ECM, and biological factors.[130-133] The co-culture of MSCs with other bone marrow cell populations, including vascular endothelial cells, hematopoietic stem cells, hematopoietic progenitor cells, and osteoblasts, has been investigated for its effect on the osteogenic differentiation of the MSCs.[134-137] As well, culturing of MSCs on mineralized ECM and with a variety of growth factors including TGF-β1, FGF-2, and BMP-2 have been

explored for their effect on the proliferation and osteogenic differentiation of MSCs.[51,74,118,138-141] Furthermore, the supplementation of the culture medium with the corticosteroid dexamethasone has been investigated for its necessity in promoting the osteogenic differentiation of osteoprogenitor cells cultured *in vitro*.[68,142] However, the co-culture of other bone marrow cell populations with MSCs in a three-dimensional mineralized ECM and with dexamethasone medium supplementation has not been explored.

To address this issue, we utilized a full factorial study design by culturing MSCs in a three-dimensional poly(ε-caprolactone) scaffold in the presence of four factors i) whole bone marrow cells, ii) *in vitro*-generated mineralized ECM, iii) dexamethasone, and iv) variations in culture duration. The focus of this study was to elucidate the effects and potential interactions of the four factors on the proliferation and osteogenic differentiation of MSCs in a three-dimensional environment.

## 3.2 Methods and Materials

### 3.2.1 Fabrication of PCL Scaffolds

Poly(ε-caprolactone) (PCL) (MW= 80000, Sigma, St. Louis, MO) was dissolved in a 5:1 (vol/vol) chloroform:methanol solution at 12 wt% (wt/wt). The PCL solution was electrospun as previously described to fabricate fiber mesh mats that were approximately 1 mm thick, with approximately 5 µm average fiber diameters.[143] PCL scaffolds were prepared by die-punching 8 mm diameter discs from the

electrospun mats. The scaffolds were then sterilized by exposure to ethylene oxide (Andersen Sterilizers Inc., Haw River, NC) for 14 hours, followed by aseptic aeration in a laminar flow cell culture hood, pre-wetted one day prior to cell seeding using an ethanol gradient series, and stored in sterile-filtered (0.22 µm) Millipore water until use.

### 3.2.2 Mesenchymal Stem Cell Isolation

Mesenchymal stem cells were harvested and pooled from the marrow of tibiae and femora of 5 male Fischer 344 rats (126 – 150g; Charles River Laboratories, Wilmington, MA) as previously described.[68] Care of the rats in this study was in accordance with the Rice University Institutional Animal Care and Use Committee. Briefly, rats were anesthetized using 4% isofluorane (Baxter Healthcare Corporation, Deerfield, IL) in $O_2$ and subsequently euthanized by $CO_2$ asphyxiation followed by a bilateral thoracotomy to ensure death. The tibiae and femora were aseptically removed and placed in Dulbecco's Modified Eagle's Medium (Invitrogen, Carlsbad, CA) with 10% Fetal Bovine Serum (FBS) (Cambrex BioScience, Walkersville, MD) and 3% penicillin-streptomycin-fungizone (Invitrogen). The epiphyses were cut, the diaphyses were pierced with a sterile 16 gauge needle, and the marrow was flushed out with 5 mL of complete osteogenic medium containing α-MEM (Invitrogen), 10% FBS (Cambrex BioScience), 10 mM β-glycerol-2-phosphate, 10 nM dexamethasone, 50 µg/mL ascorbic acid, 50 µg/mL gentamicin, 100 µg/mL ampicillin, and 0.5 µg/mL fungizone (Sigma). The collected marrow pellets were broken up by trituration,

and the cell suspension was plated in 75 $cm^2$ tissue culture flasks and cultured at 37$^oC$ in a humidified atmosphere of 95% air and 5% $CO_2$ until confluency. The medium was aspirated after 1 day to remove the non-adherent cell population and was replaced with complete osteogenic medium. Subsequent medium exchanges were performed every 2 days. In this study, we designate the adherent cell population as "mesenchymal stem cells," given the established osteogenic potential of these cells under proper culture conditions.[144] When the cells reached confluency, they were lifted using 2 mL of 0.25% (vol/vol) trypsin solution (Sigma), centrifuged at 1000 rpm for 10 minutes, and resuspended in complete osteogenic medium at a concentration of 1.25 million cells/mL.

### 3.2.3 Generation of PCL/ECM Scaffolds

Prior to cell seeding, pre-wetted PCL scaffolds were transferred into complete osteogenic medium for 2 hours, press-fit into polymethylmethacrylate (PMMA) cassettes, and maintained in the incubator. A quarter million of the isolated MSCs in 200 µL of complete osteogenic medium were seeded onto each PCL scaffold, and the MSCs were allowed to adhere to the scaffold for 2 hours in the incubator. The scaffolds were then removed from their cassettes and placed in individual wells of a 12-well tissue culture polystyrene plate with 3 mL of complete osteogenic medium per well, which was exchanged every 2 days. At day 12, the scaffolds were collected and individually placed into 1.5 mL of sterile-filtered Millipore water. The MSCs that produced the *in vitro*-generated ECM in the PCL scaffolds were then removed by a previously described decellularization

process, which involved 3 cycles of freezing in liquid $N_2$ and thawing in a 37$^{o}$C water bath, followed by 10 minutes of ultrasonication.[51,64] The resulting acellular PCL/ECM scaffolds were then aseptically dried in a laminar air flow cell culture hood and sterilized by exposure to ethylene oxide (14 hours) for later use.

### 3.2.4 Four Factor Experimental Design

The groups investigated in this study can be found in **Table 3.1**. For the acellular scaffold group, 6 acellular PCL/ECM scaffolds per culture duration were press-fit into PMMA cassettes, incubated with 200 µL of complete osteogenic medium (+media) for 2 hours, then removed to a fresh 12-well tissue culture polystyrene plate with 2 mL of +media per well. For the groups seeded with MSCs alone, 6 acellular PCL and 6 acellular PCL/ECM scaffolds per culture duration were press-fit into PMMA cassettes and seeded with 250,000 MSCs in 200 µL of either +media or complete osteogenic medium lacking dexamethasone (-media). The cells were allowed to adhere for 2 hours in the incubator, and the scaffolds were removed to 12-well tissue culture polystyrene plates with 2 mL of either +media or -media per well, accordingly. For the groups seeded with both MSCs and whole bone marrow, 6 acellular PCL and 6 acellular PCL/ECM scaffolds per culture duration were seeded with MSCs as stated above, but were left in the PMMA cassettes for 1 day in a 12-well tissue culture polystyrene plate with 2 mL of either +media or -media per well and were incubated in a humidified incubator, accordingly. The following day, whole bone marrow was isolated from rat tibiae and femora using +media or –media and triturated, then 250,000 cells from the

whole bone marrow suspension in 200 µL of +media or -media, accordingly, were seeded onto the MSC-seeded PCL and PCL/ECM scaffolds. The cells were allowed to attach for 2 hours, and the scaffolds were removed to fresh 12-well tissue culture polystyrene plates with 2 mL of either +media or -media per well, accordingly. The approximate number of MSCs, defined as the adherent cell population in whole bone marrow, present within the whole bone marrow suspension was determined by counting the number of cells attached to one tissue culture flask after 4 hours of incubation from a pool of 10,000,000 seeded whole bone marrow cells. After averaging the results from 6 flasks, approximately one MSC was observed to be attached for every 1000 plated whole bone marrow cells (data not shown), thus approximately 250 MSCs were present in the 250,000 marrow cells that were seeded onto the respective scaffolds.

### 3.2.5 Osteogenic Differentiation Assays

At the 4, 8 and 16 day culture durations, four scaffolds from each group were individually placed into 1.5 mL of sterile-filtered Millipore water, and frozen at -20$^{o}$C for later analysis. Each scaffold underwent 3 cycles of freezing and thawing followed by ultrasonication to lyse the cells and was assayed for cellularity, alkaline phosphatase (ALP) activity, and calcium content. The cellularity of the seeded scaffolds was determined with the PicoGreen assay kit (Molecular Probes, Eugene, OR). Briefly, 50 µL of cell lysate solution, 100 µL of Tris-EDTA (TE) buffer, and 150 µL of PicoGreen dye buffer were pipetted into an

opaque 96-well plate, with each sample performed in triplicate, and allowed to incubate at room temperature for 10 minutes in the dark. The excitation of the solution at 485 nm and fluorescence measurement at 528 nm was performed using a FL X800 microplate spectrophotometer (Bio-Tek Instruments, Winooski, VT). A conversion factor of 6.4 pg of DNA per cell was used to calculate cellularity and was based on DNA extracted from known numbers of MSCs (data not shown). The alkaline phosphatase activity was measured using 1.5 M alkaline buffer solution and phosphatase substrate capsules (Sigma), and compared to dilutions of a 10 mM p-nitrophenol standard solution (Sigma). Briefly, 80 µL of the cell lysate solution, 100 µL of the substrate solution and 20 µL of the buffer solution were added to a transparent 96-well plate, with each sample performed in triplicate, and allowed to incubate at 37$^{o}$C for 1 hour. The reaction was then stopped with 100 µL of 0.3 NaOH, and the absorbance was measured at 405 nm on a PowerWave X340 microplate spectrophotometer (Bio-Tek Instruments). After determining the cellularity and ALP activity, a volume of 1 N acetic acid equal to the volume remaining in each sample tube was added to each cell lysate solution and scaffold. The resulting 0.5 N acetic acid/cell lysate solution was placed on a shaker table for 1 day at 100 rpm to dissolve calcium present in the scaffold. The calcium content of the scaffolds was then determined by adding 20 µL of the acetic acid/cell lysate solution and 300 µL of calcium assay reagent containing Arsenazo III (Diagnostics Chemicals Limited, P.E.I. Canada) to a transparent 96-well plate, with each sample performed in

triplicate. The absorbance was then measured at 650 nm on a PowerWave X340 microplate spectrophotometer (Bio-Tek Instruments).

### 3.2.6 Scanning Electron Microscopy

One acellular PCL scaffold and one acellular PCL/ECM construct were fixed with 2.5% glutaraldehyde solution (Sigma) at room temperature for 2 hours and rinsed 3 times in PBS (Invitrogen). The scaffolds were then dehydrated in a gradient ethanol series, air dried in a laminar air flow cell culture hood, lyophilized, and sputter coated with gold prior to imaging. Each scaffold was imaged using a FEI Quanta 400 ESEM FEG (FEI Company, Hillsboro, OR) at 500 magnification in the center of each scaffold.

### 3.2.7 Statistical Analysis

Results are presented as means ± standard deviations. Statistical significance was determined using Tukey's Honestly Significant Differences test with a 95% confidence interval with JMP IN 5.1 software (SAS Institute Inc., Cary, NC), and global effects were determined using four-factor ANOVA with SAS system software (SAS Institute Inc.).

## 3.3 Results

### 3.3.1 Global Factor Effects

**Table 3.2** demonstrates the significance of each of the global factors. The seeding of whole bone marrow cells with MSCs onto the scaffolds was found to

have a significant effect ($p<0.05$) only in the case of the overall cellularity of the scaffolds. The presence of an ECM in the PCL scaffolds and the presence of dexamethasone each resulted in a significant effect ($p<0.05$) upon the ALP activity and the calcium deposition onto the scaffolds, although no significance was observed for cellularity in either case. The culture duration had a significant effect ($p<0.05$) upon the calcium deposition onto the scaffolds.

### 3.3.2 Cellularity of the Scaffolds

**Table 3.1** clarifies the abbreviations for the groups investigated in this study. As can be seen in **Figure 3.1**, there was a trend for the cellularity of the scaffolds to increase at day 8 and then to decrease by day 16 for four groups, PCL MSCs+, PCL/ECM MSCs+, PCL/ECM MSCs-, and PCL/ECM Co-culture-. In addition, there was a trend for the cellularity to decrease with time for the PCL Co-culture+ and PCL/ECM Co-culture+ groups. However, the PCL Co-culture- group demonstrated a significant increase ($p<0.05$) in cellularity at day 16 as compared to day 4, unlike any other group investigated.

### 3.3.3 Alkaline Phosphatase Activity

As illustrated in **Figure 3.2**, a significantly greater ($p<0.05$) ALP activity was observed at day 8 for scaffolds cultured in +media as compared to the corresponding groups cultured in -media. The PCL Co-culture+ and PCL/ECM Co-culture+ groups demonstrated a significantly greater ($p<0.05$) ALP activity than the corresponding groups seeded with MSCs alone at day 8. Additionally,

there was a trend for a peak in ALP activity at day 8 for all groups except for the acellular, PCL MSCs+, PCL MSCs-, and PCL/ECM Co-culture- groups.

### 3.3.4 Calcium Deposition

**Figure 3.3** illustrates that the amount of calcium deposited significantly increased ($p<0.05$) over time for all groups, excluding the PCL MSCs- and PCL Co-culture- groups. Both the PCL MSCs- and PCL Co-culture- groups demonstrated minimal calcium deposition. The calcium deposition at day 16 for the PCL/ECM Co-culture+ and PCL/ECM Co-culture- groups were similar to the corresponding groups seeded with MSCs alone. Interestingly, significantly increasing ($p<0.05$) calcium deposition was observed over time for the acellular group.

### 3.3.5 Scanning Electron Microscopy

**Figure 3.4** illustrates that the PCL/ECM constructs are coated with a surface layer of extracellular matrix after 12 days of culture with MSCs. Cracks in the surface layer of the dried ECM reveal uncoated electrospun PCL fibers underneath.

## 3.4 Discussion

The goal of this study was to determine the effect and interactions of four culture factors i) the presence of whole bone marrow cells, ii) the presence of *in vitro*-generated mineralized ECM, iii) the presence of dexamethasone, and iv) variations in culture duration on the proliferation and osteogenic differentiation of

MSCs cultured on an electrospun PCL scaffold. The MSCs used in this study have been characterized in a previous study and adherent marrow cell populations (MSCs) have been widely studied in bone tissue engineering.[70,145-147] Although cell markers were not utilized to directly measure osteogenic differentiation of the MSCs, two well-established and accepted biochemical markers, alkaline phosphatase activity and calcium deposition, were assessed.[148,149]

Each of the four factors had an effect on the cellularity, alkaline phosphatase activity, and calcium deposition of the MSC-seeded scaffolds. Co-culture of whole bone marrow cells with the MSCs resulted in a significant global effect on the cellularity of the scaffolds and is attributable to the increased total number of cells seeded onto these scaffolds. The other three factors were found to globally affect the alkaline phosphatase activity of the seeded cells and the calcium deposition onto the scaffolds, and are consistent with the results from our previous studies using sintered titanium mesh scaffolds.[51,64,67,68]

The results for the PCL MSCs+ and PCL/ECM MSCs+ groups are also similar to the results from our previous studies using sintered titanium mesh scaffolds.[51,64,67,68] Both groups demonstrated an increase in cellularity at day 8 with a decrease at day 16, a peak in ALP activity at day 8, a trend for greater ALP activity in +media as compared to -media, and a significant increase in calcium deposition over time. The presence of dexamethasone is well-known to

initiate differentiation of MSCs towards the osteogenic lineage.[68,150-153] An early stage marker of the osteogenic differentiation of MSCs is an increase in ALP activity, while later stages are marked by the deposition of calcium phosphate.[11] The peak in ALP activity observed at day 8 for the majority of groups investigated reflects that the MSCs have begun to differentiate along the osteogenic lineage, while the drop in ALP activity and increase in calcium deposition at day 16 indicate that the MSCs have reached late stages of osteogenic differentiation. Together, the data demonstrate that an *in vitro*-generated mineralized ECM, medium supplementation with dexamethasone, and longer culture durations encourage osteogenic differentiation of MSCs cultured on electrospun PCL fiber mesh scaffolds, a biodegradable and hydrophobic material, and this result is consistent with MSCs cultured on sintered titanium mesh scaffolds, a non-degradable and hydrophilic material.

An increase in cellularity over time was observed for the PCL Co-culture- group. This increase in scaffold cellularity can be partially explained by the greater total number of cells seeded than in groups with MSCs alone. However, the increased number of cells over time cannot be fully explained by the higher seeding density. The PCL Co-culture+ group demonstrated a decrease in the number of cells present, although there was a similar amount of cells present in the scaffold in either media condition at day 4. It is known that dexamethasone reduces the proliferation of MSCs, while increasing their osteogenic differentiation.[154] Thus, the lack of dexamethasone in the culture medium for the

PCL Co-culture- group may have allowed the MSCs to proliferate. Another explanation for the observed proliferation of the cells in this group was the low amount of calcium present in the scaffolds from this group at any time point. Low amounts of calcium in the scaffold indicates that the matrix has not mineralized, thus after cell lysis, the cellular DNA was not trapped within a mineralized matrix surrounding the cell and was likely released in its entirety into the solution. As a result, the complete cellular DNA could be detected during the DNA assay, potentially resulting in a higher cell number than the PCL Co-culture+ group. However, the PCL MSCs- group with its similarly low amount of mineralization did not demonstrate a significant increase in cellularity over time when compared to the PCL Co-culture- group. These results imply that the lack of dexamethasone in the culture medium allowed for a cell population (or populations) present in the whole bone marrow to proliferate. Indeed, in a paper by Dexter et al., *in vitro* culture of hematopoietic tissue was accomplished by culturing whole bone marrow cells on a layer of bone marrow-derived adherent cells in Fischer's medium containing only FBS and antibiotics.[155] As well, several studies have demonstrated that hematopoietic progenitor cells derived from bone marrow co-cultured with a marrow stromal cell line were able to differentiate into T Cells and B cells.[156-158]

Significantly greater ALP activity was observed at day 8 for the PCL Co-culture+ group versus the PCL MSCs+ group as well as for the PCL/ECM Co-culture+ group versus the PCL/ECM MSCs+ group. However, this result may be an

artifact of the decreasing number of cells over time for the co-culture groups, since only the differentiating MSCs are expected to produce ALP. When the ALP activity is normalized to µmoles/hour/scaffold, there is no significant difference in the ALP activity at day 8 between the PCL MSCs+ and PCL Co-culture+ groups or between the PCL/ECM MSCs+ and PCL/ECM Co-culture+ groups (data not shown). This implies that the whole bone marrow cells had no observable effect on the osteogenic differentiation of the MSCs seeded onto either type of scaffolds, as was suggested by the global effects. The lack of any observable effect of co-culture with whole bone marrow on the osteogenic differentiation of MSCs may be due to the supporting role that MSCs provide. It is known from *in vitro* experiments that MSCs produce an ECM that is supportive of hematopoeisis.[155-158] Thus, instead of whole bone marrow cells affecting the osteogenic differentiation of the MSCs, the MSCs may be promoting hematopoietic engraftment of any HSCs/HPCs present within the whole bone marrow cell population.

Significantly lower ALP activity was observed for the PCL Co-culture- and PCL/ECM Co-culture- groups as compared to the PCL Co-culture+ and PCL/ECM Co-culture+ groups. Due to the lack of the osteogenic supplement dexamethasone in the culture medium for the -groups, the MSCs present on the scaffold were not able to differentiate down the osteogenic lineage as ably as the +groups.

By day 16, there were no significant differences between the amount of calcium deposition on PCL/ECM constructs seeded with either MSCs alone or MSCs with whole bone marrow cells and cultured in either media. The similar calcium deposition levels suggest that the whole bone marrow cells had an insignificant effect on the late-stage differentiation of the MSCs, as was suggested by the global effects. In addition, the minimal calcium deposition observed for the PCL MSCs- and PCL Co-culture- groups was expected, as neither dexamethasone nor *in vitro*-generated ECM was present to induce the cells to differentiate down the osteogenic lineage.

Low cell numbers and a low ALP activity with no change over time was observed for the acellular group. This indicates that no living cells were present on the scaffold, but residual DNA and ALP was retained within the scaffold. Due to the lack of living cells present on the scaffold, the increase in calcium deposition over time for acellular PCL/ECM constructs was unanticipated. An increase in calcium deposition was not observed in a previous study with acellular titanium/ECM constructs.[51] In the current study, it is feasible that any remaining DNA, phospholipid cell fragments and ALP present on the scaffold could present nucleation sites for calcium deposition, resulting in the increase in calcium observed in this study. However, it is also plausible that a component of the extracellular matrix present in the construct induced calcium deposition. Additional studies with acellular PCL/ECM constructs washed thrice with PBS, ultrasonicated for 10 minutes, and subsequently cultured in +media

demonstrated a linear increase in calcium deposition over time, while plain PCL scaffolds treated similarly showed no calcium deposition (data not shown). The increasing calcium deposition on the acellular PCL/ECM constructs implies that the ECM construct itself is conducive to calcium deposition and may mineralize over time *in vivo* without cells. Nevertheless, the calcium deposition observed at day 16 on cell seeded PCL/ECM constructs was significantly higher as compared to acellular constructs. Thus, seeding MSCs onto the ECM constructs will be an integral part of future investigations of bone formation *in vivo*.

Significantly lower calcium deposition at all time points was observed for the PCL MSCs+ and PCL Co-culture+ groups when compared to the PCL/ECM MSCs+, PCL/ECM Co-culture+, PCL/ECM MSCs-, and PCL/ECM Co-culture- groups. This was a result of the PCL/ECM constructs being generated by osteogenically differentiated MSCs with 12 days of culture prior to decellularization. After 12 days, the deposited matrix on the construct had already started to mineralize, thus each PCL/ECM construct contained approximately 0.4 mg of $Ca^{2+}$ (data not shown) at the beginning of the second culture period, while the PCL scaffolds alone had none.

Calcium deposition at each of the culture durations was found to be similar when seeded PCL/ECM constructs were cultured in either +media or -media. However, previous results from our laboratory have shown that when MSCs were seeded onto titanium/ECM constructs in -media, there was little calcium

deposited onto the constructs.[51] Prior to seeding the MSCs onto the PCL/ECM constructs, isolation of the MSCs was performed by plating the whole bone marrow cells onto a tissue culture flask in +media and culturing the adherent cells until confluency, approximately 6 to 7 days, while the MSCs seeded onto the titanium/ECM constructs were isolated and expanded in -media for 6 days. This implies that expansion of MSCs in medium containing dexamethasone may be sufficient to direct the MSCs towards the osteogenic lineage. However, in order to maintain the osteogenic differentiation of the MSCs, either continued exposure to dexamethasone or an *in vitro*-generated ECM is necessary. This is supported by the significant increase in calcium deposition observed over time for the PCL MSCs+ and PCL/ECM MSCs- groups, while no significant difference in calcium deposition over time was observed for the PCL MSCs- group. The continued osteogenic differentiation of MSCs may be due to the retention of growth factors, secreted during the generation of the ECM scaffold, within the ECM present on the scaffold.

The osteogenic differentiation of the MSCs observed in the PCL/ECM MSCs- group has implications for future *in vivo* experiments. Continuous *in vivo* delivery of the corticosteroid dexamethasone, which is not naturally present in the body, is known to result in delayed wound healing, increased risk for infection, and diabetes mellitus, along with other side effects.[159,160] Thus, is it desirable to avoid the *in vivo* delivery of dexamethasone to cell-seeded scaffold implants. The results from this study imply that when an *in vitro*-generated ECM is present

in the scaffold, it may not be necessary to deliver an osteogenic medium supplement such as dexamethasone *in vivo* to maintain the MSCs differentiation down the osteogenic lineage.

The results of this study demonstrate that the presence of an extracellular matrix and dexamethasone are significant factors for the enhancement of the osteogenic differentiation of mesenchymal stem cells cultured *in vitro* in a three-dimensional environment. The characterization of the protein and mineral components present within the *in vitro*-generated ECM is important to understanding the proteins necessary to maintain the osteogenic differentiation of the MSCs and will be the subject of future studies. Additionally, for future studies, it would be interesting to investigate the gene expression of select groups to provide greater insight into the observations from the present study.

## 3.5 Conclusions

The goal of this study was to determine the effect of four factors on the osteogenic differentiation and proliferation of MSCs. Three factors, the presence of an *in vitro*-generated extracellular matrix contained within the electrospun PCL scaffolds, the presence of dexamethasone in the culture medium, and variations in the duration of culture were significant with regards to the osteogenic differentiation of MSCs. However, the co-culture of whole bone marrow cells with MSCs did not significantly influence the osteogenic differentiation of the MSCs under the conditions tested. This study establishes that the isolation and

expansion of MSCs in medium containing the osteogenic supplement dexamethasone initiates the osteogenic differentiation of the MSCs, and subsequent culture upon constructs containing an *in vitro*-generated ECM, even with the lack of dexamethasone in the culture medium, sustains the osteogenic differentiation of the cells. Additionally, this study suggests that the co-culture of MSCs and whole bone marrow cells without dexamethasone or *in vitro*-generated ECM enhanced the proliferation of either MSCs or another cell population (or populations) present within the whole bone marrow. The elucidation of the effects and interactions of the four factors illuminates the necessary conditions of maintaining the osteogenic differentiation and proliferation of MSCs within a three-dimensional environment.

## 3.6 Acknowledgements

This work was supported by a grant from the National Institutes of Health (R01 AR057083), a grant from the Bioengineering Research Partnership with the Baylor College of Medicine through the National Institute of Biomedical Imaging and Bioengineering (R01 EB005173), and a Ruth L. Kirschstein National Research Service Award (F31 AR055874) from the National Institute of Arthritis and Musculoskeletal and Skin Diseases. The content is solely the responsibility of the authors and does not necessarily represent the official views of the National Institute of Arthritis and Musculoskeletal and Skin Diseases or the National Institutes of Health.

| Group Names | Cells | Scaffolds | Media | Duration |
|---|---|---|---|---|
| Acellular | No Cells | PCL/ECM | With Dexamethasone (+media) | 4 days<br>8 days<br>16 days |
| PCL MSCs+ | 250,000 MSCs | PCL | With Dexamethasone (+media) | 4 days<br>8 days<br>16 days |
| PCL Co-culture+ | 250,000 MSCs<br>250,000 Marrow Cells | PCL | With Dexamethasone (+media) | 4 days<br>8 days<br>16 days |
| PCL/ECM MSCs+ | 250,000 MSCs | PCL/ECM | With Dexamethasone (+media) | 4 days<br>8 days<br>16 days |
| PCL/ECM Co-culture+ | 250,000 MSCs<br>250,000 Marrow Cells | PCL/ECM | With Dexamethasone (+media) | 4 days<br>8 days<br>16 days |
| PCL MSCs- | 250,000 MSCs | PCL | Lacks Dexamethasone (-media) | 4 days<br>8 days<br>16 days |
| PCL Co-culture- | 250,000 MSCs<br>250,000 Marrow Cells | PCL | Lacks Dexamethasone (-media) | 4 days<br>8 days<br>16 days |
| PCL/ECM MSCs- | 250,000 MSCs | PCL/ECM | Lacks Dexamethasone (-media) | 4 days<br>8 days<br>16 days |
| PCL/ECM Co-culture- | 250,000 MSCs<br>250,000 Marrow Cells | PCL/ECM | Lacks Dexamethasone (-media) | 4 days<br>8 days<br>16 days |

**Table 3.1:** Names of the groups investigated in this study. The acellular group was taken as the control. Each of the other groups represents one combination of the four factors: cells seeded, scaffold type, media composition, and duration.

| Factor Comparison | Cellularity | ALP/DNA | Calcium Deposition |
|---|---|---|---|
| No Cells vs. MSCs | p<0.05 | p<0.05 | p<0.05 |
| No Cells vs. Co-culture | p<0.05 | p<0.05 | p<0.05 |
| MSCs vs. Co-culture | p<0.05 | N.S. | N.S. |
| PCL vs. PCL/ECM | N.S. | p<0.05 | p<0.05 |
| +media vs. -media | N.S. | p<0.05 | p<0.05 |
| Day 4 vs. Day 8 | N.S. | p<0.05 | p<0.05 |
| Day 4 vs. Day 16 | N.S. | N.S. | p<0.05 |
| Day 8 vs. Day 16 | p<0.05 | p<0.05 | p<0.05 |

**Table 3.2:** Global effect of the four factors investigated in this study. Significance levels were determined by using four-factor ANOVA and Tukey's HSD with the SAS system software. Not significant is abbreviated as N.S.

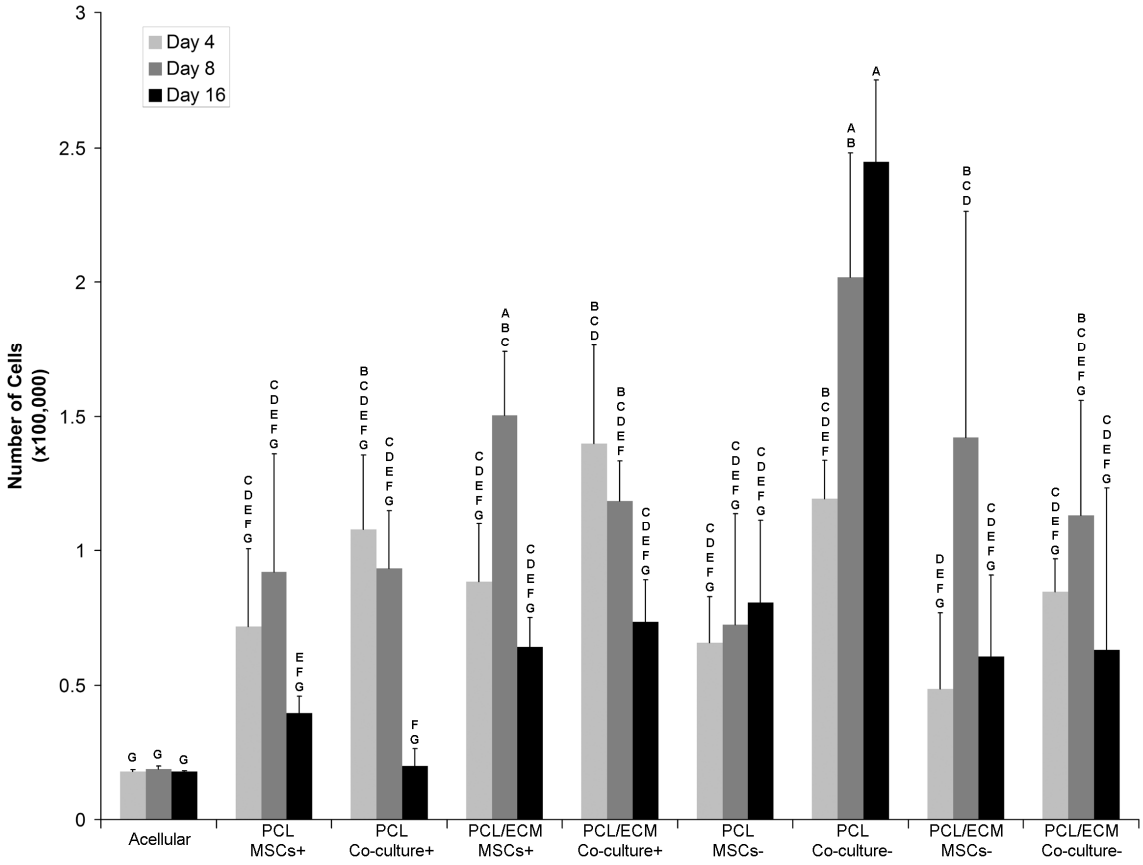


**Figure 3.1:** Cellularity of scaffolds seeded with MSCs or whole bone marrow cells and MSCs. Cell numbers were determined with a PicoGreen assay kit and are represented as mean ± standard deviation with n = 4. Groups not connected by the same letter are significantly different ($p<0.05$).

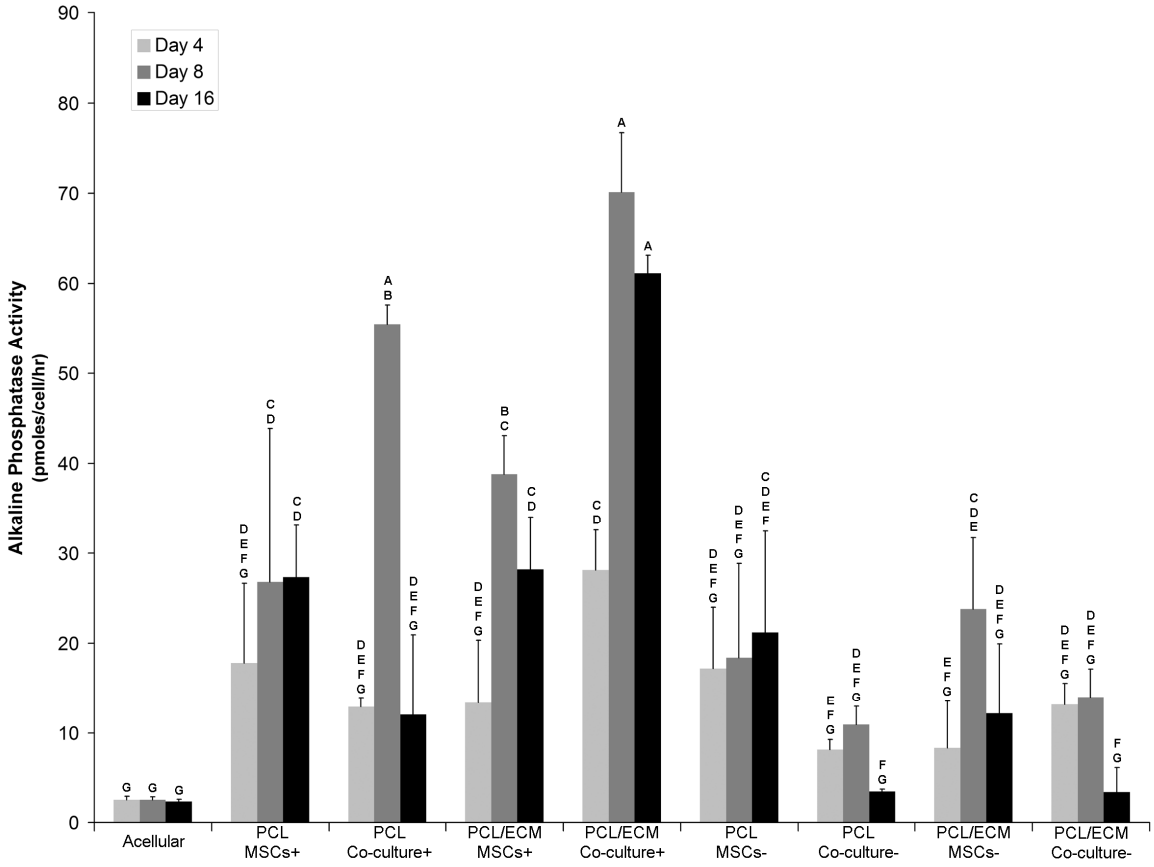


**Figure 3.2:** Alkaline phosphatase activity of scaffolds seeded with MSCs or whole bone marrow cells and MSCs. ALP activity was determined by absorbance spectroscopy and are represented as mean ± standard deviation with n = 4. Groups not connected by the same letter are significantly different ($p<0.05$).

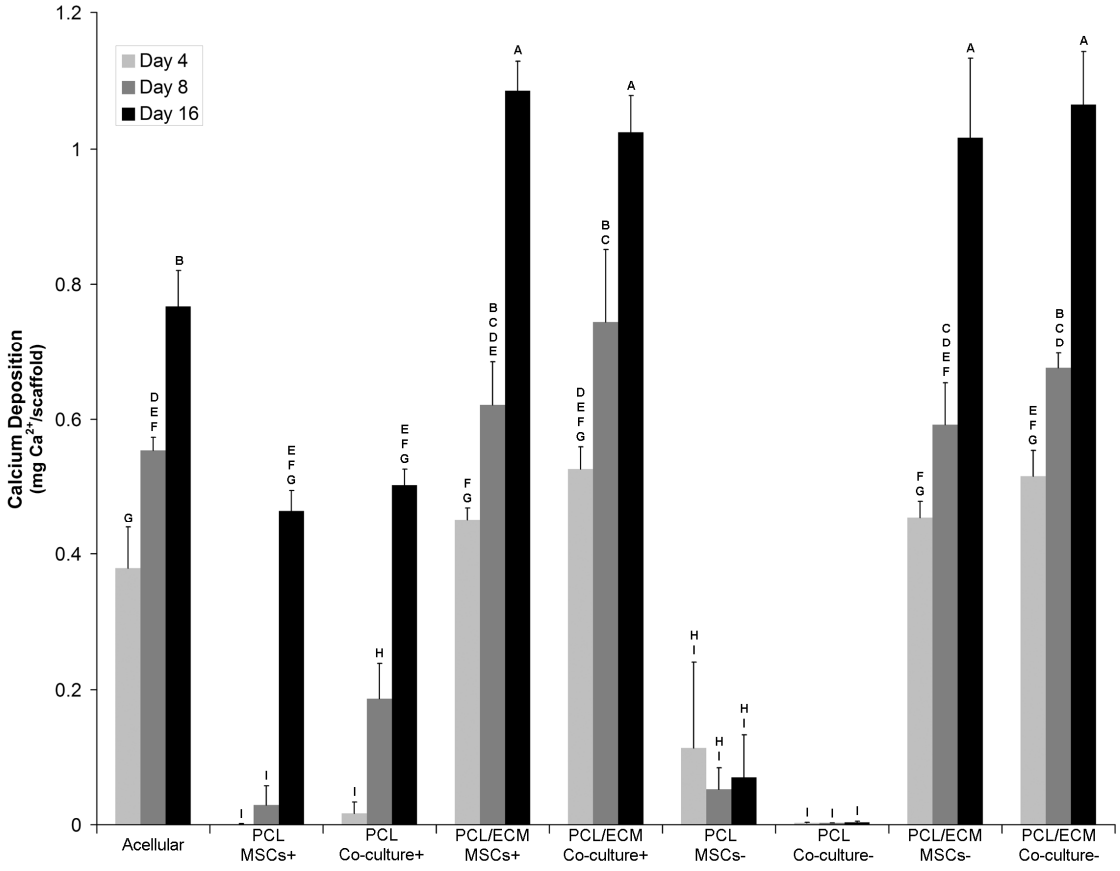


**Figure 3.3:** Calcium ion amount present on scaffolds seeded with MSCs or whole bone marrow cells and MSCs. Calcium amount was determined by absorbance spectroscopy and are represented as mean ± standard deviation with n = 4. Groups not connected by the same letter are significantly different ($p<0.05$).

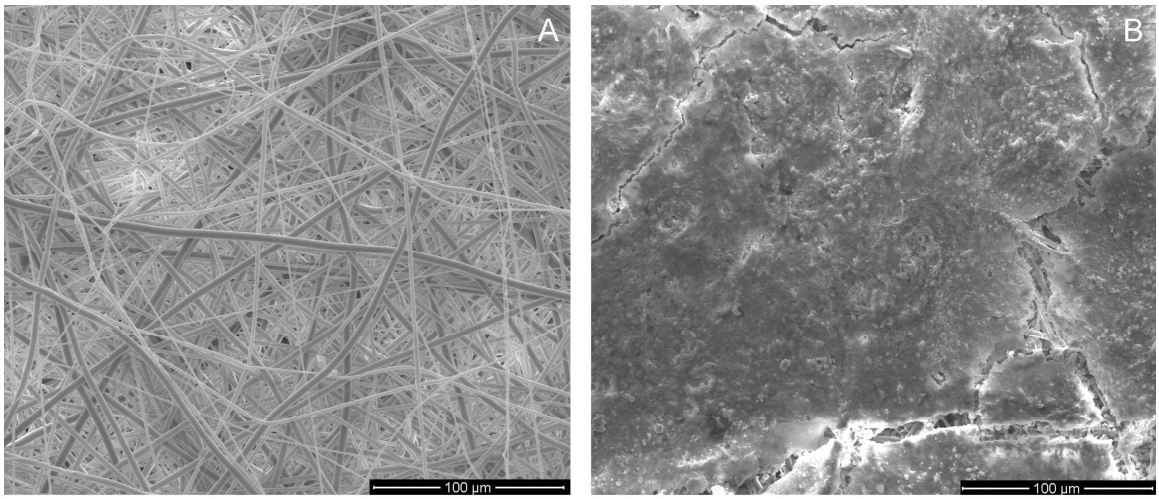


**Figure 3.4:** Scanning electron micrographs of A) PCL scaffolds and B) PCL/ECM constructs at a magnification of 500X. The scale bar represents 100 µm.

# CHAPTER 4

## Protein and Mineral Composition of Osteogenic Extracellular Matrix Constructs Generated with a Flow Perfusion Bioreactor


### Abstract

This study investigated the temporal composition of an osteogenic extracellular matrix construct generated by culturing mesenchymal stem cells in an electrospun biodegradable poly(ε-caprolactone) fiber mesh scaffold within a flow perfusion bioreactor. Constructs of different extracellular matrix maturities were analyzed for their protein and mineral composition at several culture durations by liquid chromatography-tandem mass spectroscopy, scanning electron microscopy, energy dispersive X-ray diffraction, X-ray diffraction, and calcium and phosphate assays. The analysis revealed that at short culture durations the cells deposited cellular adhesion proteins as a prerequisite protein network for further bone formation. At the later culture durations, the extracellular matrix was composed of collagen 1, hydroxyapatite, matrix remodeling proteins, and regulatory proteins. These results suggest that the later culture duration constructs would allow for improved bone regeneration due to the ability to mineralize and the capabilities for future remodeling.


---

* This manuscript was prepared as presented for submission to Biomacromolecules

## 4.1 Introduction

Bone defects can arise from a variety of sources, including trauma, resection of tumors, and congenital disorders. Autograft bone stands as the gold standard material for reconstruction of the missing bony tissue, due to its ability to integrate with the surrounding bone and to grow with the patient.[1,161] However, autograft bone is of limited availability and may present an associated donor site morbidity.[162,163] Bone tissue engineering seeks to develop alternative materials to overcome the limitations of bone grafts by providing a supporting environment and incorporating bioactive and biomimetic domains found in mature bone to induce bone formation and regeneration.

The organic phase of the extracellular matrix (ECM) of mature bone is composed largely of collagen 1, while the mineral component consists of hydroxyapatite.[11] Other proteins such as collagen 5, fibril-associated collagens, proteoglycans, glycoproteins, growth factors, and matrix metalloproteinases (MMPs) are present in minor quantities, but are also important components of the composition of bone.[11] Collagen 5 and the fibril-associated collagens help regulate the correct fibril diameter of collagen 1 in the tissue. The proteoglycans and glycoproteins bind to growth factors, nucleate hydroxyapatite deposition, and facilitate bone cell attachment. Select growth factors promote osteoblast infiltration and blood vessel ingrowth into the bone, while the MMPs allow for the remodeling of bone.

Many bone tissue engineering scaffolds have been designed incorporating domains that mimic the varied components, structures, and bioactive nature of mature bone. Examples include, prefabricated polymers also containing collagen with deposited apatite crystals, calcium phosphate cements with growth factor releasing microspheres, and gelatin hydrogels with adsorbed or absorbed growth factors.[164-168] In our laboratory, we have investigated an osteogenic tissue engineered construct, comprising an electrospun poly(ε-caprolactone) (PCL) scaffold and an ECM coating generated by osteogenically differentiated mesenchymal stem cells (MSCs) cultured for 12 days within a flow perfusion bioreactor (PCL/ECM constructs).[18,169] We have demonstrated that osteogenically pre-differentiated MSCs cultured on acellular PCL/ECM constructs retained their differentiation without the presence of osteogenic cell culture supplements.[18,169] Moreover, these acellular PCL/ECM constructs supported continued mineralization in culture medium.[18] These constructs were shown to contain the major bone components: collagens, glycosaminoglycans, and a calcium-bearing mineral.[64,74]

In this study, we hypothesize that the ECM deposited by MSCs within the constructs cultured under flow perfusion conditions replicates the proteins and minerals found in mature bone and that there is a temporal effect in the deposition of these components during *in vitro* culture. To test these hypotheses, we analyzed the protein and mineral compositions of *in vitro* MSC-generated ECM constructs at different culture durations after a decellularization and drying

procedure. Electrospun PCL scaffolds were seeded with osteogenically pre-differentiated MSCs and cultured within a flow perfusion bioreactor for 8, 12, and 16 days in osteogenic differentiation medium. Day 12 constructs were decellularized, dried, sterilized, reseeded with fresh pre-differentiated MSCs, and cultured in osteogenic medium within a flow perfusion bioreactor for an additional 4, 8, and 16 days. Each construct group was decellularized and air dried prior to imaging with scanning electron microscopy (SEM), protein analysis with liquid chromatography-tandem mass spectroscopy (LC-MS/MS), and mineral analysis with energy dispersive x-ray diffraction (EDX), x-ray diffraction (XRD), calcium assay, and phosphate assay.

## 4.2 Materials and Methods

### 4.2.1 Fabrication of PCL Scaffolds

PCL with an inherent viscosity of 0.68 dL/g, number average molecular weight of 61000 ± 2500 Da, and a weight average molecular weight of 88500 ± 2700 Da (DURECT Corporation, Pelham, AL) was dissolved in a 5:1 (vol/vol) chloroform:methanol solution at 22 wt% (wt/wt). The PCL solution was electrospun as previously described to produce fiber mesh mats with a porosity of 84% and an average fiber diameter of approximately 5 μm, from which disc-shaped scaffolds 8 mm in diameter and approximately 1 mm thick were prepared using a biopsy punch.[143] The scaffolds were then sterilized by exposure to ethylene oxide (Andersen Sterilizers Inc., Haw River, NC) for 14 hours and pre-wetted using an ethanol gradient one hour prior to cell seeding.

### 4.2.2 MSC Isolation

MSCs were harvested and pooled from the marrow of tibiae and femora of 4 male Fischer 344 rats (150 – 175 g; Charles River Laboratories, Wilmington, MA) as previously described.[68] Care of the rats in this study was in accordance with a protocol approved by the Rice University Institutional Animal Care and Use Committee. The MSCs were cultured in complete osteogenic media (α-MEM (Invitrogen, Carlsbad, CA), 10% FBS (Gemini Bio-Products, West Sacramento, CA), 10 mM β-glycerol-2-phosphate, 10 nM dexamethasone, 50 µg/mL ascorbic acid, 50 µg/mL gentamicin, 100 µg/mL ampicillin, and 0.5 µg/mL fungizone (all from Sigma-Aldrich, St. Louis, MO)) for 7 days to pre-differentiate them along the osteogenic pathway.[68] Rat femora from select MSC isolations were cleaned of soft tissues and retained frozen in Millipore-filtered water for later mineral content analysis.

### 4.2.3 MSC Culture on PCL Scaffolds

Prior to cell seeding, seventy-eight pre-wetted PCL scaffolds were transferred into complete osteogenic medium for 2 hours, press-fit into cassettes, and maintained briefly in an incubator. A quarter-million of the isolated MSCs in 200 µL of complete osteogenic medium were seeded onto each PCL scaffold, and the MSCs were allowed to adhere to the scaffold overnight in the incubator. Subsequently, the scaffold-containing cassettes were placed into a flow perfusion bioreactor at a flow rate of 1 mL/min with 200 mL of complete osteogenic medium per bioreactor, which was exchanged every 2 days.[61] Twelve

constructs each were removed from the bioreactors at day 8 (PCL day 8) and day 16 (PCL day 16), while a total of fifty-four constructs were removed at day 12 (PCL day 12). The MSCs that generated the osteogenic ECM in the PCL scaffolds *in vitro* were then removed by a decellularization process, which involved 3 cycles of freezing in liquid $N_2$ and thawing in a 37$^{o}$C water bath, followed by 10 min. of ultrasonication. Forty-two of the day 12 constructs previously generated were aseptically air dried and sterilized for 14 hours in ethylene oxide (PCL/ECM constructs). Six of the day 12 constructs (PCL/ECM 0) were retained for LC-MS/MS analysis as a control for the remaining PCL/ECM constructs.

### 4.2.4 MSC Culture on PCL/ECM Constructs

Prior to seeding with fresh MSCs, acellular PCL/ECM constructs were transferred to complete osteogenic media for 2 hours, press-fit into cassettes, and maintained briefly in the incubator. MSCs were seeded and cultured on the constructs as described in the previous section. Twelve constructs each were removed from the bioreactors at day 4 (PCL/ECM day 4), day 8 (PCL/ECM day 8), and day 16 (PCL/ECM day 16), and the reseeded MSCs were removed by the decellularization procedure described in the previous section.

### 4.2.5 Protein Extraction

Six constructs from each group were combined and minced with microscissors, then placed in 1.5 mL of 7 M urea buffer (7 M urea, 2 mM sodium EDTA, 50 mM

tris(hydroxymethyl)amino-methane, 0.5% triton X-100, 1% protease inhibitor cocktail, 2 mM dithiothreitol, 1 mM phenylmethylsulfonyl fluoride (all from Sigma-Aldrich)) and rotated at 4$^{o}$C overnight. The solution was strained to remove PCL fragments, centrifuged at 2000 rpm for 10 min. to pellet the mineral components, and the supernatant containing the protein extract was aliquoted into two 750 µL samples and frozen at -20$^{o}$C.

### 4.2.6 LC-MS/MS Analysis

One of the frozen 750 µL supernatant samples from each group was defrosted and analyzed at the proteomics core facility at M.D. Anderson Cancer Center via LC-MS/MS according to their standard operating procedure. Briefly, the protein solutions were precipitated using an equal volume of 3.9 M ammonium sulfate and centrifuged at 13000 rpm for 30 min. at 4$^{o}$C. The pellet was resuspended in Rapidgest (Waters, Milford, Massachusetts) containing trypsin and 50 mM sodium bicarbonate, incubated overnight at 37$^{o}$C, and subsequently injected into a liquid chromatography column connected to a tandem mass spectrometer (LC-MS/MS). The resulting spectra, excluding the peaks from human keratin and bovine trypsin, were analyzed using the Mascot search engine.[97] Search parameters were limited to the Rattus taxonomy (66908 sequences) and with the trioxidation of cysteine and oxidation of methionines as a variable modification. Peptide mass tolerances were set to 2 Daltons, fragment mass tolerances were set to 1 Dalton, and two missed cleavages were accepted. Searches were performed using the non-redundant proteins at the National Center for

Biotechnology Information (NCBInr version 20100908 (11756863 sequences, 4014994744 residues)). Protein hits were scored using standard Mascot scoring and a Mascot score greater than 30 was regarded as significant ($p<0.05$). An exponentially modified Protein Abundance Index (emPAI) score for each protein hit was also determined by the software. The emPAI score is roughly correlated to protein concentration and can be used for relative quantitation.[98] Manual analysis of the protein hit list was used to identify the ECM proteins present within each group.

### 4.2.7 Calcium and Phosphate Assays

Three constructs from each group were rinsed twice with sterile Millipore-filtered water, and 1 mL of 1 N acetic acid was added to each construct. The constructs were minced with microscissors and placed on a shaker table at room temperature for 1 day at 75 rpm to dissolve any mineral salts present in the construct. Three femora were fragmented with a mortar and pestle and placed into 1 mL of 12 N hydrochloric acid overnight at room temperature. The calcium content of the constructs and bones were determined as previously described, with each sample measured in triplicate.[18] The phosphate content of the constructs and bones was measured in triplicate and was determined by following the protocol supplied by the manufacturer of the assay kit (R & D Systems, Minneapolis, MN).

### 4.2.8 SEM and EDX Analysis

Femora fragments and one construct from each group were fixed with 2.5% glutaraldehyde solution (Sigma-Aldrich) at room temperature for 45 min., dried using an ethanol gradient, frozen, and then lyophilized. The bone fragments and constructs were sputter coated with gold prior to imaging with an FEI Quanta 400 ESEM FEG (FEI Company, Hillsboro, OR) at 1000x magnification in the center of each sample. Additionally, each specimen was scanned at 1000x magnification at three different spots using an EDX (EDAX Inc., Mahwah, NJ) integrated with the SEM until the relative intensities of the peaks became stable, and the resulting peaks were identified using the EDAX Genesis software package (EDAX Inc.). Each element identified was quantified into an atomic percentage by the EDAX software, and the Ca:P ratio was determined by dividing the calcium percentage by the phosphorous percentage.

### 4.2.9 XRD Analysis

The mineral pellets for each group, isolated during the protein extraction step, were washed twice with Millipore-filtered water to remove soluble salts remaining in the pellet and subsequently air dried. Femora fragments were crushed into a fine powder using a ceramic mill. The powder from each group was placed on a zero background wafer (Rigaku, The Woodlands, TX) and analyzed using a D/Max XRD (Rigaku). The powders were scanned for a fixed time of 12 seconds per step from $10^{o}$ to $60^{o}$ using a 2 mm divergent slit, a step size of $0.10^{o}$, and a variable receiving slit. Spectrum identification was performed using Jade 9

software (MDI, Livermore, CA) and matched with crystals from the PDF 4 database provided with the Jade 9 software using a chemistry filter for compounds containing only calcium, phosphorous, oxygen, and carbon. The spectra were matched according to best figure of merit and a 2θ offset between -0.100 and 0.100, and any peaks not accounted for by the first identification procedure were matched with the same database. The percent crystallinity was determined by adding a linear background, manually identifying peaks, and fitting the peak profiles to the spectra until the residual stabilized. This procedure was repeated three times and the resulting crystallinities were averaged.

### 4.2.10 Statistical Analysis

Results are presented as means ± standard deviations. Statistical significance for the calcium and phosphate assay data was determined using Tukey's Honestly Significant Differences test with a 95% or a 99% confidence interval with JMP IN 5.1 software (SAS Institute Inc., Cary, NC).

## 4.3 Results

### 4.3.1 LC-MS/MS Analysis

No ECM proteins were detected by LC-MS/MS analysis for the PCL day 8 constructs **(Table 4.1)**. The PCL day 12 constructs were found to contain fibronectin, a cell binding protein that forms a fibrillar network extending between adjacent cells; fibulin-1, a protein that binds to fibronectin and regulates its fibril diameter; procollagen 6, a cell binding protein that interacts with fibronectin and

collagen 1 and is suggested to anchor the basement membrane to underlying connective tissue; periostin, a protein that plays a role in the formation of collagen cross-links, interacts with fibronectin, and directly binds to bone morphogenic protein-1 (BMP-1); collagen 1, the main structural protein of bone; and MMP-2, a gelatinase that may play a role in angiogenesis by remodeling the ECM.[11,170-174] The emPAI score for fibronectin was higher than for collagen 1, periostin, procollagen 6, and MMP-2 in the PCL day 12 constructs, and no score was reported for fibulin-1.

The PCL day 16 constructs were found to retain all proteins observed in the PCL day 12 constructs, with the exception of fibulin-1, based on LC-MS/MS analysis. Three additional proteins were found within the constructs, including: high-temperature requirement A serine peptidase 1 (HtrA1), a peptidase that degrades fibronectin and inhibits transforming growth factor-β (TGF-β)/BMP signaling; thrombospondin 2 (TSP-2), a protein that inhibits angiogenesis and binds to fibronectin; and pigment epithelium-derived factor (PEDF), another protein that inhibits angiogenesis, expressed during early bone development, and may counteract vascular endothelial growth factor A (VEGF-A).[175-177] The emPAI score was higher for fibronectin than for all other proteins detected in the PCL day 16 constructs, with the exception of TSP-2, which reported no score.

The PCL/ECM 0 constructs were found by LC-MS/MS to contain fibronectin, fibulin-1, HtrA1, collagen 1, procollagen 6, and thrombospondin 1 (TSP-1), a

protein that inhibits angiogenesis, activates the TGFβ family of proteins, and binds to glycosaminoglycans.[178] The emPAI score for HtrA1 was higher than for all other proteins detected in the PCL/ECM 0 constructs.

LC-MS/MS detected the presence of two ECM proteins in the PCL/ECM day 4 constructs: osteopontin, a calcium-binding glycoprotein that binds cells and preferentially accumulates at ECM discontinuities including healing bone surfaces and at cell-matrix interfaces, such as on activated bone surfaces; and secreted phosphoprotein 2, 24 kDa (SPP-24 or SPP-2), a protein that binds BMP-2 and hydroxyapatite, and regulates the bioavailability of BMP-2.[179,180] Within these constructs, osteopontin presented a higher emPAI score than SPP-24.

LC-MS/MS analysis of the PCL/ECM day 8 constructs detected periostin at a higher level than procollagen 6 (as reflected by the emPAI scores), while osteopontin and SPP-24 were no longer present. The PCL/ECM day 16 constructs contained procollagen 6, fibronectin, and PEDF along with fibulin-1 and alkaline phosphatase, an enzyme that hydrolyzes pyrophosphates and is an early marker of osteogenic differentiation.[181] The emPAI scores for procollagen 6 and fibulin-1 were higher than the scores for alkaline phosphatase, PEDF, and fibronectin.

### 4.3.2 Calcium and Phosphate Assays

The number of moles of calcium ions and phosphate ions present in the constructs was found to increase with increasing culture durations **(Figure 4.1)**. The PCL day 8 and PCL day 12 constructs demonstrated a significantly lower ($p<0.05$) amount of calcium ions present as compared to PCL/ECM day 16 constructs. The PCL day 8 constructs also exhibited a significantly lower ($p<0.05$) amount of calcium ions as compared to the PCL/ECM day 8 constructs. In addition, the PCL day 8 constructs were observed to have a significantly lower ($p<0.05$) amount of phosphate ions as compared to PCL/ECM day 16 constructs. The ratio of calcium to phosphorous (Ca:P) as determined by the calcium and phosphate assays for each group is illustrated in **Table 4.2**. The Ca:P ratio for PCL day 12 constructs was significantly lower ($p<0.01$) than that of mature bone, when using the calcium and phosphate assay results. Additionally, the Ca:P ratio for the PCL day 16, PCL/ECM day 4, PCL/ECM day 8, and PCL/ECM day 16 constructs were significantly lower ($p<0.05$) than that of mature bone, when using the calcium and phosphate assay results.

### 4.3.3 Scanning Electron Microscopy

Nodules were found by SEM to be present on the constructs, and the abundance of nodules was found qualitatively to increase with increasing culture durations **(Figure 4.2)**. PCL day 8 constructs demonstrated sparse nodules with a matrix coating on the electrospun PCL, whereas PCL day 16 constructs showed large amounts of nodules present on top of the matrix coating. PCL/ECM day 8 and

PCL/ECM day 16 constructs demonstrated a full coating of nodules on the surface.

### 4.3.4 Electron Dispersive X-ray Spectroscopy

The EDX spectrum in **Figure 4.3** illustrates that the PCL day 16 constructs had carbon, oxygen, phosphorous, calcium and gold atoms present. The gold atoms were an artifact related to the gold coating necessary for SEM imaging. The ratio of calcium to phosphorous (Ca:P), as calculated from the atomic percentage data obtained from the EDAX software in the EDX analysis, of the entire scanned region seen in the SEM micrographs in **Figure 4.2** is presented in **Table 4.2**.

### 4.3.5 X-Ray Diffraction Analysis

The XRD spectra of the various groups are illustrated in **Figure 4.4**. As the ECM matured for each of the PCL and PCL/ECM based constructs, there was an increase in intensity of the peaks at 2θ angles of $26^o$, $28^o$, $32^o$, $40^o$, and $50^o$ and a slight decrease of the peak at $21^o$. The analysis demonstrated that all constructs had a major phase composed of hydroxyapatite (HAp) and a minor phase composed of tricalcium phosphate (TCP), except for the PCL day 8 constructs **(Table 4.3)**. Each construct demonstrated crystallinities over 80%, with the exception of the PCL day 8 construct. The figures of merit for all groups were large, which indicated a poor fit of the spectra of the mineral content of the constructs to the database values for pure HAp and TCP. However, the 2θ offset, which represents how much the software had to shift the peaks to match

the HAp and TCP spectra within the database, was nil for some constructs, including PCL day 12 HAp, PCL/ECM day 4 HAp, PCL/ECM day 8 TCP, and mature bone HAp. The software was unable to match the minerals from the PCL day 8 constructs to any of the compounds in the database that contained the elements found by EDX analysis and was unable to determine the percent crystallinity.

## 4.4 Discussion

Prior analyses of constructs developed within our laboratory have demonstrated that the *in vitro*-generated ECM deposited by MSCs onto PCL and titanium constructs promoted osteogenic differentiation of MSCs *in vitro* and that the titanium-based constructs comprised collagens, glycosaminoglycans, and a calcium-based mineral.[18,64] The goal of this study was to determine whether the ECM deposited by MSCs within the constructs cultured under flow perfusion conditions replicates the proteins and minerals found in mature bone and if there is a temporal effect in the deposition of these components during *in vitro* culture.

For the PCL day 8 constructs no secreted proteins were detected by LC-MS/MS. However, an extracellular matrix coating appeared to be present via SEM for these constructs. The lack of detected protein via LC-MS/MS may reflect that the amount of protein extracted from the constructs was below the threshold for detection.

For the PCL day 12 constructs, a high abundance of fibronectin was observed, which may facilitate cell adhesion to the PCL scaffold. Further, fibulin-1 was detected within the PCL day 12 constructs. Fibulin-1 is known to regulate the fibril diameter of fibronectin and may reflect that the fibronectin was in a fibrillar form.[174] However, an emPAI score for fibulin-1 was not generated, which suggests that the protein was a weak hit and may not be present within the constructs. The presence of secreted collagen 1 and periostin within the constructs suggests the production of a collagenous network by the cells, as periostin plays a role in cross-linking collagen.[172] Also, the presence of procollagen 6 in similar quantities to collagen 1 may reflect that it was deposited to assist in anchoring the collagen 1 network to the deposited fibronectin within the construct. MMP-2 was observed in similar quantities to collagen 1, which may suggest that the MSCs secreted the protease so that it would be able to degrade any malformed collagen that may have been deposited.

For the PCL day 16 constructs, high levels of fibronectin remained present within the constructs. A slight decrease in procollagen 6 as compared to the PCL day 12 constructs was also observed. However, there were similar amounts of collagen 1, MMP-2, and periostin in PCL day 12 and PCL day 16 constructs. The loss of fibulin-1 may be explained by the appearance of TSP-2, which binds to fibronectin as well. However, similar to fibulin-1, the emPAI score was not given for TSP-2 and thus it may not be present within the constructs. The decrease in fibronectin may suggest that HtrA1 degraded some of the deposited

fibronectin. A decrease in procollagen 6 may also be linked to the decrease in fibronectin, since it is a linker protein between collagen 1 and fibronectin. The appearance of PEDF and TSP-2 may suggest that the MSCs were beginning the mineralization process of the constructs. PEDF and TSP-2 are known to bind to collagen 1, found in developing bone matrix, and PEDF is secreted at high levels by osteoblasts, while TSP-2 is secreted by MSCs undergoing osteogenic differentiation.[176,182-184] In addition, TSP-2 and PEDF are anti-angiogenic factors, thus their presence may imply that the MSCs are regulating an angiogenic factor, such as VEGF-A or bFGF.

With respect to the PCL/ECM day 4 constructs, both osteopontin and SPP-24 were observed with high emPAI scores. SPP-24 is found at high levels in the bones of neonates and may be important in neonatal skeletal development and the acquisition of peak bone mass.[179] The presence of both osteopontin and SPP-24 may reflect that the reseeded MSCs recognized the PCL/ECM scaffold as a bony surface and were depositing proteins that encouraged cell adhesion to the surface.

For the PCL/ECM day 8 constructs, the disappearance of both osteopontin and SPP-24 may imply that the proteins have performed their function of recruiting more cells to the damaged bony surface and were not necessary for further development. With the deposition of procollagen 6 and periostin, it appears that

the MSCs were developing the pre-requisite matrix for further mineralization of the constructs.

Regarding the PCL/ECM day 16 constructs, the presence of procollagen 6, fibulin-1, and fibronectin suggests that the MSCs are further developing the extracellular matrix. The disappearance of periostin may be due to batch differences between the MSCs used for generation of the scaffold. The secretion of alkaline phosphatase indicates that the MSCs were undergoing osteogenic differentiation inducing further mineralization of the constructs. The deposition of PEDF also signifies that the MSCs had fully differentiated into osteoblasts.

Of interest is the fact that there were no similar proteins observed between the PCL/ECM day 4 and either the PCL day 12 or the PCL/ECM 0 constructs. This is surprising since the PCL/ECM day 4 constructs were derived from MSCs cultured for 4 days on sterilized, dried, and decellularized PCL day 12 constructs (i.e., PCL/ECM 0 constructs). However, the PCL day 12 constructs were not sterilized prior to analysis. Consequently, the PCL/ECM 0 constructs provide a baseline for comparison, as they were prepared in the same manner as the PCL day 12 constructs, with the exception that the PCL/ECM 0 constructs were sterilized via exposure to ethylene oxide prior to matrix analysis.

Similar proteins were found to be present in the PCL 12 and PCL/ECM 0 constructs, based on LC-MS/MS analysis, as expected. Specifically, fibronectin,

fibulin-1, collagen 1, and procollagen 6 were detected in both constructs. However, HtrA1 and thrombospondin 1 were measured in the PCL/ECM 0 construct, while MMP-2 and periostin were not detected. The difference may reflect slight variability between the batches of MSCs used to generate the constructs or limitations of the LC-MS/MS technique itself, but it does not appear to indicate a detrimental effect of the sterilization procedure on the matrix, as characterized by LC-MS/MS. Interestingly, the PCL/ECM 4 scaffolds did not retain any of the proteins detected in the PCL/ECM 0 scaffolds. The MSCs seeded onto the PCL/ECM 0 constructs may have degraded the proteins present, which by day 4 of culture (PCL/ECM day 4) could have been below the threshold level for detection.

The protein compositions of the constructs as measured by LC-MS/MS in the present study did not fully resemble the known composition of mature or developing bone. However, the constructs began to consist of several of the mature bone proteins as culture duration increased. Mature and developing bone is composed of collagen 1, fibronectin, glycosaminoglycan substituted proteoglycans such as decorin and biglycan, MMPs such as MMP-2 and MMP-9, and growth factors such as BMP-2, VEGF, and basic fibroblast growth factor (bFGF).[11] From our prior studies, collagen 1 and some glycosaminoglycans (GAGs) were expected.[64,169] However, no GAG substituted proteoglycans were detected in any of the constructs and this may be due to the amount of proteoglycans extracted being below the threshold of LC-MS/MS detection.

Alternatively, the lack of detected proteoglycans and GAGs may be due to the lack of deglycosylation and chondroitinase treatment of the protein extract.

The appearance of growth factors was expected within the constructs, nevertheless, only the anti-angiogenic growth factor PEDF was reported. The lack of expression of VEGF-A is not unexpected due to its high diffusivity and its lack in ability to bind to ECM molecules when it is present in its shortest splice form.[185] As well, bFGF has a short half-life *in vivo* and washes easily away if it is not bound to heparan sulfate.[186,187] Furthermore, the lack of VEGF-A or bFGF may be due to a low amount of it being secreted by the MSCs, thus it would not be detected by the LC-MS/MS technique. However, the lack of detection of TGFβ-1 and BMP-2 was unexpected. Both TGFβ-1 and BMP-2 encourage bone formation and may be expected to be secreted by the MSCs, especially in the PCL/ECM based scaffolds since they resemble bone to a higher degree than the PCL scaffolds.[139] However, these growth factors, although absent in the present analyses, may appear at longer culture durations or the extracted amount may be below the detection level of the LC-MS/MS. Indeed, previous studies employing immunohistochemistry analysis of matrix produced by MSCs cultured under flow perfusion conditions on scaffolds comprising a blend of starch and PCL were found to contain several bone-related growth factors, including TGFβ-1, fibroblast growth fator-2, VEGF and BMP-2.[188] As none of these growth factors were detected by LC-MS/MS in the present study, the sensitivity of the

LC-MS/MS technique may not have been sufficient for full characterization of the protein component of ECM constructs of the dimensions explored in this study.

The mineral component of the constructs was demonstrated to contain $Ca^{2+}$ and $PO_4^{3-}$ ions, and the amount of these ions increased over time. The increase in $Ca^{2+}$ is similar to what has been previously observed in bioreactor studies using titanium and PCL fiber mesh scaffolds in our laboratory.[18,64,67] It can also be seen through the Ca:P ratio that the concentration of the $Ca^{2+}$ and $PO_4^{3-}$ ions were very similar to each other at each culture period, excluding the case of the PCL day 8 constructs. Comparing to the ratio found in mature bone, it can be seen that the ratio was almost double what is found in the constructs. The difference may be accounted for by the method of generating the constructs, which may leave DNA fragments and cell debris throughout the constructs. These cellular remnants are potential sources of $PO_4^{3-}$, and may skew the Ca:P ratio towards a lower value.

The EDX spectrum in **Figure 4.3** demonstrated that the constructs were composed of carbon, oxygen, phosphorous, and calcium. Comparing the EDX spectrum from PCL day 8 constructs to PCL day 16 constructs (data not shown), there was a noticeably lower intensity for the calcium and phosphorous peaks in the PCL day 8 constructs. Combined with a lower visible number of nodules in the SEM micrograph of the PCL day 8 construct, this implies that the nodules are the main source of the calcium and phosphorous peaks seen in the EDX spectra

of all the constructs. However, in the absence of a more detailed analysis, the nodules cannot be irreproachably shown to be the mineral deposits found within the constructs.

**Table 4.2** shows the calculated Ca:P ratio from the EDS spectra and demonstrates that the Ca:P ratio of all the constructs, excluding the PCL day 8 and PCL/ECM day 8 constructs, was similar to mature bone. From the ratios, it can be seen that the minerals are not pure HAp, which has a ratio of 1.67. However, the HAp present in bone has many substitutes including $Na^{+}$, $Mg^{2+}$, $HPO_4^{2-}$, $CO_3^{2-}$, $OH^{-}$, $Cl^{-}$, and $F^{-}$, thus an observed ratio within the range of 1.41 to 1.99 would not be unexpected.[189] The observed Ca:P ratios in the constructs and bone also suggest that the minerals could be amorphous calcium phosphate (ACP), due to the varied stoichiometry of ACP, octacalcium phosphate (OCP), or a mixture of several mineral phases.[189,190] However, combining the Ca:P ratio with the analysis of the XRD spectra suggests that the minerals were a mixture of two phases, composed mainly of HAp with a minor phase of TCP present, with the exception of the PCL day 8 constructs.

Nevertheless, the analysis of the minerals may have been affected by the decellularization procedure and isolation of the mineral pellets from the constructs. The decellularization procedure requires multiple freeze and thaw steps in water and a drying step, while the isolation of the mineral pellets required a water wash step to remove any remnant protein extract solution and a

subsequent drying step. The water wash and drying steps may have dissolved amorphous mineral components or altered the crystallinity of the minerals. However, all samples for the various mineral analyses were treated in the same fashion, thus any changes that may have occurred would be consistent across samples.

The peak locations and breadths visible in the XRD spectra for PCL day 16 and PCL/ECM day 16 constructs and the Ca:P ratios derived from the EDX spectra of both of these constructs were similar to that of the mature bone. The spectra of both of these constructs developed broad and minor peaks at $28^{o}$, $40^{o}$, and $50^{o}$, similar to that seen in the spectrum of mature bone and, with the increase in intensity of the major peaks at $26^{o}$ and $32^{o}$ as the constructs increased in culture duration, suggests that the mineral composition is approaching that of mature bone. Encouragingly, the figure of merits of each mineral type in the construct started to approach 0, which indicates that the minerals were beginning to resemble pure hydroxyapatite and tricalcium phosphate. In addition, there was a trend of increasing crystallinity that approached that of mature bone as the culture duration increased.

It can also be observed that the spectrum of PCL day 16 constructs rather than that of PCL/ECM day 4 constructs had a greater resemblance to mature bone, although both constructs were cultured for the same length of time. This may be because the scaffolding for the PCL/ECM based constructs was based on the

PCL day 12 constructs. As can be seen, the spectrum of the PCL/ECM day 4 constructs appears to resemble that of the PCL day 12 constructs. The reseeding procedure covers the surface of the decellularized PCL day 12 constructs with MSCs, and osteopontin deposited by the MSCs may have prevented the maturation of the previously deposited minerals. However, the maturation of the minerals may have also been affected by the decellularization procedure or by the reseeding of the pre-differentiated MSCs. Only by day 16 of culture for the PCL/ECM constructs does the spectrum start to resemble that of mature bone.

However, the nodules on the surface of the constructs seen in **Figure 4.2** do not resemble the mineralized surface of mature bone. Mature bone is known to have a highly ordered surface composed of plate-like crystals of nano-crystalline HAp with many ion substitutes.[189,191-193] Even the longest culture period constructs, PCL day 16 and PCL/ECM day 16, which have some nodules that look needle-like, do not resemble mature bone (SEM micrograph not shown). Nevertheless, the surface of the constructs may change at a later point, due to the crystals growing larger and fusing together or through an organization of the ECM.

## 4.5 Conclusions

Overall, this study demonstrates that MSCs seeded upon PCL-based constructs and cultured under engineered conditions with a flow perfusion bioreactor deposit cell adhesive, structural, remodeling, and regulatory proteins as well as

hydroxyapatite minerals found in developing and mature bone. The protein composition of the constructs as they are cultured over time revealed that the MSCs deposited cellular adhesion proteins, such as fibronectin, at short culture durations, while they deposited matrix remodeling and regulatory proteins, such as MMP-2 and PEDF, at long culture durations. The constructs were seen to contain the major components of mature bone, collagen 1 and hydroxyapatite. The constructs also contain fibril-regulating proteins that help to organize collagen 1 and fibronectin, and matrix remodeling proteins, thus the ECM has started to resemble that of mature bone. However, only one anti-angiogenic growth factor and no glycosaminoglycan-substituted proteoglycans were identified. Further analysis will be needed to determine the effect that ECM maturity has on bone formation and regeneration *in vivo*.

## 4.6 Acknowledgements

This work was supported by a grant from the National Institutes of Health (R01 AR057083), a grant from the Bioengineering Research Partnership with the Baylor College of Medicine through the National Institute of Biomedical Imaging and Bioengineering (R01 EB005173), and a Ruth L. Kirschstein National Research Service Award (F31 AR055874) from the National Institute of Arthritis and Musculoskeletal and Skin Diseases. The content is solely the responsibility of the authors and does not necessarily represent the official views of the National Institute of Arthritis and Musculoskeletal and Skin Diseases or the National Institutes of Health.

| Construct | Accession.Version (NCBInr) | Protein | Mass (Da) | Mascot Score | No. of Unique Peptides | emPAI |
|---|---|---|---|---|---|---|
| PCL day 8 | N/A | None Detected | N/A | N/A | N/A | N/A |
| PCL day 12 | EDL75262.1 | Fibronectin 1, isoform CRA-d (**FN1**) | 262747 | 604 | 12 | 0.21 |
| PCL day 12 | EDM14936.1 | Periostin, osteoblast specific factor (predicted), isoform CRA_d (**Postn**) | 90251 | 199 | 4 | 0.09 |
| PCL day 12 | EDL92064.1 | Procollagen, type VI, α3 (predicted), isoform CRA_d (**Col6**) | 233804 | 166 | 4 | 0.05 |
| PCL day 12 | CAB01633.1 | Collagen α1, type I (**Col1**) | 137885 | 94 | 2 | 0.06 |
| PCL day 12 | CAA50583.1 | Type IV collagenase (**MMP-2**) | 74181 | 82 | 1 | 0.06 |
| PCL day 12 | NP_001121019.1 | Fibulin-1 (**FBLN1**) | 78071 | 68 | 2 | None |
| PCL day 16 | EDL75262.1 | Fibronectin 1, isoform CRA_d (**FN1**) | 262747 | 616 | 12 | 0.17 |
| PCL day 16 | EDL92061.1 | Procollagen, type VI, α3 (predicted), isoform CRA_b (**Col6**) | 311351 | 124 | 3 | 0.03 |
| PCL day 16 | CAB01633.1 | Collagen α1, type I (**Col1**) | 132885 | 105 | 2 | 0.06 |
| PCL day 16 | EDM14936.1 | Periostin, osteoblast specific factor (predicted), isoform CRA_d (**Postn**) | 90251 | 93 | 2 | 0.05 |
| PCL day 16 | CAA50583.1 | Type IV collagenase (**MMP-2**) | 74181 | 71 | 1 | 0.06 |
| PCL day 16 | NP_001162609.1 | Thrombospondin 2 precursor (**TSP-2**) | 129726 | 65 | 2 | None |
| PCL day 16 | NP_113909.1 | HtrA serine peptidase 1 (**HtrA1**) | 51330 | 63 | 1 | 0.08 |
| PCL day 16 | NP_808788.1 | Pigment epithelium-derived factor (**PEDF**) | 46465 | 51 | 1 | 0.09 |
| PCL/ECM 0 | PO4937.2 | Fibronectin 1 (**FN1**) | 272341 | 65 | 2 | 0.03 |
| PCL/ECM 0 | NP_001121019.1 | Fibulin-1 (**FBLN1**) | 78019 | 61 | 2 | 0.10 |
| PCL/ECM 0 | NP_113909.1 | HtrA serine peptidase 1 (**HtrA1**) | 51298 | 59 | 3 | 0.23 |
| PCL/ECM 0 | CAB01633.1 | Collagen α1, type I (**Col1**) | 137802 | 48 | 3 | 0.05 |
| PCL/ECM 0 | NP_001013080.1 | Thrombospondin 1 (**TSP-1**) | 129588 | 39 | 1 | 0.03 |
| PCL/ECM 0 | EDL97133.1 | Procollagen, type VI, α1 (predicted) | 75928 | 32 | 1 | 0.05 |
| PCL/ECM day 4 | AAA41762.1 | Osteopontin precursor (**OPN**) | 34929 | 270 | 5 | 0.78 |
| PCL/ECM day 4 | AAA87903.1 | Secreted phosphoprotein-24 precursor (**SPP-24/SPP-2**) | 20687 | 73 | 1 | 0.21 |
| PCL/ECM day 8 | EDL92061.1 | Procollagen, type VI, α3 (predicted), isoform CRA_b (**Col6**) | 311351 | 49 | 1 | 0.01 |
| PCL/ECM day 8 | EDM14934.1 | Periostin, osteoblast specific factor (predicted), isoform CRA_b (**Postn**) | 77695 | 43 | 1 | 0.05 |
| PCL/ECM day 16 | EDL92063.1 | Procollagen, type VI, α3 (predicted), isoform CRA_d (**Col6**) | 233804 | 808 | 12 | 0.23 |
| PCL/ECM day 16 | NP_001121019.1 | Fibulin-1 (**FBLN1**) | 78071 | 91 | 2 | 0.11 |
| PCL/ECM day 16 | EDL75260.1 | Fibronectin 1, isoform CRA-b (**FN1**) | 253107 | 78 | 2 | 0.03 |
| PCL/ECM day 16 | CAA68703.1 | Alkaline phosphatase (**ALP**) | 57810 | 56 | 2 | 0.07 |
| PCL/ECM day 16 | NP_808788.1 | Pigment epithelium-derived factor (**PEDF**) | 46465 | 51 | 1 | 0.09 |

**Table 4.1:** The proteins present within each type of construct as found by LC-MS/MS. The best match for each protein and the associated Mascot score are presented. The emPAI score gives a rough estimate of the quantity of the protein within the constructs.

| Construct | Ca & $PO_4$ Assay Ca:P ratio | EDX Ca:P ratio |
|---|---|---|
| PCL day 8 | 1.47 ± 0.52 | 1.12 ± 0.05 |
| PCL day 12 | 1.02 ± 0.29 | 1.45 ± 0.13 |
| PCL day 16 | 1.24 ± 0.09 | 1.51 ± 0.07 |
| PCL/ECM day 4 | 1.14 ± 0.21 | 1.36 ± 0.05 |
| PCL/ECM day 8 | 1.09 ± 0.14 | 1.62 ± 0.02 |
| PCL/ECM day 16 | 1.10 ± 0.15 | 1.53 ± 0.04 |
| Mature Bone | 1.99 ± 0.11 | 1.41 ± 0.02 |

**Table 4.2:** The ratio of calcium to phosphorous present on the constructs as determined by the calcium and phosphate assays and by EDX analysis. The Ca:P ratio is indicative of the type of calcium phosphate present, with pure hydroxyapatite having a Ca:P ratio of 1.67. Data are expressed as means ± standard deviation for n=3 for the Ca and $PO_4$ assay. EDX data are expressed as means ± standard deviation for three separate spots analyzed on a single sample.

| Construct | Crystallinity | Mineral | Figure of Merit | 2θ offset |
|---|---|---|---|---|
| PCL day 8 | N/A | N/A | N/A | N/A |
| PCL day 12 | 82.12 ± 6.58% | Hydroxyapatite (M) | 41.3 | 0.000 |
| | | Tricalcium Phosphate (m) | 25.1 | 0.060 |
| PCL day 16 | 89.10 ± 0.75% | Hydroxyapatite (M) | 11.7 | 0.080 |
| | | Tricalcium Phosphate (m) | 10.9 | 0.080 |
| PCL/ECM day 4 | 82.54 ± 3.64% | Hydroxyapatite (M) | 33.8 | 0.000 |
| | | Tricalcium Phosphate (m) | 23.3 | -0.060 |
| PCL/ECM day 8 | 80.05 ± 6.92% | Hydroxyapatite (M) | 24.3 | 0.100 |
| | | Tricalcium Phosphate (m) | 28.3 | 0.000 |
| PCL/ECM day 16 | 85.91 ± 10.11% | Hydroxyapatite (M) | 28.4 | 0.040 |
| | | Tricalcium Phosphate (m) | 29.5 | 0.080 |
| Mature Bone | 84.39 ± 1.23% | Hydroxyapatite (M) | 25.2 | 0.000 |
| | | Tricalcium Phosphate (m) | 18.4 | -0.020 |

**Table 4.3:** The crystallinity and figure of merit for the fit of each mineral type present as determined by XRD. The 2θ offset represents the shift (in degrees) required by the software to match the respective spectra to the HAp or TCP peaks within the PDF 4 database. The (M) represents a major phase and the (m) represents a minor phase. Data are expressed as means ± standard deviation for three manual fittings of the spectra obtained from a single sample comprising the combined mineral component of six constructs.

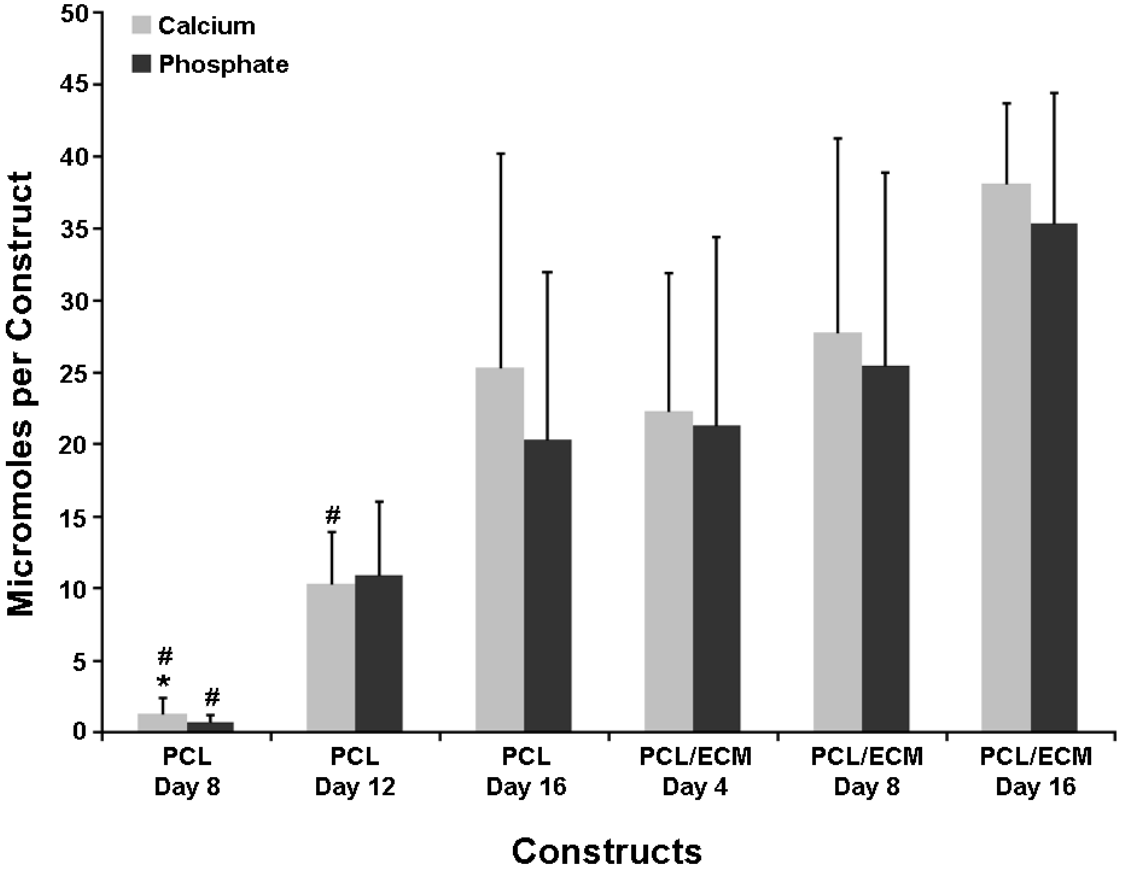


**Figure 4.1:** The amount of calcium and phosphate ions present in each scaffold at different stages of the ECM maturity. The * symbol represents a significant difference of $p<0.05$ to the PCL/ECM day 8 group and the # symbol represents a significant difference of $p<0.05$ to the PCL/ECM day 16 group. Data are expressed as means ± standard deviation for n=3.

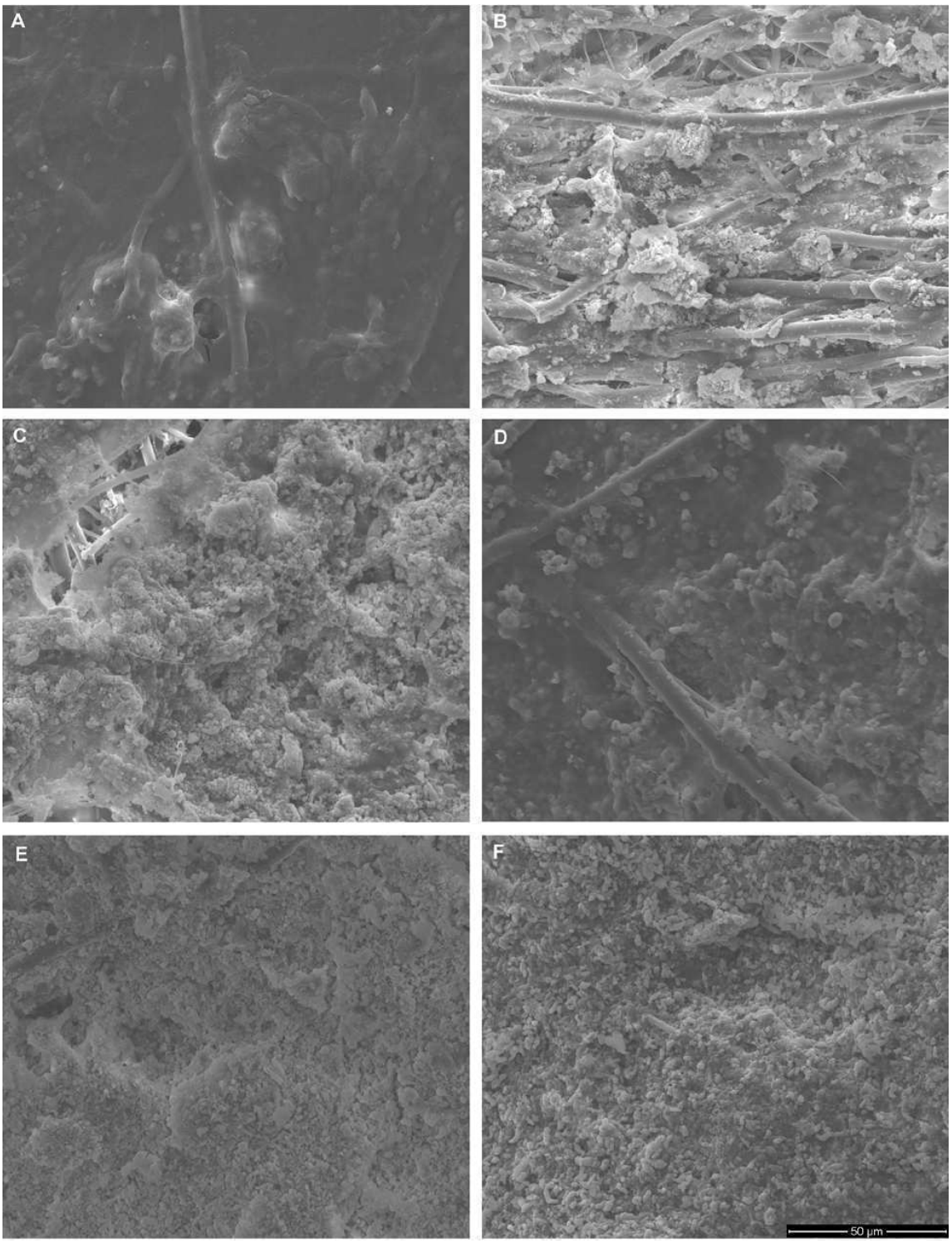


**Figure 4.2:** SEM micrographs of the top of the flow generated acellular constructs. A) PCL day 8, B) PCL day 12, C) PCL day 16, D) PCL/ECM day 4, E) PCL/ECM day 8, F) PCL/ECM day 16. As culture duration increases, there is an appearance and growth of mineral nodules on the surface.

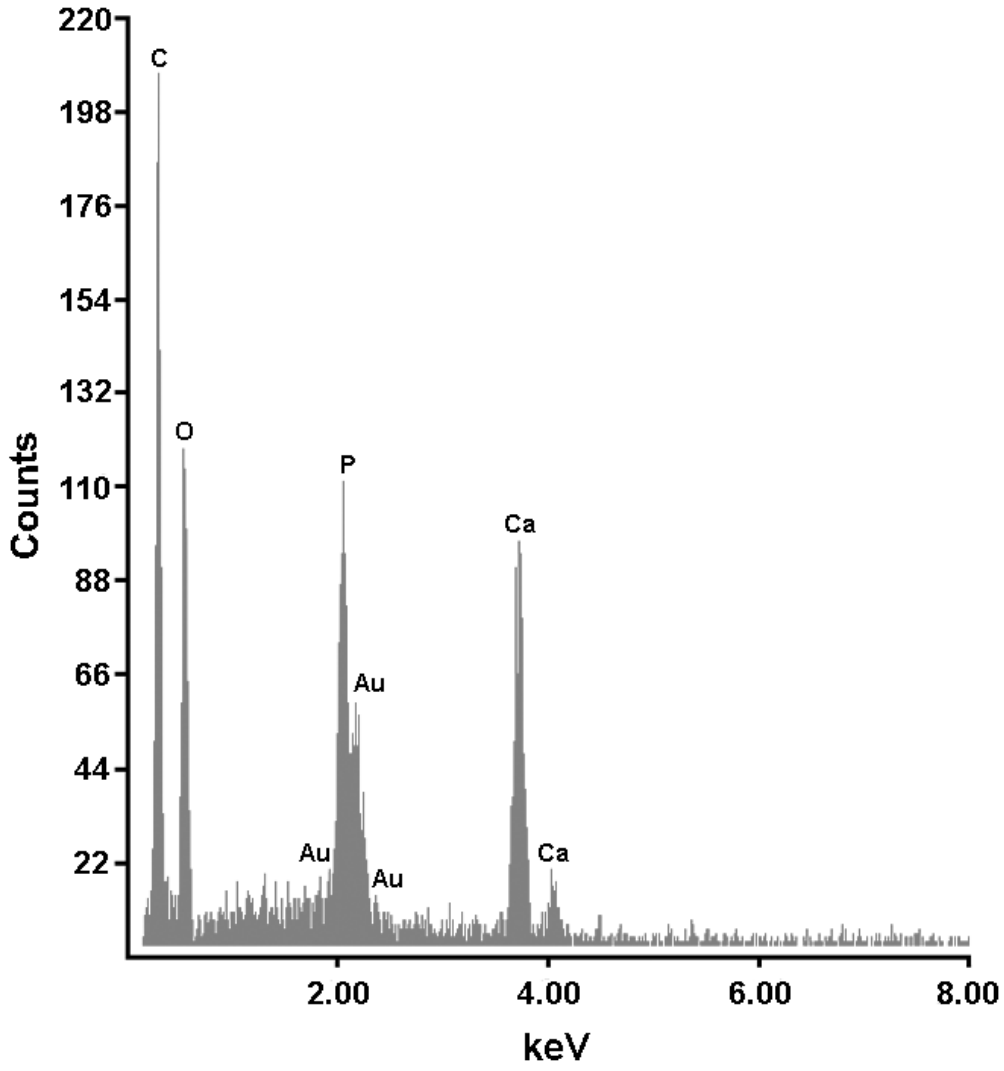


**Figure 4.3:** A representative EDX spectrum of the constructs. EDX analysis demonstrates the presence of carbon, oxygen, calcium, phosphorous, and gold on the surface of the constructs. The presence of gold is due to its use in coating the constructs for SEM imaging.

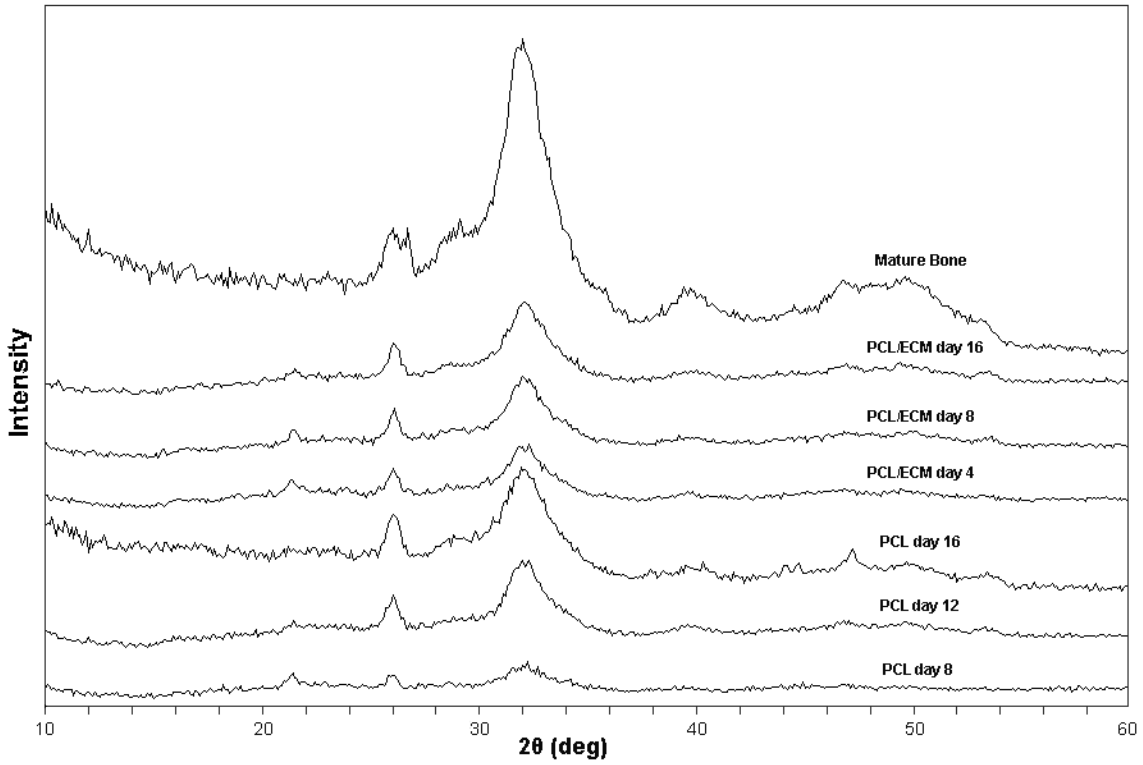


**Figure 4.4:** XRD spectra of the constructs. The PCL day 8 construct demonstrates minor broad peaks within the scan range. All other constructs demonstrate broad peaks at $26^{o}$ and $32^{o}$. Peaks at $28^{o}$, $40^{o}$, and $50^{o}$ can be seen in PCL day 16 and PCL/ECM day 16 constructs, similar to those seen in mature bone.

# CHAPTER 5

## Osteogenic Differentiation of Mesenchymal Stem Cells on Demineralized and Devitalized Poly(ε-caprolactone) and Extracellular Matrix Hybrid Constructs


### Abstract

Devitalization and demineralization processing of polymer and extracellular matrix (ECM) hybrid constructs was explored for the effect on the retention of ECM components and construct osteogenicity. Hybrid constructs were generated by seeding osteogenically pre-differentiated rat mesenchymal stem cells (MSCs) onto electrospun poly(ε-caprolactone) fiber mesh scaffolds and culturing in osteogenic medium for 12 or 16 days within a flow perfusion bioreactor to create an ECM coating. The constructs were either untreated, devitalized (using a freeze-thaw or a detergent technique), or devitalized and demineralized, and subsequently characterized for DNA, glycosaminoglycan (GAG), collagen, and calcium content. The osteogenicity of each construct was investigated by culturing MSCs on the hybrid constructs within a flow perfusion bioreactor for 4, 8 and 12 days in osteogenic medium. Cellular proliferation was determined by DNA assay, while osteogenic differentiation of MSCs was determined by the alkaline phosphatase activity and calcium assays. Distribution of the ECM throughout the processed and MSC-seeded constructs was visualized by scanning electron microscopy and histological staining. This study establishes that the freeze-thaw devitalization method disturbs the ECM coating


---

* This manuscript was prepared as presented for submission to Journal of Biomedical Materials Research Part A. The Supplementary Figures are included as well.

the least and provides beneficial void spaces in the surface ECM coating, allowing cells access to the interior of the construct.

## 5.1 Introduction

Craniofacial defects caused by trauma, disease, and congenital deformity can be clinically repaired using the current gold standard, autologous bone, if the defect is of limited size.[194] However, some patients have defects encompassing a large volume which cannot be adequately repaired using their own bone tissue. To address this issue, allogeneic bone and demineralized bone matrix (DBM) have been employed to provide the necessary amount of graft material to repair large defects.[195] However, these graft materials have had limited success at bone regeneration and integration with the surrounding bone at the defect site.[122,196,197] This limited success may be due to the devitalization and sterilization processes required to generate allogeneic bone and DBM. Both allogeneic bone and DBM, prior to being used as bone graft material, are rendered acellular and sterile although an additional morselization and demineralization step is required for DBM.[120] These processing steps have been shown to reduce the osteogenic and osteoinductive properties of the graft materials as compared to autologous bone.[194,197]

The goal of tissue engineering is to create an osteogenic and osteoinductive construct that regenerates bone for use in bone defect repair. Our laboratory has developed a cell-generated extracellular matrix (ECM) coated polymer construct as a potential bone regenerative material.[18,143] Previous investigation into these constructs has determined that they are comprised of collagen type I and hydroxyapatite, along with other important cell-adhesive and regulatory proteins

that are present within native bone.[76] In addition, pre-differentiated mesenchymal stem cells (MSCs) cultured on these constructs under static conditions and in medium lacking osteogenic supplements have displayed increased osteogenic differentiation when compared to MSCs cultured on only the polymer material.[18] However, prior to the seeding of the MSCs, the constructs underwent a devitalization and sterilization process.[18,76] Therefore, analogous to allogeneic bone grafts and DBM, these processed constructs may have a reduced osteogenic and osteoinductive potential as compared to untreated constructs.

The devitalization and demineralization techniques employed in this study have been adapted from the processing of bone grafts and tissues.[198,199] Indeed, other cell-generated ECM coated scaffolds have been devitalized using these techniques, but there is little investigation into the effects of various devitalization methods on the composition of the cell-generated ECM coatings.[51,57,200-203] Accordingly, this study investigates whether these modified bone graft processing techniques affect the retention of the ECM components and the osteogenic differentiation of MSCs cultured onto these constructs. Constructs were generated by seeding osteogenically pre-differentiated MSCs onto electrospun poly(ε-caprolactone) (PCL) and culturing them within a flow perfusion bioreactor for 12 days or 16 days in osteogenic medium. Subsequently, they were either i) sterilized, ii) sterilized and devitalized using a freeze-thaw method, iii) sterilized and devitalized using a detergent procedure, or iv) sterilized and

devitalized and demineralized using a freeze-thaw method combined with an acid treatment. Each construct was characterized by measuring the amount of DNA, glycosaminoglycans (GAGs), collagen, and calcium within each construct to determine the extent of loss of biological material due to processing. Scanning electron microscopy (SEM) and histological staining for GAGs, collagen, and calcium was also performed to determine the distribution of each component within the constructs. Furthermore, osteogenically pre-differentiated MSCs were seeded onto each cell-generated ECM polymer construct and cultured in osteogenic medium within a flow perfusion bioreactor for 4, 8, and 12 days. The cellularity and mineralization of the construct, along with the alkaline phosphatase (ALP) activity of the MSCs was determined to elucidate the effects of processing on the osteogenic differentiation of cultured MSCs within the constructs. Additionally, SEM and histological staining was performed to determine ECM distribution throughout the constructs seeded with MSCs.

## 5.2 Methods and Materials

### 5.2.1 Materials

PCL with an inherent viscosity of 0.68 dL/g was purchased from DURECT Corporation (Pelham, AL). The ethylene oxide was obtained from Andersen Sterilizers Inc. (Haw River, NC). The Fischer 344 rats were purchased from Charles River Laboratories (Wilmington, MA). The α-MEM was obtained from Invitrogen (Carlsbad, CA) while the fetal bovine serum was purchased from Gemini Bio-Products (West Sacramento, CA). The PicoGreen assay was

purchased from Molecular Probes (Eugene, OR). The Arsenazo III was purchased from Diagnostics Chemicals Limited (P.E.I., Canada). The rest of the chemical were purchased from Sigma-Aldrich (St. Louis, MO).

### 5.2.2 Fabrication of PCL Scaffolds

The PCL was characterized using gel permeation chromatography and polystyrene standards to determine that it had a number average molecular weight of 61000 ± 2500 Da and a weight average molecular weight of 88500 ± 2700 Da. The PCL was dissolved in a 5:1 (v/v) chloroform:methanol solution at 18% (w/w) prior to being electrospun as previously described to produce fiber mesh mats with a porosity of 87% and an average fiber diameter of approximately 10 μm.[143] Disc-shaped scaffolds 8 mm in diameter and approximately 1 mm thick were prepared from the PCL mats using a biopsy punch, then subsequently sterilized by exposure to ethylene oxide for 14 hours, and pre-wetted using an ethanol gradient prior to cell seeding.

### 5.2.3 MSC Isolation

MSCs were harvested and pooled from the marrow of tibiae and femora of 4 male Fischer 344 rats (150 – 175 g) as previously described.[68] NIH guidelines for the care and use of laboratory animals (NIH Publication #85-23 Rev. 1985) have been observed. The MSCs were cultured in complete osteogenic media (α-MEM, 10% fetal bovine serum, 10 mM β-glycerol-2-phosphate, 10 nM dexamethasone, 50 μg/mL ascorbic acid, 50 μg/mL gentamicin, 100 μg/mL

ampicillin, and 0.5 µg/mL fungizone) for 7 days to pre-differentiate them along the osteogenic pathway.[68]

### 5.2.4 MSC Culture on PCL Scaffolds

Prior to cell seeding, pre-wetted PCL scaffolds (n = 128) were transferred into complete osteogenic medium for 2 hours, press-fit into cassettes, and maintained briefly in an incubator. A quarter-million of the isolated MSCs in 200 µL of complete osteogenic medium were seeded onto each PCL scaffold, and the MSCs were allowed to adhere to the scaffold overnight in the incubator. Subsequently, the cassettes containing cell-seeded scaffolds were placed into flow perfusion bioreactors with a flow rate of 0.7 mL/min and 200 mL of complete osteogenic medium per bioreactor, which was exchanged every 3 days.[61] Sixty-four constructs each were removed from the bioreactors at day 12 (PCL/ECM 12) and day 16 (PCL/ECM 16).

### 5.2.5 Construct Processing

The PCL/ECM 12 and PCL/ECM 16 constructs were processed using four different methods (n = 16) and is described in **Table 5.1**. Constructs from each processed group (n = 3) was digested using Proteinase K to generate a sample solution and analyzed by the DNA, GAG, hydroxyproline, and calcium assays. One additional construct was fixed in 2.5% (v/v) glutaraldehyde for 45 minutes and cut in half for use in histological analysis and SEM.

### 5.2.6 Seeding of the ECM-Coated Constructs with MSCs

Constructs from each of the groups listed in **Table 5.1** (n = 12) were treated and seeded with MSCs in a similar manner as previously described in the MSC culture on PCL scaffolds section. Three constructs were removed from each group after 4, 8, and 12 days and placed in Millipore water. Each culture period underwent a repeated freeze-thaw procedure to generate a sample solution, which was later analyzed by the DNA, ALP, and calcium assays. To determine the calcium amount, a volume of 1 N acetic acid equal to the volume of solution present in each sample tube was added to each sample solution and construct. The resulting 0.5 N acetic acid/sample solution was placed on a shaker table for 1 day at 100 rpm to dissolve calcium present in the construct. One construct was removed for each group at each culture period, fixed in 2.5% (v/v) glutaraldehyde for 45 minutes, cut in half, and retained for histological analysis and SEM.

### 5.2.7 Proteinase K Digestion

Proteinase K solution was made by adding 100 mg Proteinase K into 100 mL of Pepstatin A buffer and placing the solution within a 56$^{o}$C water bath for 2 hours.[169] Constructs from each of the processed groups (n = 3) were individually placed into 1 mL of Proteinase K solution and placed into a 56$^{o}$C water bath for 16 hours. Afterwards, the constructs and solution underwent 3 cycles of freezing and thawing followed by 10 minutes of ultrasonication.

### 5.2.8 Biochemical Assays

The amount of DNA present within the constructs was determined with the PicoGreen assay kit which uses an excitation at 480 nm and the emission was measured at 520 nm as previously described.[169] The amount of GAGs within each construct was determined with the 1,9-dimethyl-methylene blue (DMMB) assay and measured at 520 nm as previously described.[169] The amount of collagen within each construct was determined with the hydroxyproline assay and measured at 570 nm as previously described.[169] The measured hydroxyproline amounts were converted to collagen amounts by using a hydroxyproline to collagen ratio of 1:10.[204] The calcium amount was determined by the Arsenazo III kit and measured at 650 nm as previously described.[18,205] The ALP activity was measured using phosphatase substrate capsules and measured at 405 nm as previously described.[18]

### 5.2.9 Scanning Electron Microscopy

After glutaraldehyde fixation, half of a construct was dehydrated in a gradient ethanol series, air dried in a laminar air flow cell culture hood, lyophilized, and sputter coated with 20 nm of gold prior to imaging. Each construct was imaged using a FEI Quanta 400 ESEM FEG (FEI Company) at a magnification of 250 in the center of each construct.

### 5.2.10 Histological Stains

Sectioning of the processed constructs prior to seeding was performed by placing half of a construct into Histoprep overnight, followed by embedding and freezing them into blocks at -20$^{o}$C. The blocks were sectioned into 5 μm sections that were placed onto 4X UV adhesive slides (Electron Microscope Sciences) kept at -20$^{o}$C and adhered to the slide via a brief exposure to 345 nm UV light prior to defrosting of the slide at room temperature. Safranin O, picrosirius red, and alizarin red stains were performed on each of these sectioned constructs.[206-208] For the sectioning of the MSC-seeded constructs, half of a construct was placed into Histoprep over night, embedded, and frozen into blocks at -20$^{o}$C. The blocks were sectioned into 5 μm sections that were adhered to super frost plus slides (VWR) and placed on a slide warmer set for 45$^{o}$C for 1 day. Hematoxylin and eosin staining was performed on each of these sections.[209]

### 5.2.11 Statistical Analysis

Results are presented as means ± standard deviations. Statistical significance between all constructs was determined using Tukey's Honestly Significant Differences test with 95% confidence interval using JMP 9 software (SAS Institute).

## 5.3 Results

### 5.3.1 Amount of DNA, GAGs, Collagen, and Calcium within ECM-Coated Constructs

As can be seen in **Figure 5.1**, the EO 12 and EO 16 constructs, contained significantly more ($p<0.05$) DNA as compared to their respective FT, Tri, and dM constructs. The processed constructs with the same ECM maturity contained similar amount of DNA to each other. The processed PCL/ECM 16 constructs contained significantly more ($p<0.05$) DNA than the processed PCL/ECM 12 constructs. **Figure 5.2** demonstrates that there was no significant difference in GAG amounts between EO 12 and EO 16 as compared to their respective FT, Tri, and dM constructs. However, there was a significant difference ($p<0.05$) between the amounts of GAGs present within the PCL/ECM 16 constructs as compared to their respective PCL/ECM 12 constructs. As illustrated in **Figure 5.3**, there was no significant difference in the amount of collagen contained within each construct between 12 and EO 16 as compared to their respective FT, Tri, and dM constructs. However, there was a significant difference ($p<0.05$) between the amounts of collagen contained within the PCL/ECM 16 constructs and their respective PCL/ECM 12 constructs with the exception of the FT 12 and FT 16 constructs. **Figure 5.4** reveals that there was no significant difference between the calcium amount within the processed constructs as compared to the sterilized constructs, EO 12 and EO 16. Nevertheless, there was a trend of lower amounts of calcium contained in the FT 12 and dM 12 constructs as compared to EO 12. This was also observed between the dM 16 and EO 16 constructs.

### 5.3.2 Distribution of ECM Components within the Processed Constructs

The SEM micrographs in **Figure 5.5** show the presence of an ECM coating in the EO 12, FT 12, and Tri 12 constructs with minimal amounts of ECM present on the dM 12 constructs. The ECM coating was seen to completely cover the top surface of the EO 16, FT 16, and Tri 16 constructs with a minimal presence of void spaces. In contrast, the dM 16 construct contained many void spaces in the surface ECM coating.

**Figure 5.6i** and **Figure 5.6ii** demonstrate that there was an approximately 100 micron thick layer of ECM composed of GAGs and collagen at the top of the EO 12 constructs. The GAG and collagen layers were approximately 40 microns thick in the FT 12 construct, but negligible amounts were present in the Tri 12 and dM 12 constructs. The EO 16 construct demonstrated an ECM coating throughout the entirety of the construct. The FT 16 constructs had a 70 micron layer of GAGs at the top of the construct with some GAGs present in pockets within the interior of the constructs. Both the Tri 16 and dM 16 constructs contained an approximately 20 micron thick layer of GAGs present at the top of the constructs. In addition, the Tri 16 and dM 16 constructs contained an approximately 80 micron thick layer of collagen present at the top of each construct. The FT 16 construct was also seen to have collagen present throughout the interior of the construct. **Figure 5.6iii** shows that the calcium was localized in the same area as the collagen component and follows the same trends as collagen.

### 5.3.3 Cellularity of the MSC Seeded Processed Constructs

**Figure 5.7** demonstrates that there was no significant difference in cell number in the EO 12, FT 12, and dM 12 constructs at day 12. However, there was a significant difference ($p < 0.05$) in cell number between Tri 12 and EO 12 constructs at day 12. The dM 12 constructs had a significantly lower ($p<0.05$) amount of cells present as compared to EO 12, FT 12, and Tri 12 at day 8. With the EO 16, FT 16, and Tri 16 constructs, there was no significant difference in cell number at any culture period. However, the dM 16 constructs had a significantly higher ($p<0.05$) cell number as compared to the EO 16, FT 16, and Tri 16 constructs at day 12. A significantly higher ($p<0.05$) number of cells was seen within EO 12, FT 12, and Tri 12 constructs when compared respectively to the EO 16, FT 16, and Tri 16 constructs at day 8. There was no significant difference in the cell number between dM 12 and dM 16 constructs at day 4, day 8, and day 12.

### 5.3.4 Alkaline Phosphatase Activity of MSCs Seeded on Processed Constructs

The alkaline phosphatase activity of the MSCs seeded onto the ECM coated constructs is illustrated in **Figure 5.8**. There was no significant difference between the EO 12, FT 12, Tri 12, and dM 12 constructs at day 4, day 8, and day 12. However, EO 16 constructs demonstrated a significantly higher ($p<0.05$) ALP activity as compared to the dM 16 constructs at day 8. Comparing between the EO 16, FT 16, and Tri 16 constructs, there was a significant difference

($p<0.05$) in ALP activity at day 12. The EO 16 constructs had a significantly higher ($p<0.05$) ALP activity when compared to EO 12 constructs at day 4 and day 12. Similarly, the FT 16 constructs had a significantly higher ($p<0.05$) ALP activity than FT 12 constructs at day 12.

### 5.3.5 Calcium Deposition of MSC Seeded Processed Constructs

**Figure 5.9** demonstrates that there was no significant difference in calcium deposition between the EO 12, FT 12, and Tri 12 constructs at any timepoint. However, the Tri 12 constructs had a significantly higher ($p<0.05$) amount of calcium as compared to dM 12 constructs at day 12. The EO 16 constructs had a significantly higher ($p<0.05$) amount of calcium when compared to either FT 16 or dM 16 constructs at day 8 and day 12. Nevertheless, there was no significant difference between the EO 12, FT 12, Tri 12, and dM 12 constructs when compared respectively to the EO 16, FT 16, Tri 16, and dM 16 constructs at any timepoint.

### 5.3.6 Extracellular Matrix Distribution within MSC Seeded Processed Constructs

The SEM micrographs seen in **Figure 5.10** demonstrate an ECM coating on each of the constructs, with only the Tri 12 construct lacking a full coating. In addition, the EO 16 construct was seen to have 2 layers of ECM present at the top surface of construct.

**Figure 5.11i** demonstrates that the EO 12 constructs had filled with ECM by day 12. Additionally, the EO 16 construct was seen to have 2 layers of ECM with the top layer approximately 25 microns thick and a bottom layer of ECM present throughout the construct by day 12. **Figure 5.11ii** shows that the FT 12 construct produced an approximately 80 micron thick layer of ECM at the top of the construct with ECM present in the interior by day 12. The FT 16 construct was seen to have ECM present throughout the construct and an approximately 160 micron thick layer of ECM present at both the top and bottom of the construct at day 4 which increased to approximately 300 microns thick at the top and approximately 230 microns thick at the bottom by day 12. **Figure 5.11iii** demonstrates that both the Tri 12 and Tri 16 constructs produced an approximately 100 micron thick layer of ECM at the top of each construct by day 8, but this disappeared to become an approximately 20 micron thick layer of ECM present at the top of the construct by day 12. **Figure 5.11iv** shows that the dM 12 constructs produced an approximately 120 micron thick layer of ECM at the top of the construct by day 8, which increased to approximately 200 microns thick by day 12. The dM 16 constructs demonstrated minor amounts of ECM present at both day 4 and day 8, however, by day 12 there is an approximately 80 micron thick layer of ECM present at the top of the construct.

## 5.4 Discussion

The goal of this study was to determine the effects of devitalization and demineralization processing of flow perfusion cell-generated ECM constructs on

the retention of ECM components and construct osteogenicity. Characterization of the constructs explored the amount and distribution of DNA, GAGs, collagen, and calcium, while MSC-seeding of the constructs investigated cellular proliferation using DNA amounts and osteogenic differentiation using the well-established markers of ALP activity and calcium mineralization.[148,149]

The characterization of the constructs demonstrated that all of the devitalization and demineralization techniques were successful in removing cells and calcium bearing minerals. The amount of DNA present in the EO 12 and EO 16 constructs was significantly higher than those in any of the processed constructs. Each processed construct contained similar amounts of DNA, suggesting that no devitalization technique was successful in removing all of the nuclear material. However, if complete removal of the nuclear material was desired, treatment of the constructs with DNases and RNases may potentially be a solution.[210,211] Undetectable levels of calcium were observed for both of the dM 12 and dM 16 constructs after demineralization demonstrating that the 2% EDTA treatment for 2 hours is sufficient to remove the calcium deposits. In addition to the successful devitalization and demineralization, no significant difference in the amounts of GAGs, collagen, and calcium was measured in each of the FT, Tri, and dM constructs when compared to the EO constructs. This implies that devitalization and demineralization had minimal impact on the amount of GAGs, collagen, and calcium present in the constructs.

However, visual examination of the SEM micrographs in **Figure 5.5** provides more information with lower amounts of ECM observed on the dM 12 constructs as compared to the EO 12, FT 12, and Tri 12 constructs and markedly lower amounts of ECM observed on the dM 16 constructs as compared to the EO 16, FT 16, and Tri 16 constructs. Similarly, the histological sections reveal that there is a drastic loss in the thickness of the GAG, collagen, and calcium layers within the constructs after devitalization and demineralization. The discrepancy between the quantitative and qualitative analysis may be a result of the methodology used to gather the images. The SEM micrographs obtained can only demonstrate the amount of ECM coating present on the surface of the construct and does not provide the amount of ECM present within the interior of the constructs. With regards to the histological images, the processing performed to create the FT, Tri, and dM constructs may have allowed for ECM loss to occur while generating fixed and embedded samples for sectioning.

Further study of the histological images illustrates that there are differences seen in the thickness of the GAG layer for both PCL/ECM 12 and PCL/ECM 16 constructs. The EO constructs have a thicker layer of GAGs as compared to the FT constructs which in turn has a thicker layer of GAGs than either the Tri or dM constructs. A similar loss in collagen thickness is observed in the picrosirius red staining of the FT, Tri, and dM constructs as compared to the EO constructs. Nevertheless, the FT constructs contain a thicker layer of collagen than either the Tri or dM constructs. In each treatment, the processed constructs are either

exposed to water or ammonium hydroxide in order to cause cell lysis, but these neither destroy nor remove the GAGs or collagen from the ECM.[199,212] However, exposure of the PCL/ECM constructs to freezing and thawing, ultrasonication, or continuous stirring can disrupt the ECM while Triton X-100 exposure has been shown to remove GAGs in addition to disrupting the ECM.[199] This can explain the observation of a thinner layer of GAGs and collagen in the Tri construct as compared to the EO and FT constructs. The loss of GAGs and collagen observed in the dM constructs as compared to the FT constructs may also be explained by the additional demineralization step. The dM constructs underwent the same devitalization steps as the FT constructs, but they are also soaked in a 2% EDTA solution which was continuously stirred for 2 hours. The extra time the dM constructs were agitated could potentially disrupt the ECM to a greater extent, resulting in a thinner layer of GAGs and collagen.

In a similar trend to the collagen distribution, the alizarin red staining of the FT, Tri, and dM constructs demonstrated that there was a thinner layer of calcium present as compared to the EO constructs, but the FT constructs contained a thicker layer of calcium than the Tri or dM constructs. This may be explained by the initiation and preferential deposition of calcium minerals along the collagen fibers in bone formation.[11,12] The devitalization and demineralization techniques removed some of the collagen fibers and thus the calcium minerals bound to the collagen fibers would also be removed. The end result is a similar trend between the calcium staining and collagen staining.

The MSC culture on the constructs demonstrated that cellular proliferation was similar on all of the PCL/ECM 12 constructs, but the dM 16 constructs had a significantly higher number of cells as compared to the EO 16, FT 16, and Tri 16 constructs. Examining the SEM micrographs of each of the constructs seen in **Figure 5.5**, it can be observed that each of the PCL/ECM 12 constructs had void spaces allowing access to the interior of the construct. However, between the PCL/ECM 16 constructs, the EO 16 constructs have minimal void space, the FT 16 and Tri 16 constructs have some void space, while a large amount is observed in the dM 16 constructs.

The void spaces observed within all of these cell-generated ECM constructs may potentially also be caused by the various devitalization and demineralization conditions. Each of the treatments used within this study has been shown to disrupt the ECM.[199] In the freeze-thaw devitalization method, numerous small ice crystals are created by the rapid freezing of water and thus leaving gaps where the cells were present and ice crystals had formed.[213] With the detergent method, the lipids present in the cell membrane would be dissociated, creating spaces where cells once were.[214] In the case of the demineralization procedure, some proteins and proteoglycans present within the ECM layer may have been solubilized or disrupted by the chelating agent, EDTA.[215] In addition, the agitation caused by the magnetic stir bar during the demineralization procedure generates convective forces throughout the construct.[216] Both EDTA and

agitation would cause some loss of ECM components from the constructs, thus leaving gaps in the surface ECM layer.

With the presence of void spaces, the MSCs seeded onto the PCL/ECM 12 constructs and dM 16 constructs may have been able to infiltrate into the interior and proliferate. Indeed, this is supported by similar levels of cell number seen on dM 16 constructs at day 12 as compared to the PCL/ECM 12 constructs at day 12. Histological staining also supports this with the EO 12, FT 12, dM 12, and dM 16 constructs filling with ECM in the interior of the constructs.

MSCs seeded onto Tri 12 constructs were also able to access the interior of the construct and generated an ECM layer at the top of the construct by day 8, but by day 12, the ECM coating had largely disappeared. Potentially, there may be some remnants of Triton X-100 left within the constructs which could cause cell lysis. Consequently, proteases may have been released which would have digested the ECM, resulting in a thin layer of ECM remaining by day 12.

Meanwhile the histological staining of the EO 16 constructs demonstrate that the MSCs were having difficulty in accessing the interior of the construct and instead have generated a second layer of ECM above the first ECM coating. However, the FT 16 constructs allowed some MSC access into the interior of the construct and had increases in ECM deposition at the top and bottom layers of the construct with minimal increase in matrix in the interior of the constructs.

Similarly, the Tri 16 constructs allowed MSCs access and had ECM present at the top layer of the construct at day 8, but the ECM deposited in the Tri 16 constructs later disappeared by day 12, possibly due to the same reason as the Tri 12 constructs.

The cell proliferation data also shows that the dM 12 constructs had a significantly lower number of cells present at day 8 when compared to the EO 12, FT 12, and Tri 12 constructs. This may be a result of the dM 12 construct having lost a greater thickness of GAGs and collagen than the other PCL/ECM 12 constructs. With this loss of ECM components, the MSCs may have had difficulty proliferating until they deposited enough ECM within the construct.

The ALP activity of the seeded MSCs demonstrates that there was no significant difference in activity between any of the PCL/ECM 12 constructs. This suggests that the processing techniques didn't remove any of the osteogenic components from the deposited ECM. However, the EO 16 construct had a significantly higher ALP activity as compared to dM 16 and Tri 16 at day 8 and day 12, respectively. In this case, the demineralization and detergent processing may have removed an osteogenic component present in the unprocessed constructs, since this effect isn't seen in the FT 16 construct. In fact, the FT 16 constructs demonstrated a significantly higher ALP activity at day 12 as compared to the EO 16, Tri 16, and dM 16 constructs. This may be due to the combination of higher amounts of ECM components as compared to the Tri 16 and dM 16 constructs in

conjunction with greater access to the interior of the construct as compared to the EO 16 constructs, which may have prolonged the osteogenic differentiation of the MSCs. In addition, since the difference in ALP activity between the processed constructs is only seen in the PCL/ECM 16 constructs, there may be an important osteogenic component present in the PCL/ECM 16 not found in the PCL/ECM 12. This is also supported by the significantly higher difference in ALP activity seen between the EO 12 and EO 16 constructs at day 4 and day 12 and the FT 12 and FT 16 constructs at day 12.

The calcium data illustrates that there was no significant difference in the calcium deposition between the EO 12, FT 12, and Tri 12 constructs. This may be explained by the similarity between their ECM coatings seen in the SEM micrographs and the histological images. Indeed, the cell proliferation and ALP activity data demonstrates that there were no significant differences between the constructs. However, there was a significant difference in calcium deposited for the dM 12 and dM 16 constructs at day 12 as compared to the EO 12 and EO 16 constructs, respectively. Nevertheless, this is not surprising, since these constructs started off with much less mineralization as compared to any of the other constructs.

The significant difference observed between the calcium deposition in FT 16 and EO 16 constructs may be related to the ALP activity. ALP activity is an early osteogenic differentiation marker and calcium deposition is a late stage marker.

Since the MSCs seeded onto FT 16 constructs demonstrated a significantly higher ALP activity than MSCs seeded onto EO 16 constructs, the MSCs may have not differentiated into osteoblasts by day 12.

Interestingly, there were no significant differences in calcium amounts between the PCL/ECM 12 constructs and their respective PCL/ECM 16 constructs. This may suggest that both the 12 day and 16 day ECM coatings are equally osteogenic. However, on the other hand, it may be a result of minimal amounts of ECM present in the PCL/ECM 12 constructs and the lack of access into the interior of the construct for the PCL/ECM 16 constructs.

## 5.5 Conclusions

This study explored the effect of various devitalization and demineralization techniques on the retention of ECM components within cell-generated ECM constructs and the osteogenic differentiation of MSCs seeded onto these constructs. Of all the processing techniques examined, histological analysis demonstrated that the freeze-thaw method contained the thickest layer of GAGs, collagen, and calcium within the constructs. In addition, the culture of MSCs on freeze-thaw treated PCL/ECM 16 constructs affected their osteogenic differentiation, with a significantly higher ALP activity and minimal amounts of calcium deposition at late stage culture as compared to untreated PCL/ECM 16 constructs. Moreover, each of the devitalization and demineralization techniques generated void spaces in surface of the ECM coating due to cell lysis, ice crystal

formation, and loss of ECM components. The presence of these void spaces enhanced cell infiltration and proliferation within the constructs. Overall, this study establishes that the freeze-thaw technique is the least harsh method of devitalization of cell-generated ECM constructs and additionally generates void spaces in the ECM coating allowing access of MSCs into the interior of the constructs.

## 5.6 Acknowledgements

This work was supported by a grant from the National Institutes of Health (R01 AR057083). R.A.T. also acknowledges the Ruth L. Kirschstein National Research Service Award (F31 AR055874) from the National Institute of Arthritis and Musculoskeletal and Skin Diseases. The content is solely the responsibility of the authors and does not necessarily represent the official views of the National Institute of Arthritis and Musculoskeletal and Skin Diseases or the National Institutes of Health.

| Processing Type | Technique | Initial Construct | Resulting Construct |
|---|---|---|---|
| Sterilization Only | 1. Exposure to ethylene oxide for 14 hours | PCL/ECM 12 | EO 12 |
| | | PCL/ECM 16 | EO 16 |
| Freeze-Thaw Devitalization | 1. Place in 1 mL of Millipore filtered water<br>2. 3 cycles of freezing at -196$^{o}$C followed by thawing at 37$^{o}$C<br>3. 10 minutes of ultrasonication<br>4. 2 rinses with Millipore filtered water<br>5. Air dry<br>6. Exposure to ethylene oxide for 14 hours | PCL/ECM 12 | FT 12 |
| | | PCL/ECM 16 | FT 16 |
| Detergent Devitalization | 1. Place in 1 mL of 0.5% v/v Triton-X 100 and 0.05% v/v $NH_4OH$<br>2. Shake at 100 rpm for 1 hour at room temperature<br>3. 3 rinses with Millipore filtered water<br>4. Air dry<br>5. Exposure to ethylene oxide for 14 hours | PCL/ECM 12 | Tri 12 |
| | | PCL/ECM 16 | Tri 16 |
| Demineralization and Devitalization | 1. Place in 1 mL of Millipore filtered water<br>2. 3 cycles of freezing at -196$^{o}$C followed by thawing at 37$^{o}$C<br>3. 10 minutes of ultrasonication<br>4. Place in 40 mL of 2% w/v ethylenediaminetetraacetic acid (EDTA)<br>5. Stir at 72 rpm for 2 hours<br>6. 2 rinses with Millipore filtered water<br>7. Exposure to ethylene oxide for 14 hours | PCL/ECM 12 | dM 12 |
| | | PCL/ECM 16 | dM 16 |

**Table 5.1:** The processing methods and the techniques used to generate devitalized and demineralized constructs.

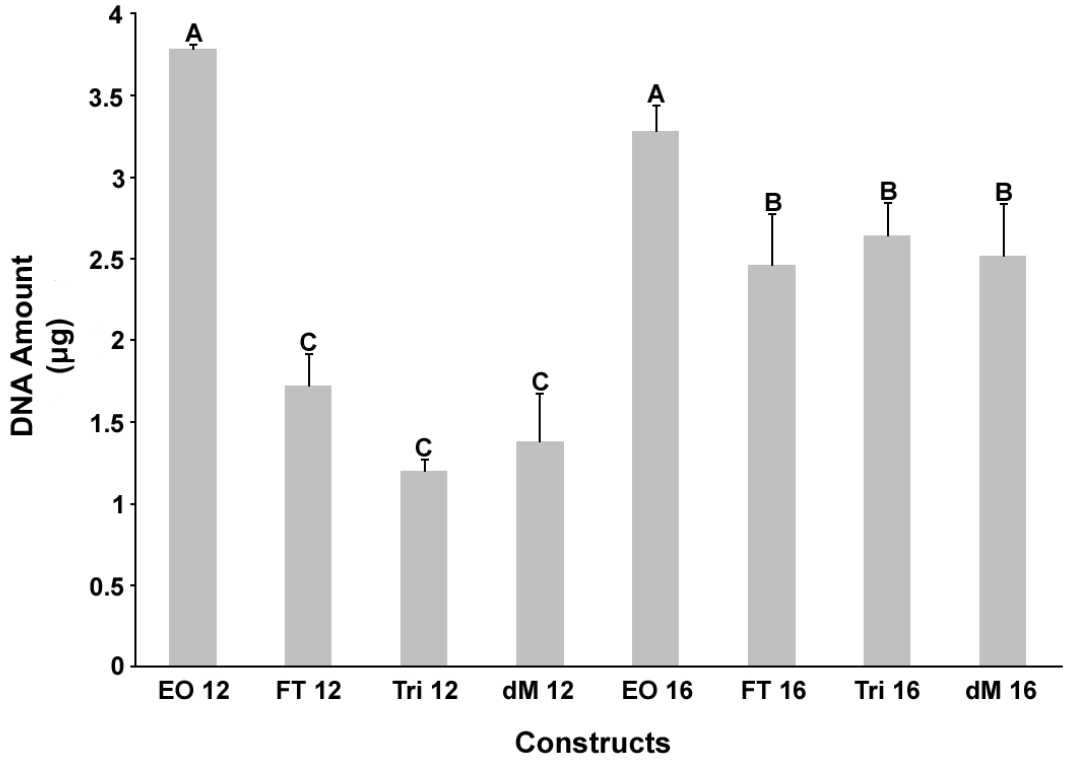


**Figure 5.1:** DNA content within each of the different processed constructs prior to being reseeded with MSCs. Groups not connected by the same letter indicates significant difference ($p<0.05$). Data are expressed as means ± standard deviation for n=3.

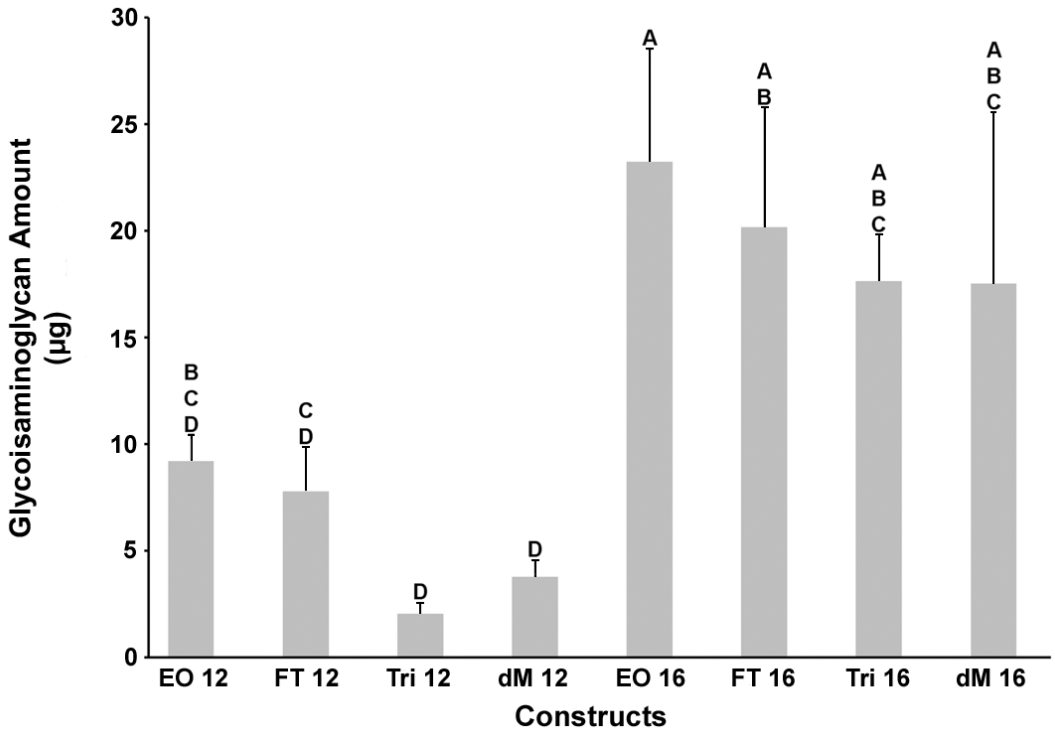


**Figure 5.2:** Glycoasminoglycan content within each of the different processed constructs prior to being reseeded with MSCs. Groups not connected by the same letter indicates significant difference ($p<0.05$). Data are expressed as means ± standard deviation for n=3.

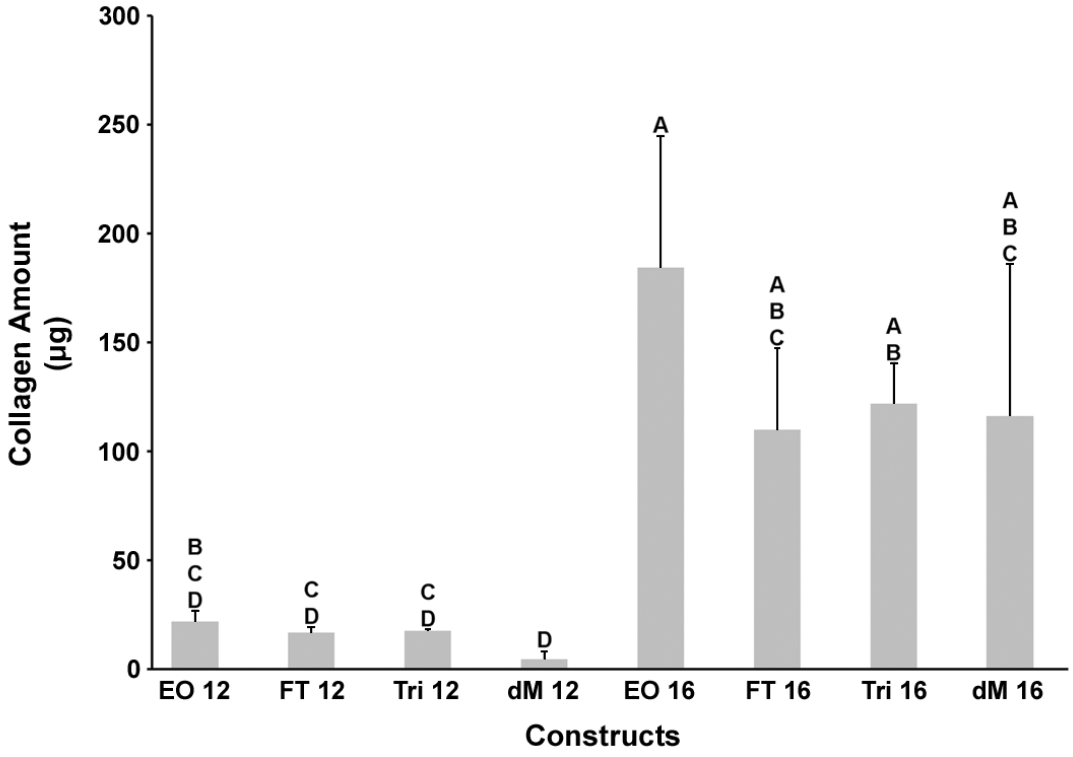


**Figure 5.3:** Collagen content within each of the different processed constructs prior to being reseeded with MSCs. Groups not connected by the same letter indicates significant difference ($p<0.05$). Data are expressed as means ± standard deviation for n=3.

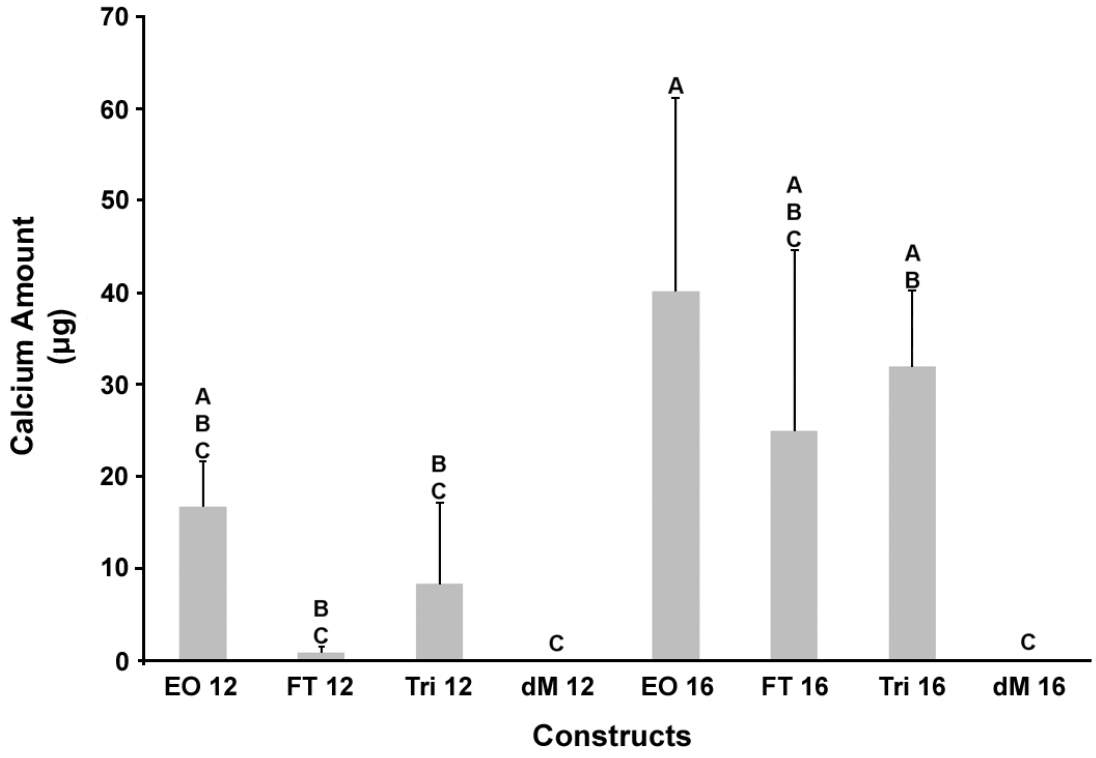


**Figure 5.4:** Calcium content within each of the different processed constructs prior to being reseeded with MSCs. Groups not connected by the same letter indicates significant difference ($p<0.05$). Data are expressed as means ± standard deviation for n=3.

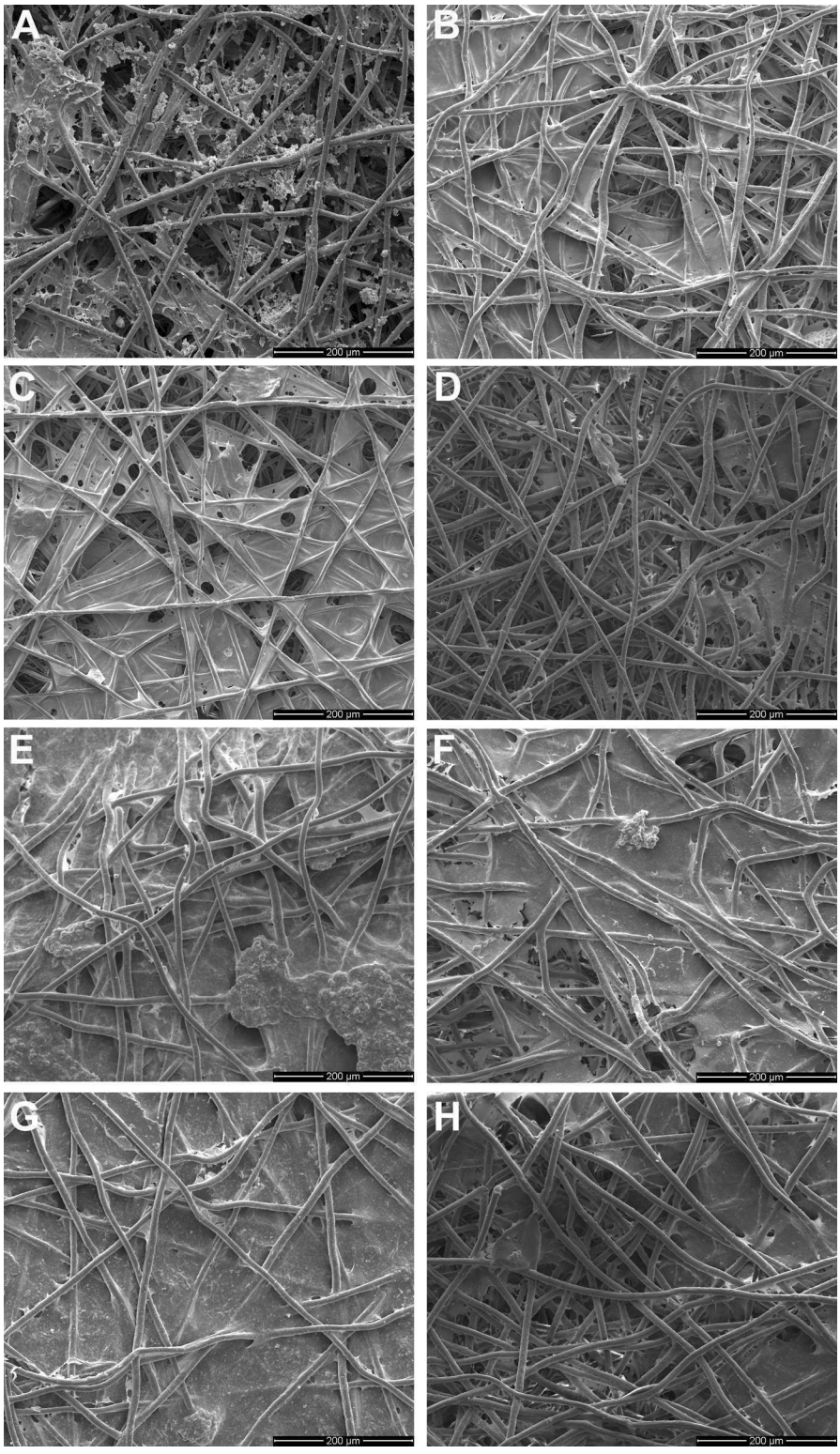


**Figure 5.5:** Scanning electron micrograph of the processed constructs at a 250X magnification. Each micrograph demonstrates the void spaces generated in the ECM coating by the devitalization and demineralization techniques. A) EO 12, B) FT 12, C) Tri 12, D) dM 12, E) EO 16, F) FT 16, G) Tri 16, H) dM 16.

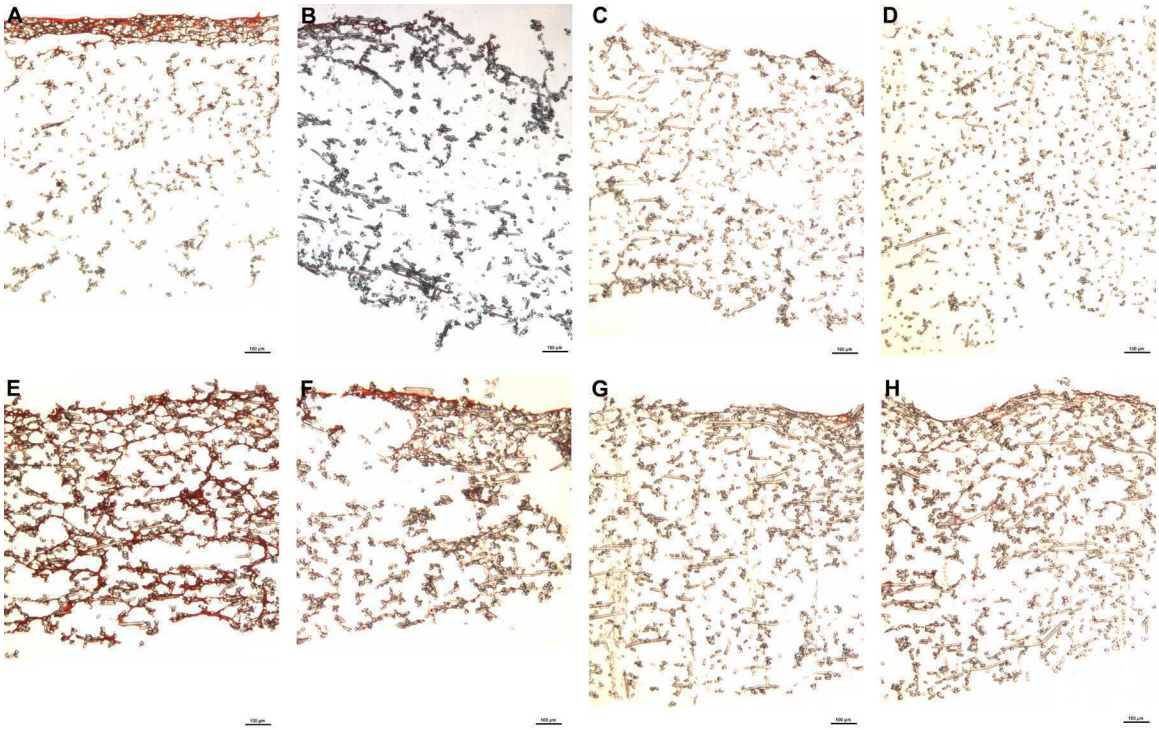


**Figure 5.6i:** Histological images of the processed constructs at 5X magnification. Constructs were cut into 5 µm sections and stained with Safranin O.A) EO 12, B) FT 12, C) Tri 12, D) dM 12, E) EO 16, F) FT 16, G) Tri 16, H) dM 16.

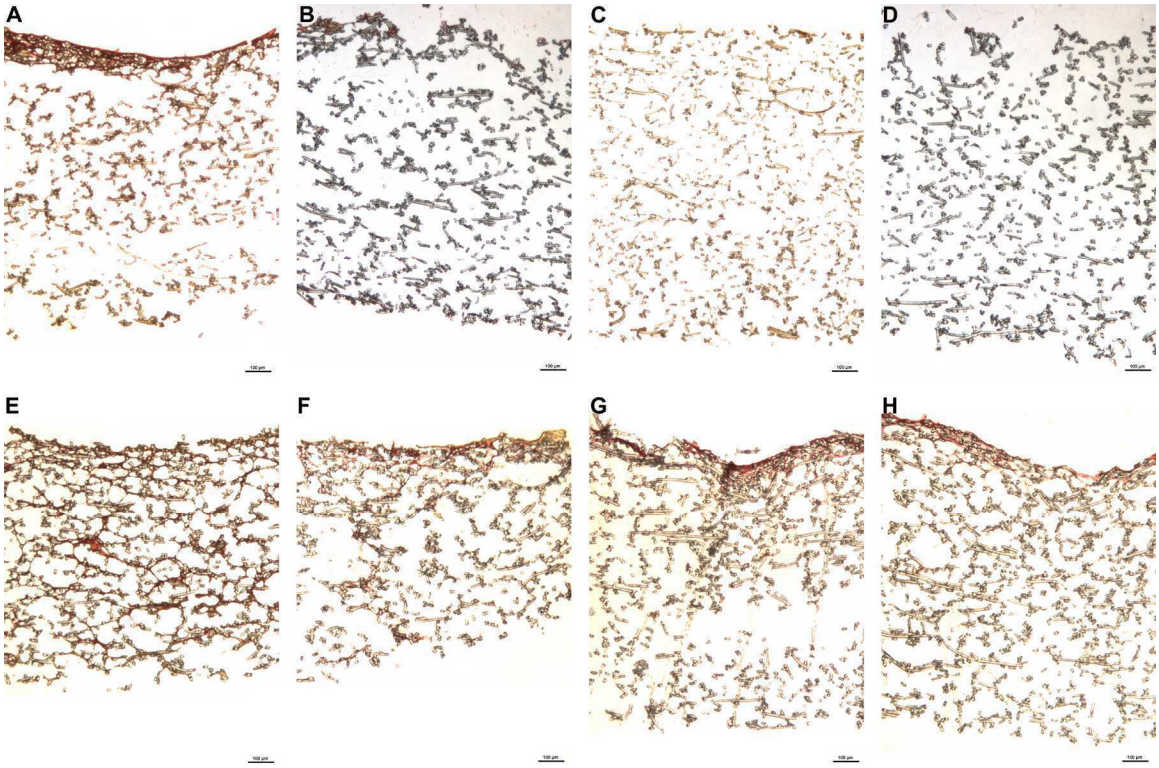


**Figure 5.6ii:** Histological images of the processed constructs at 5X magnification. Constructs were cut into 5 µm sections and stained with Picrosirius Red. A) EO 12, B) FT 12, C) Tri 12, D) dM 12, E) EO 16, F) FT 16, G) Tri 16, H) dM 16.

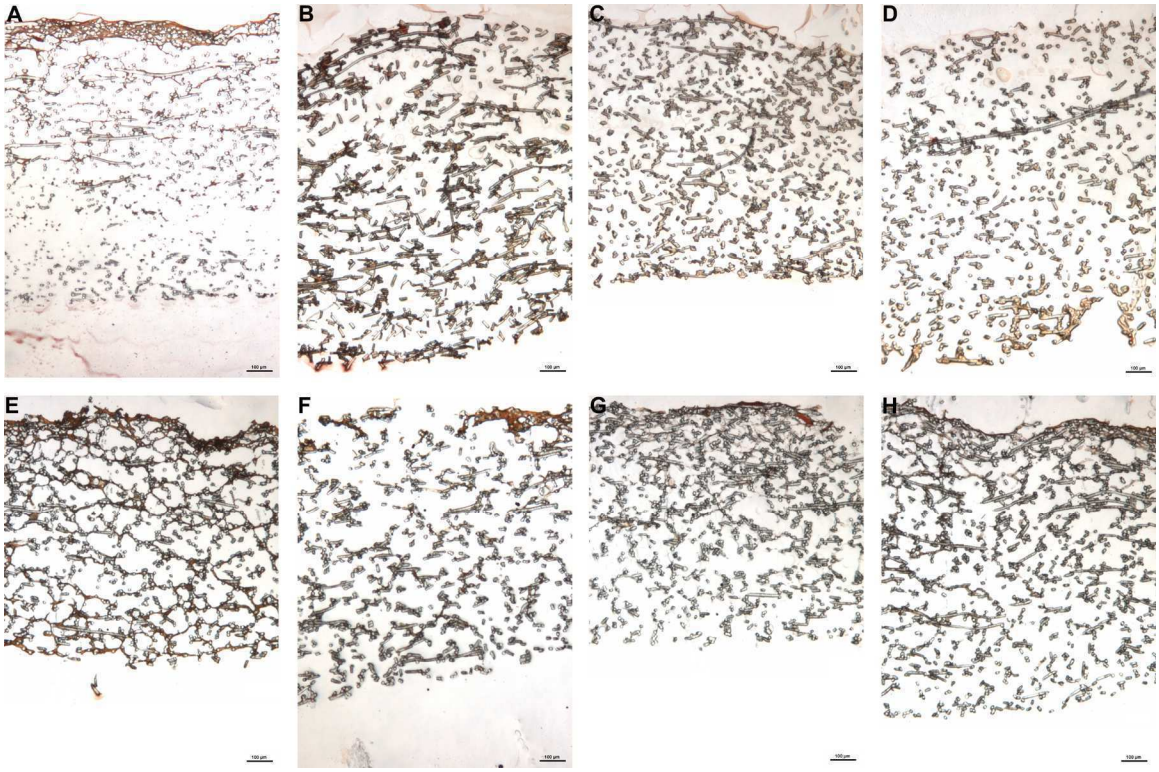


**Figure 5.6iii:** Histological images of the processed constructs at 5X magnification. Constructs were cut into 5 µm sections and stained with Alizarin Red. A) EO 12, B) FT 12, C) Tri 12, D) dM 12, E) EO 16, F) FT 16, G) Tri 16, H) dM 16.

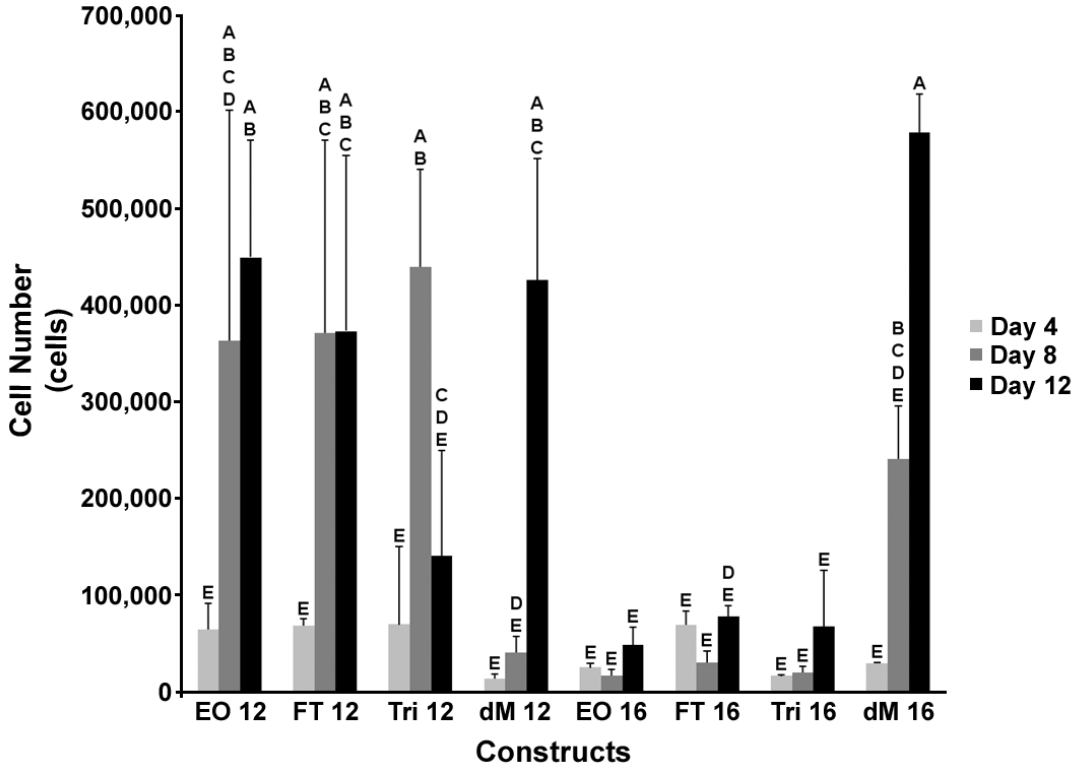


**Figure 5.7:** Cellularity of the reseeded constructs at day 4, day 8, and day 12. Groups not connected by the same letter indicates significant difference ($p<0.05$). Data are expressed as means ± standard deviation for n=3.

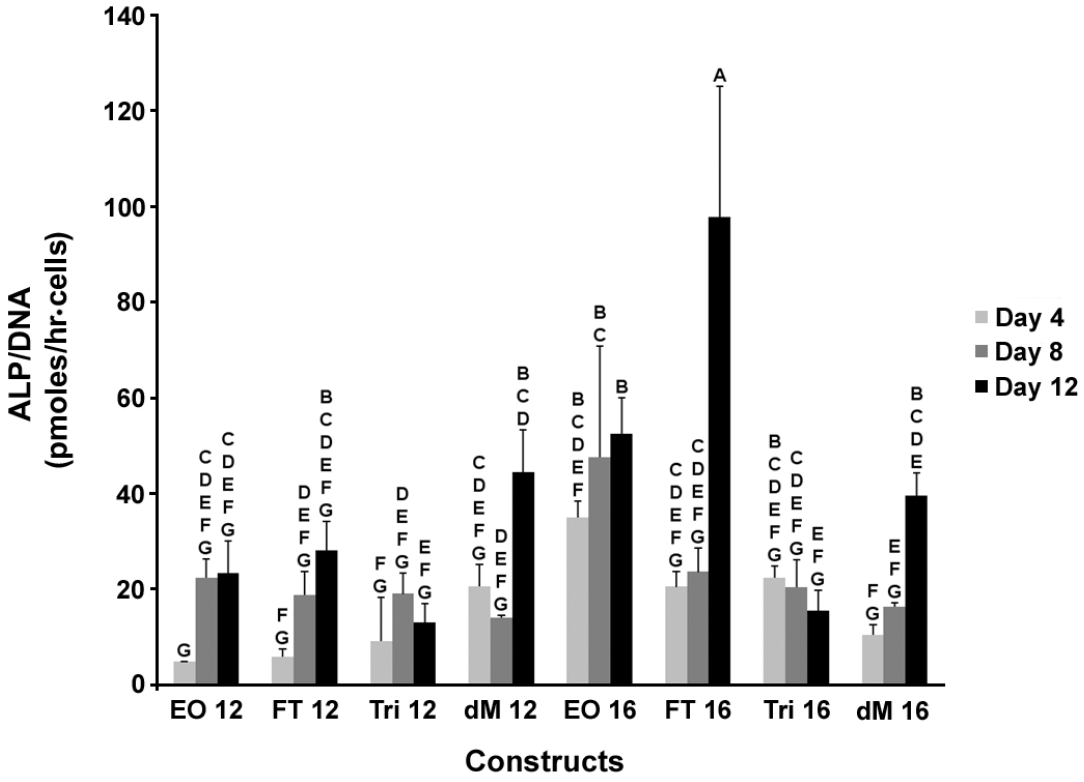


**Figure 5.8:** Alkaline phosphatase activity of the reseeded constructs at day 4, day 8, and day 12. Groups not connected by the same letter indicates significant difference ($p<0.05$). Data are expressed as means ± standard deviation for n=3.

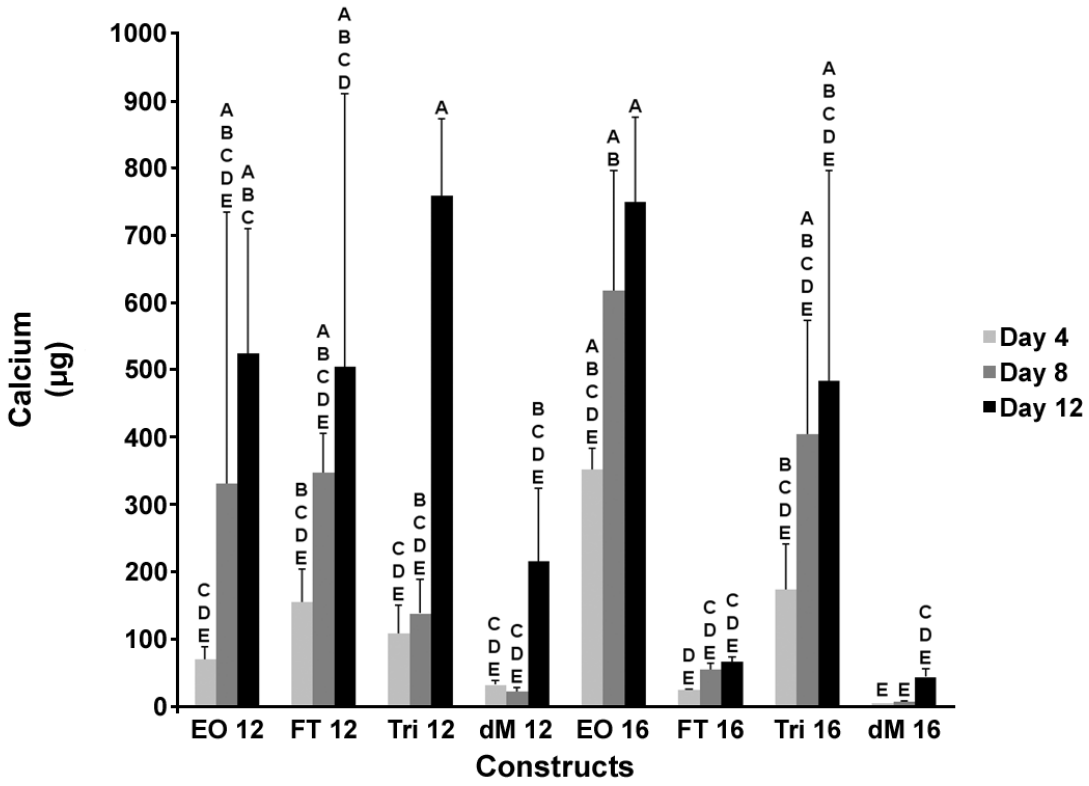


**Figure 5.9:** Calcium amounts present on each reseeded constructs at day 4, day 8, and day 12. Groups not connected by the same letter indicates significant difference ($p<0.05$). Data are expressed as means ± standard deviation for n=3.

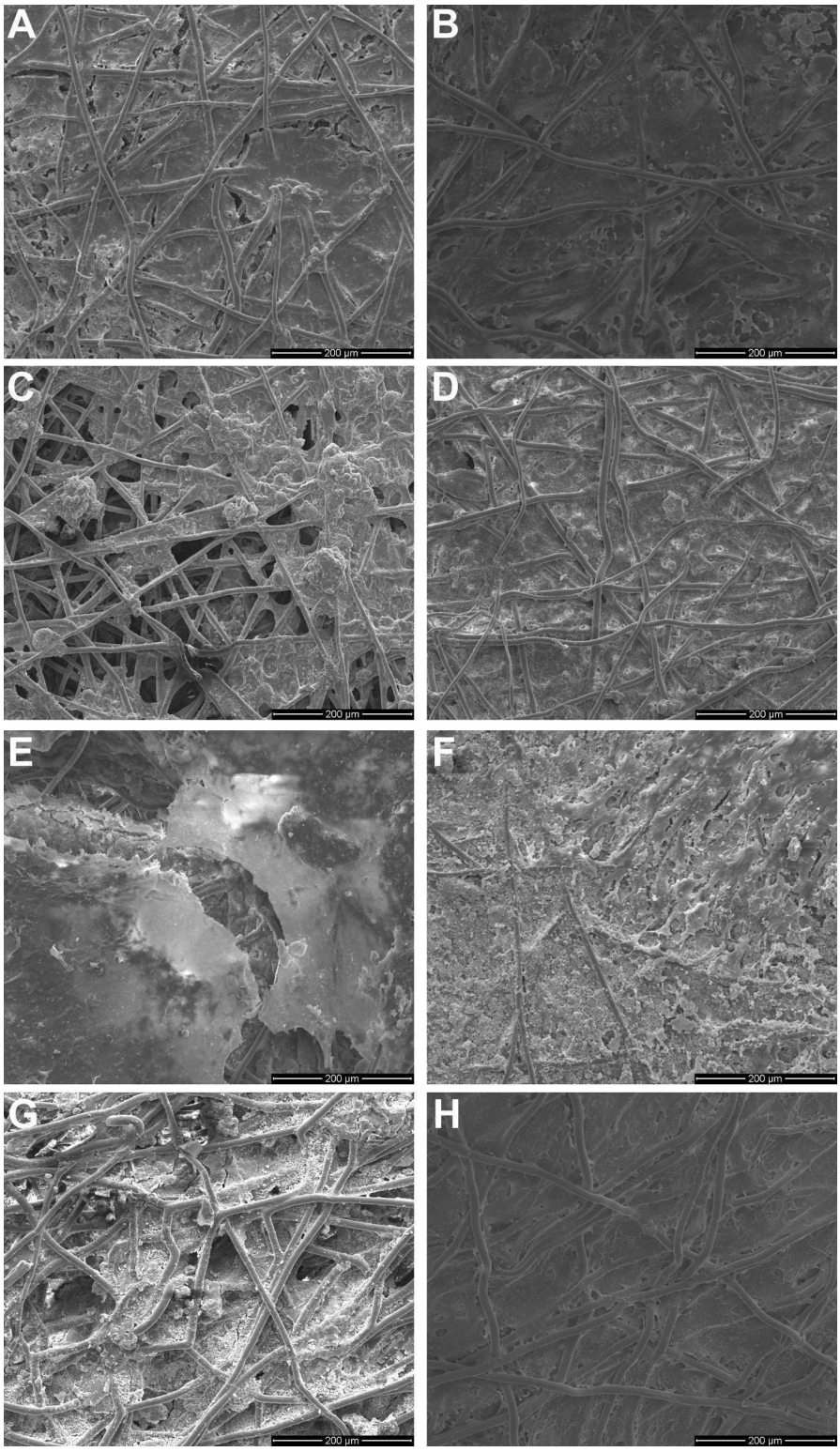


**Figure 5.10:** Scanning electron micrograph of the reseeded processed constructs at day 12 at a 250X magnification. Each micrograph demonstrates the coating of ECM produced by the reseeded MSCs. A) EO 12, B) FT 12, C) Tri 12, D) dM 12, E) EO 16, F) FT 16, G) Tri 16, H) dM 16.

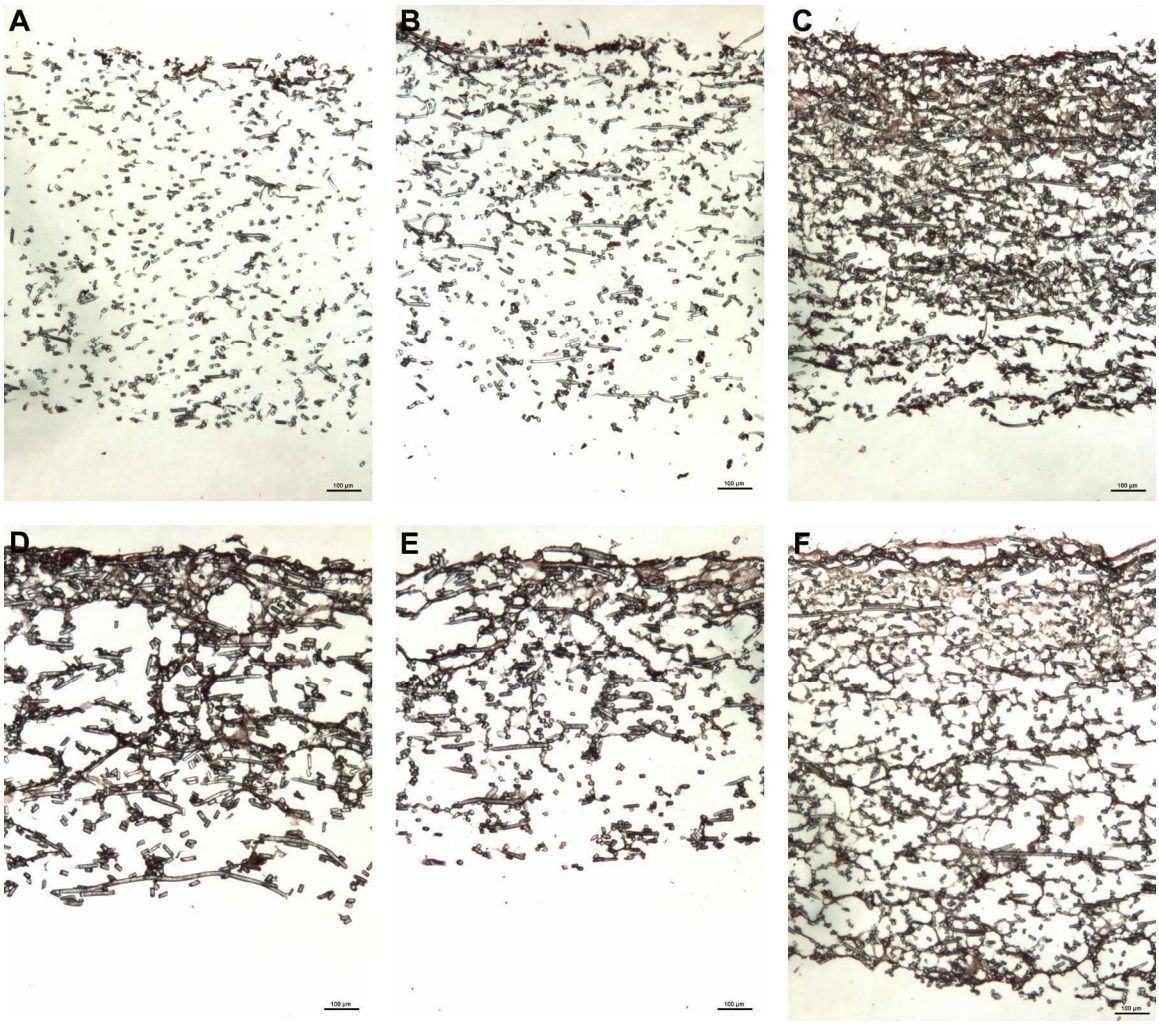


**Figure 5.11i:** Histological images of the reseeded processed constructs at 5X magnification for the day 4, day 8, and day 12 timepoints. Constructs were cut into 5 µm sections and stained with H & E. A) EO 12 day 4, B) EO 12 day 8, C) EO 12 day 12, D) EO 16 day 4, E) EO 16 day 8, F) EO 16 day 12.

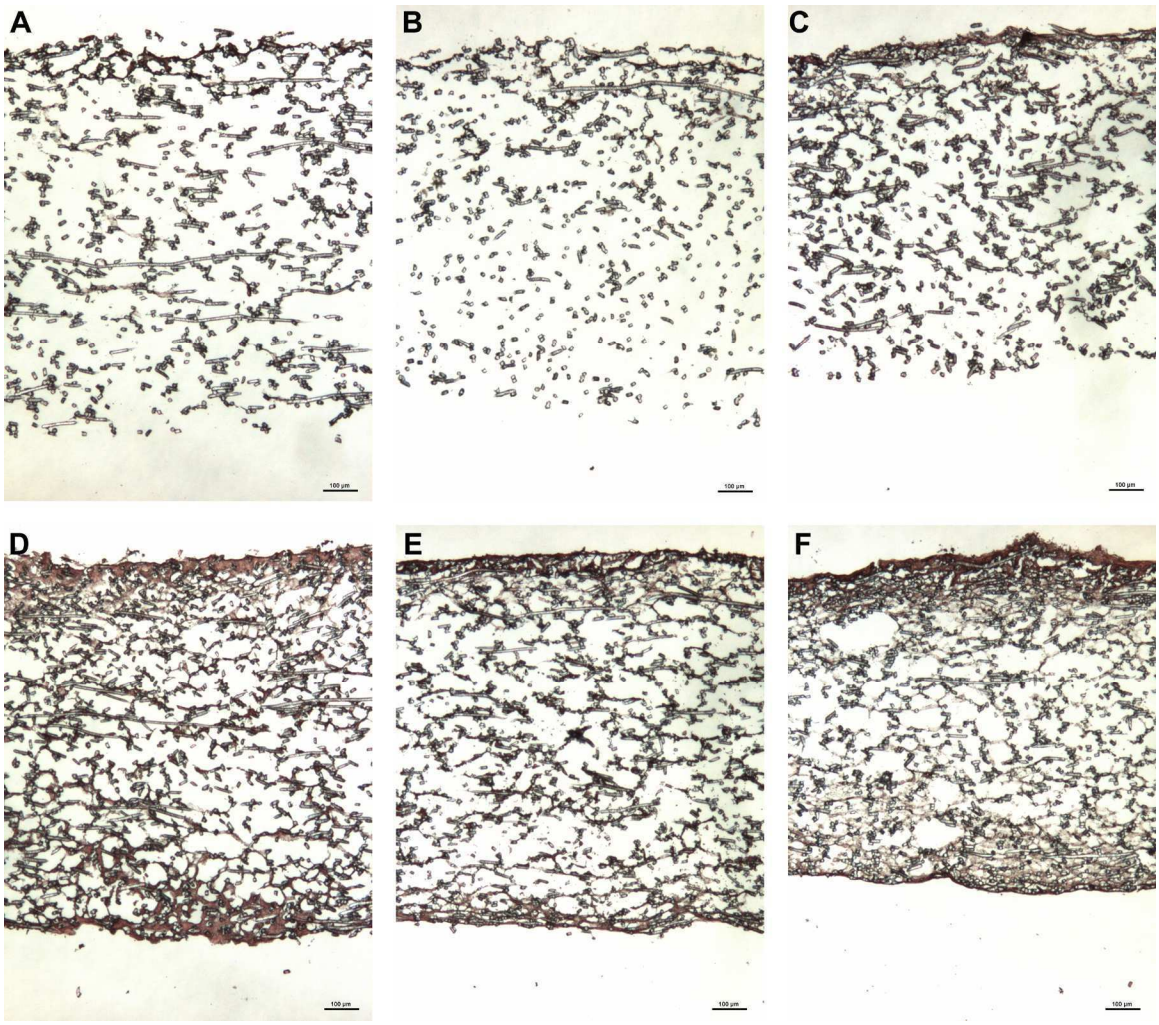


**Figure 5.11ii:** Histological images of the reseeded processed constructs at 5X magnification for the day 4, day 8, and day 12 timepoints. Constructs were cut into 5 μm sections and stained with H & E. A) FT 12 day 4, B) FT 12 day 8, C) FT 12 day 12, D) FT 16 day 4, E) FT 16 day 8, F) FT 16 day 12.

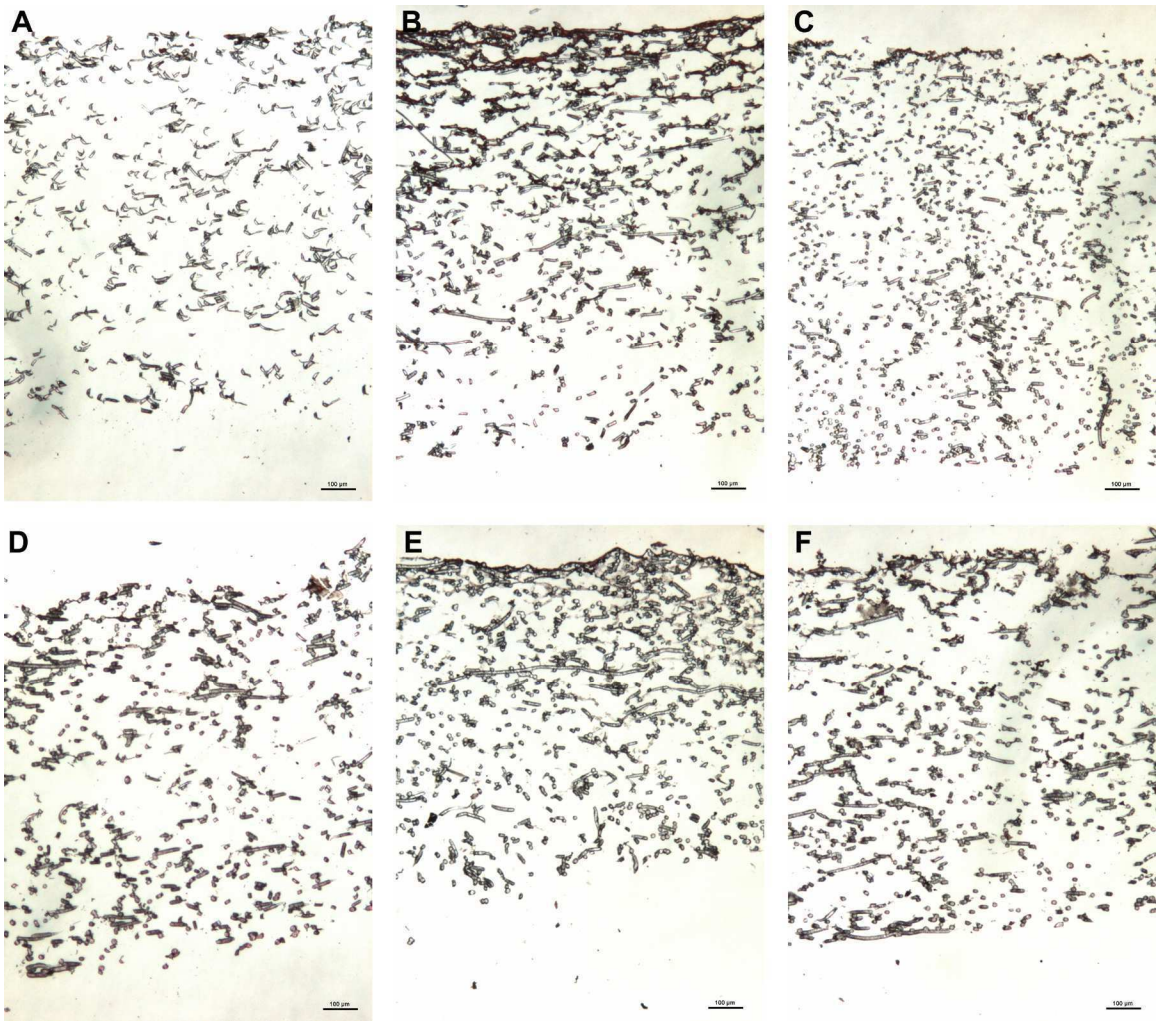


**Figure 5.11iii:** Histological images of the reseeded processed constructs at 5X magnification for the day 4, day 8, and day 12 timepoints. Constructs were cut into 5 µm sections and stained with H & E. A) Tri 12 day 4, B) Tri 12 day 8, C) Tri 12 day 12, D) Tri 16 day 4, E) Tri 16 day 8, F) Tri 16 day 12.

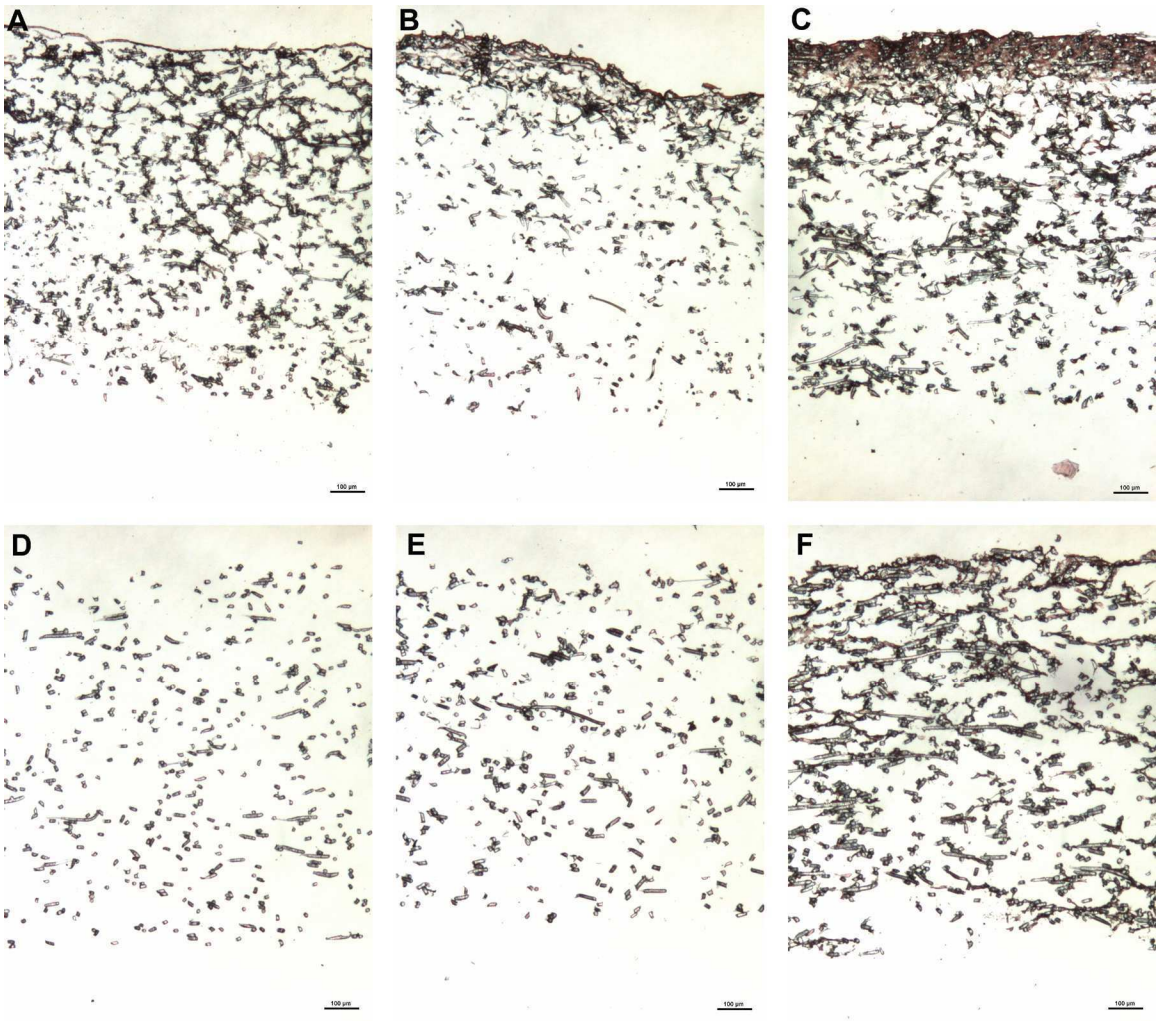


**Figure 5.11iv:** Histological images of the reseeded processed constructs at 5X magnification for the day 4, day 8, and day 12 timepoints. Constructs were cut into 5 µm sections and stained with H & E. A) dM 12 day 4, B) dM 12 day 8, C) dM 12 day 12, D) dM 16 day 4, E) dM 16 day 8, F) dM 16 day 12.

# CHAPTER 6

## Conclusions and Future Work

The overall goal of this research work was to develop a MSC-generated ECM and PCL construct, determine its osteogenicity, and identify the components in the ECM that encourage the osteogenic differentiation of MSCs seeded onto the construct. The specific aims outlined in the thesis overview allowed for confirmation of the osteogenicity of the PCL/ECM constructs and identification of the ECM components that were present within the osteogenic construct.

Chapter 3 demonstrated that the statically cultured acellular PCL/ECM constructs contained a component that is conducive to calcium deposition and may mineralize over time *in vivo* without cells. It was also shown that the *in vitro* cell-generated ECM can sustain the osteogenic differentiation of MSCs even with the lack of the osteogenic supplement, dexamethasone. In addition, it was demonstrated that the cell-generated ECM enhanced the proliferation of either MSCs or another cell population (or populations) present within the whole bone marrow.

Given the information from the study presented in Chapter 3, it was logical to explore the changes in protein and mineral composition of the osteogenic PCL/ECM constructs over time. Chapter 4 showed that at early ECM maturities, it was composed of cellular adhesion proteins, such as fibronectin. Meanwhile, at later stages of ECM maturities, it was mainly composed of matrix remodeling

and regulatory proteins, such as MMP-2 and PEDF. The constructs were also found to contain the major components of mature bone, collagen 1 and hydroxyapatite along with fibril-regulating proteins that help to organize both collagen 1 and fibronectin, thus demonstrating that the ECM has started to resemble mature bone.

The PCL/ECM constructs studied previously have all undergone a freeze-thaw devitalization procedure. Chapter 5 explored the effect of various devitalization and demineralization processes on the retention of major ECM components and the osteogenicity of the treated constructs. The freeze-thaw devitalization method was shown to disrupt the ECM the least, retaining a thicker layer of GAGs, collagen, and calcium within the constructs as compared to the other processing methods. In addition, this study demonstrates that void spaces in the surface of the ECM coating on the constructs are important for allowing access of MSCs into the interior of the constructs enhancing matrix production within the constructs.

The result of the research described in this thesis reveals that osteogenically pre-differentiated MSC-generated PCL/ECM constructs are osteogenic and contain some of the components of mature bone. Furthermore, devitalizing the constructs using a minimally disruptive process, such as freeze-thaw cycles enhances MSC access to the interior of the construct as compared to untreated constructs.

Of further interest would be the exploration of the creation of the ECM coating on well-characterized and pre-designed scaffolds. Electrospun scaffolds are well-characterized, but it is difficult to create clinically relevant shapes using only electrospinning. 3D printing allows for the generation of scaffolds that are able to be formed into irregular shapes but with known pore sizes. Future studies can investigate whether drastically different pore sizes affects the composition of the ECM deposited by the cells.

Additional future studies investigating the performance of the PCL/ECM constructs in an *in vivo* environment, whether it be at an ectopic or orthotopic site would provide insight into the inflammatory nature of the construct as well as the integration of the construct to the surrounding bone of a defect and the extent of bone formation within the entirety of the construct. These investigations would provide more conclusive evidence of the osteogenicity of the constructs and validate the results observed within this thesis.

## References


1. M Artico, L Ferrante, FS Pastore, EO Ramundo, D Cantarelli, D Scopelliti, and G Iannetti, *Bone autografting of the calvaria and craniofacial skeleton: historical background, surgical results in a series of 15 patients, and review of the literature.* Surg Neurol 2003, **60**, 71-79.

2. SN Khan, JF Fraser, HS Sandhu, FP Cammisa, Jr., FP Girardi, and JM Lane, *Use of osteopromotive growth factors, demineralized bone matrix, and ceramics to enhance spinal fusion.* J Am Acad Orthop Surg 2005, **13**, 129-137.

3. Z Li and M Kawashita, *Current progress in inorganic artificial biomaterials.* J Artif Organs 2011, **14**, 163-170.

4. DK Rah, *Art of replacing craniofacial bone defects.* Yonsei Med J 2000, **41**, 756-765.

5. Z Ge, Z Jin, and T Cao, *Manufacture of degradable polymeric scaffolds for bone regeneration.* Biomed Mater 2008, **3**, 022001.

6. PV Giannoudis, H Dinopoulos, and E Tsiridis, *Bone substitutes: an update.* Injury 2005, **36 Suppl 3**, S20-27.

7. MH Ho, DM Wang, HJ Hsieh, HC Liu, TY Hsien, JY Lai, and LT Hou, *Preparation and characterization of RGD-immobilized chitosan scaffolds.* Biomaterials 2005, **26**, 3197-3206.

8. WJ Li, R Tuli, X Huang, P Laquerriere, and RS Tuan, *Multilineage differentiation of human mesenchymal stem cells in a three-dimensional nanofibrous scaffold.* Biomaterials 2005, **26**, 5158-5166.

9. G Wang, L Zheng, H Zhao, J Miao, C Sun, N Ren, J Wang, H Liu, and X Tao, *In vitro assessment of the differentiation potential of bone marrow-derived mesenchymal stem cells on genipin-chitosan conjugation scaffold with surface hydroxyapatite nanostructure for bone tissue engineering.* Tissue Eng Part A 2011, **17**, 1341-1349.

10. P Yilgor, K Tuzlakoglu, RL Reis, N Hasirci, and V Hasirci, *Incorporation of a sequential BMP-2/BMP-7 delivery system into chitosan-based scaffolds for bone tissue engineering.* Biomaterials 2009, **30**, 3551-3559.

11. JP Bilezikian, LG Raisz, and GA Rodan, *Principles of Bone Biology*. 2nd ed. 2002, San Diego: Academic Press.

12. A Tampieri, S Sprio, M Sandri, and F Valentini, *Mimicking natural bio-mineralization processes: a new tool for osteochondral scaffold development.* Trends Biotechnol 2011, **29**, 526-535.

13. X Li, J Xie, X Yuan, and Y Xia, *Coating electrospun poly(epsilon-caprolactone) fibers with gelatin and calcium phosphate and their use as biomimetic scaffolds for bone tissue engineering.* Langmuir 2008, **24**, 14145-14150.

14. HS Yun, SH Kim, D Khang, J Choi, HH Kim, and M Kang, *Biomimetic component coating on 3D scaffolds using high bioactivity of mesoporous bioactive ceramics.* Int J Nanomedicine 2011, **6**, 2521-2531.

15. SF Badylak, K Park, N Peppas, G McCabe, and M Yoder, *Marrow-derived cells populate scaffolds composed of xenogeneic extracellular matrix.* Exp Hematol 2001, **29**, 1310-1318.

16. CB Thomas, S Maxson, and KJ Burg, *Preparation and characterization of a composite of demineralized bone matrix fragments and polylactide beads for bone tissue engineering.* J Biomater Sci Polym Ed 2011, **22**, 589-610.

17. HJ Kim, UJ Kim, G Vunjak-Novakovic, BH Min, and DL Kaplan, *Influence of macroporous protein scaffolds on bone tissue engineering from bone marrow stem cells.* Biomaterials 2005, **26**, 4442-4452.

18. RA Thibault, LS Baggett, AG Mikos, and FK Kasper, *Osteogenic differentiation of mesenchymal stem cells on pregenerated extracellular matrix scaffolds in the absence of osteogenic cell culture supplements.* Tissue Eng Part A 2010, **16**, 431-440.

19. W Harrington and P Vonhippel, *The Structure of Collagen and Gelatin.* Adv Protein Chem 1961, **16**, 1-138.

20. X Liu, LA Smith, J Hu, and PX Ma, *Biomimetic nanofibrous gelatin/apatite composite scaffolds for bone tissue engineering.* Biomaterials 2009, **30**, 2252-2258.

21. SA Sell, MJ McClure, K Garg, PS Wolfe, and GL Bowlin, *Electrospinning of collagen/biopolymers for regenerative medicine and cardiovascular tissue engineering.* Adv Drug Deliv Rev 2009, **61**, 1007-1019.

22. Y Chen, AF Mak, M Wang, and J Li, *Composite coating of bonelike apatite particles and collagen fibers on poly L-lactic acid formed through an accelerated biomimetic coprecipitation process.* J Biomed Mater Res B Appl Biomater 2006, **77**, 315-322.

23. J Doshi and DH Reneker, *Electrospinning Process and Applications of Electrospun Fibers.* J Electrostat 1995, **35**, 151-160.

24. S Yang, KF Leong, Z Du, and CK Chua, *The design of scaffolds for use in tissue engineering. Part II. Rapid prototyping techniques.* Tissue Eng 2002, **8**, 1-11.

25. H Schoof, J Apel, I Heschel, and G Rau, *Control of pore structure and size in freeze-dried collagen sponges.* J Biomed Mater Res 2001, **58**, 352-357.

26. P Schaaf, JC Voegel, L Jierry, and F Boulmedais, *Spray-assisted polyelectrolyte multilayer buildup: from step-by-step to single-step polyelectrolyte film constructions.* Adv Mater 2012, **24**, 1001-1016.

27. T Kokubo and H Takadama, *How useful is SBF in predicting in vivo bone bioactivity?* Biomaterials 2006, **27**, 2907-2915.

28. AC Jayasuriya and S Kibbe, *Rapid biomineralization of chitosan microparticles to apply in bone regeneration.* J Mater Sci Mater Med 2009, **21**, 393-398.

29. Y Zhang, VJ Reddy, SY Wong, X Li, B Su, S Ramakrishna, and CT Lim, *Enhanced biomineralization in osteoblasts on a novel electrospun biocomposite nanofibrous substrate of hydroxyapatite/collagen/chitosan.* Tissue Eng Part A 2010, **16**, 1949-1960.

30. MB Eslaminejad, H Mirzadeh, Y Mohamadi, and A Nickmahzar, *Bone differentiation of marrow-derived mesenchymal stem cells using beta-tricalcium phosphate-alginate-gelatin hybrid scaffolds.* J Tissue Eng Regen Med 2007, **1**, 417-424.

31. KL Sellgren and T Ma, *Perfusion conditioning of hydroxyapatite-chitosan-gelatin scaffolds for bone tissue regeneration from human mesenchymal stem cells.* J Tissue Eng Regen Med 2012, **6**, 49-59.

32. J Li, Y Chen, AF Mak, RS Tuan, L Li, and Y Li, *A one-step method to fabricate PLLA scaffolds with deposition of bioactive hydroxyapatite and collagen using ice-based microporogens.* Acta Biomater 2010, **6**, 2013-2019.

33. J Li, X Yuan, F He, and AF Mak, *Hybrid coating of hydroxyapatite and collagen within poly(D,L-lactic-co-glycolic acid) scaffold.* J Biomed Mater Res B Appl Biomater 2008, **86**, 381-388.

34. R Ravichandran, JR Venugopal, S Sundarrajan, S Mukherjee, and S Ramakrishna, *Precipitation of nanohydroxyapatite on PLLA/PBLG/Collagen nanofibrous structures for the differentiation of adipose derived stem cells to osteogenic lineage.* Biomaterials 2012, **33**, 846-855.

35. N Hild, OD Schneider, D Mohn, NA Luechinger, FM Koehler, S Hofmann, JR Vetsch, BW Thimm, R Muller, and WJ Stark, *Two-layer membranes of calcium phosphate/collagen/PLGA nanofibres: in vitro biomineralisation and osteogenic differentiation of human mesenchymal stem cells.* Nanoscale 2010, **3**, 401-409.

36. C Weinand, R Gupta, E Weinberg, I Madisch, CM Neville, JB Jupiter, and JP Vacanti, *Toward regenerating a human thumb in situ.* Tissue Eng Part A 2009, **15**, 2605-2615.

37. AC Jayasuriya and NA Ebraheim, *Evaluation of bone matrix and demineralized bone matrix incorporated PLGA matrices for bone repair.* J Mater Sci Mater Med 2009, **20**, 1637-1644.

38. BG Kurkalli, O Gurevitch, A Sosnik, D Cohn, and S Slavin, *Repair of bone defect using bone marrow cells and demineralized bone matrix supplemented with polymeric materials.* Curr Stem Cell Res Ther 2010, **5**, 49-56.

39. PY Ni, M Fan, ZY Qian, JC Luo, CY Gong, SZ Fu, S Shi, F Luo, and ZM Yang, *Synthesis and characterization of injectable, thermosensitive, and biocompatible acellular bone matrix/poly(ethylene glycol)-poly (epsilon-caprolactone)-poly(ethylene glycol) hydrogel composite.* J Biomed Mater Res A 2011, **100**, 171-179.

40. H Iwata, S Sakano, T Itoh, and TW Bauer, *Demineralized bone matrix and native bone morphogenetic protein in orthopaedic surgery.* Clin Orthop Relat Res 2002, **395**, 99-109.

41. T Hagino and Y Hamada, *Accelerating bone formation and earlier healing after using demineralized bone matrix for limb lengthening in rabbits.* J Orthop Res 1999, **17**, 232-237.

42. S Badylak, S Meurling, M Chen, A Spievack, and A Simmons-Byrd, *Resorbable bioscaffold for esophageal repair in a dog model.* J Pediatr Surg 2000, **35**, 1097-1103.

43. TK Sampath and AH Reddi, *Distribution of bone inductive proteins in mineralized and demineralized extracellular matrix.* Biochem Biophys Res Commun 1984, **119**, 949-954.

44. MR Urist, *Bone: formation by autoinduction.* Science 1965, **150**, 893-899.

45. WS Pietrzak, SN Ali, D Chitturi, M Jacob, and JE Woodell-May, *BMP depletion occurs during prolonged acid demineralization of bone: characterization and implications for graft preparation.* Cell Tissue Bank 2011, **12**, 81-88.

46. E Gruskin, BA Doll, FW Futrell, JP Schmitz, and JO Hollinger, *Demineralized bone matrix in bone repair: History and use.* Adv Drug Deliv Rev 2012, in press.

47. DJ Holt and DW Grainger, *Demineralized bone matrix as a vehicle for delivering endogenous and exogenous therapeutics in bone repair.* Adv Drug Deliv Rev 2012, in press.

48. G Syftestad and MR Urist, *Degradation of bone matrix morphogenetic activity by pulverization.* Clin Orthop Relat Res 1979, **141**, 281-285.

49. D Cohn, A Sosnik, and A Levy, *Improved reverse thermo-responsive polymeric systems.* Biomaterials 2003, **24**, 3707-3714.

50. M Lovett, K Lee, A Edwards, and DL Kaplan, *Vascularization strategies for tissue engineering.* Tissue Eng Part B Rev 2009, **15**, 353-370.

51. N Datta, HL Holtorf, VI Sikavitsas, JA Jansen, and AG Mikos, *Effect of bone extracellular matrix synthesized in vitro on the osteoblastic differentiation of marrow stromal cells.* Biomaterials 2005, **26**, 971-977.

52. L Fassina, E Saino, L Visai, MA Avanzini, MG Cusella De Angelis, F Benazzo, S Van Vlierberghe, P Dubruel, and G Magenes, *Use of a gelatin cryogel as biomaterial scaffold in the differentiation process of human bone marrow stromal cells.* Conf Proc IEEE Eng Med Biol Soc 2010, 247-250.

53. H Hagenmuller, S Hofmann, T Kohler, HP Merkle, DL Kaplan, G Vunjak-Novakovic, R Muller, and L Meinel, *Non-invasive time-lapsed monitoring and quantification of engineered bone-like tissue.* Ann Biomed Eng 2007, **35**, 1657-1667.

54. AM Martins, QP Pham, PB Malafaya, RA Sousa, ME Gomes, RM Raphael, FK Kasper, RL Reis, and AG Mikos, *The role of lipase and alpha-amylase in the degradation of starch/poly(epsilon-caprolactone) fiber meshes and the osteogenic differentiation of cultured marrow stromal cells.* Tissue Eng Part A 2009, **15**, 295-305.

55. E Saino, S Grandi, E Quartarone, V Maliardi, D Galli, N Bloise, L Fassina, MG De Angelis, P Mustarelli, M Imbriani, and L Visai, *In vitro calcified matrix deposition by human osteoblasts onto a zinc-containing bioactive glass.* Eur Cell Mater 2011, **21**, 59-72.

56. BW Thimm, S Wust, S Hofmann, H Hagenmuller, and R Muller, *Initial cell pre-cultivation can maximize ECM mineralization by human mesenchymal stem cells on silk fibroin scaffolds.* Acta Biomater 2011, **7**, 2218-2228.

57. G Tour, M Wendel, and I Tcacencu, *Cell-derived matrix enhances osteogenic properties of hydroxyapatite.* Tissue Eng Part A 2011, **17**, 127-137.

58. Y Ikada, *Tissue Engineering Fundamentals and Applications*. 2006, San Diego, CA, USA: Elsevier.

59. MR Kreke, WR Huckle, and AS Goldstein, *Fluid flow stimulates expression of osteopontin and bone sialoprotein by bone marrow stromal cells in a temporally dependent manner.* Bone 2005, **36**, 1047-1055.

60. I Owan, DB Burr, CH Turner, J Qiu, Y Tu, JE Onyia, and RL Duncan, *Mechanotransduction in bone: osteoblasts are more responsive to fluid forces than mechanical strain.* Am J Physiol 1997, **273**, C810-815.

61. GN Bancroft, VI Sikavitsas, and AG Mikos, *Design of a flow perfusion bioreactor system for bone tissue-engineering applications.* Tissue Eng 2003, **9**, 549-554.

62. RL Dahlin, VV Meretoja, M Ni, FK Kasper, and AG Mikos, *Design of a High Throughput Flow Perfusion Bioreactor System for Tissue Engineering.* Tissue Eng Part C Methods 2012, in press.

63. GN Bancroft, VI Sikavitsas, J van den Dolder, TL Sheffield, CG Ambrose, JA Jansen, and AG Mikos, *Fluid flow increases mineralized matrix deposition in 3D perfusion culture of marrow stromal osteoblasts in a dose-dependent manner.* Proc Natl Acad Sci USA 2002, **99**, 12600-12605.

64. N Datta, QP Pham, U Sharma, VI Sikavitsas, JA Jansen, and AG Mikos, *In vitro generated extracellular matrix and fluid shear stress synergistically enhance 3D osteoblastic differentiation.* Proc Natl Acad Sci USA 2006, **103**, 2488-2493.

65. L Fassina, L Visai, L Asti, F Benazzo, P Speziale, MC Tanzi, and G Magenes, *Calcified matrix production by SAOS-2 cells inside a*

*polyurethane porous scaffold, using a perfusion bioreactor.* Tissue Eng 2005, **11**, 685-700.

66. ME Gomes, VI Sikavitsas, E Behravesh, RL Reis, and AG Mikos, *Effect of flow perfusion on the osteogenic differentiation of bone marrow stromal cells cultured on starch-based three-dimensional scaffolds.* J Biomed Mater Res A 2003, **67**, 87-95.

67. HL Holtorf, N Datta, JA Jansen, and AG Mikos, *Scaffold mesh size affects the osteoblastic differentiation of seeded marrow stromal cells cultured in a flow perfusion bioreactor.* J Biomed Mater Res A 2005, **74**, 171-180.

68. HL Holtorf, JA Jansen, and AG Mikos, *Flow perfusion culture induces the osteoblastic differentiation of marrow stroma cell-scaffold constructs in the absence of dexamethasone.* J Biomed Mater Res A 2005, **72**, 326-334.

69. FW Janssen, J Oostra, A Oorschot, and CA van Blitterswijk, *A perfusion bioreactor system capable of producing clinically relevant volumes of tissue-engineered bone: in vivo bone formation showing proof of concept.* Biomaterials 2006, **27**, 315-323.

70. FW Janssen, R van Dijkhuizen-Radersma, A Van Oorschot, J Oostra, JD de Bruijn, and CA Van Blitterswijk, *Human tissue-engineered bone produced in clinically relevant amounts using a semi-automated perfusion bioreactor system: a preliminary study.* J Tissue Eng Regen Med 2010, **4**, 12-24.

71. D Li, T Tang, J Lu, and K Dai, *Effects of flow shear stress and mass transport on the construction of a large-scale tissue-engineered bone in a perfusion bioreactor.* Tissue Eng Part A 2009, **15**, 2773-2783.

72. AM Martins, A Saraf, RA Sousa, CM Alves, AG Mikos, FK Kasper, and RL Reis, *Combination of enzymes and flow perfusion conditions improves osteogenic differentiation of bone marrow stromal cells cultured upon starch/poly(epsilon-caprolactone) fiber meshes.* J Biomed Mater Res A 2010, **94**, 1061-1069.

73. QP Pham, FK Kasper, AS Mistry, U Sharma, AW Yasko, JA Jansen, and AG Mikos, *Analysis of the osteoinductive capacity and angiogenicity of an in vitro generated extracellular matrix.* J Biomed Mater Res A 2009, **88**, 295-303.

74. QP Pham, FK Kasper, LS Baggett, RM Raphael, JA Jansen, and AG Mikos, *The influence of an in vitro generated bone-like extracellular matrix on osteoblastic gene expression of marrow stromal cells.* Biomaterials 2008, **29**, 2729-2739.

75. VI Sikavitsas, GN Bancroft, HL Holtorf, JA Jansen, and AG Mikos, *Mineralized matrix deposition by marrow stromal osteoblasts in 3D perfusion culture increases with increasing fluid shear forces.* Proc Natl Acad Sci USA 2003, **100**, 14683-14688.

76. RA Thibault, AG Mikos, and FK Kasper, *Protein and mineral composition of osteogenic extracellular matrix constructs generated with a flow perfusion bioreactor.* Biomacromolecules 2011, **12**, 4204-4212.

77. J van den Dolder, GN Bancroft, VI Sikavitsas, PH Spauwen, JA Jansen, and AG Mikos, *Flow perfusion culture of marrow stromal osteoblasts in titanium fiber mesh.* J Biomed Mater Res A 2003, **64**, 235-241.

78. H Terai, D Hannouche, E Ochoa, Y Yamano, and JP Vacanti, *In vitro engineering of bone using a rotational oxygen-permeable bioreactor system.* Mater Sci Eng C 2002, **20**, 3-8.

79. M Shin, H Yoshimoto, and JP Vacanti, *In vivo bone tissue engineering using mesenchymal stem cells on a novel electrospun nanofibrous scaffold.* Tissue Eng 2004, **10**, 33-41.

80. SA Steigman, A Ahmed, RM Shanti, RS Tuan, C Valim, and DO Fauza, *Sternal repair with bone grafts engineered from amniotic mesenchymal stem cells.* J Pediatr Surg 2009, **44**, 1120-1126.

81. CS Young, H Abukawa, R Asrican, M Ravens, MJ Troulis, LB Kaban, JP Vacanti, and PC Yelick, *Tissue-engineered hybrid tooth and bone.* Tissue Eng 2005, **11**, 1599-1610.

82. W Zhang, H Abukawa, MJ Troulis, LB Kaban, JP Vacanti, and PC Yelick, *Tissue engineered hybrid tooth-bone constructs.* Methods 2009, **47**, 122-128.

83. G Vunjak-Novakovic, LE Freed, RJ Biron, and R Langer, *Effects of mixing on the composition and morphology of tissue-engineered cartilage.* AIChE J 1996, **42**, 850-860.

84. S Hofmann, H Hagenmuller, AM Koch, R Muller, G Vunjak-Novakovic, DL Kaplan, HP Merkle, and L Meinel, *Control of in vitro tissue-engineered bone-like structures using human mesenchymal stem cells and porous silk scaffolds.* Biomaterials 2007, **28**, 1152-1162.

85. JH Jansen, OP van der Jagt, BJ Punt, JA Verhaar, JP van Leeuwen, H Weinans, and H Jahr, *Stimulation of osteogenic differentiation in human*

*osteoprogenitor cells by pulsed electromagnetic fields: an in vitro study.* BMC Musculoskelet Disord 2010, **11**, 188-198.

86. LY Sun, DK Hsieh, PC Lin, HT Chiu, and TW Chiou, *Pulsed electromagnetic fields accelerate proliferation and osteogenic gene expression in human bone marrow mesenchymal stem cells during osteogenic differentiation.* Bioelectromagnetics 2010, **31**, 209-219.

87. JR Mauney, S Sjostorm, J Blumberg, R Horan, JP O'Leary, G Vunjak-Novakovic, V Volloch, and DL Kaplan, *Mechanical stimulation promotes osteogenic differentiation of human bone marrow stromal cells on 3-D partially demineralized bone scaffolds in vitro.* Calcif Tissue Int 2004, **74**, 458-468.

88. A Sittichokechaiwut, JH Edwards, AM Scutt, and GC Reilly, *Short bouts of mechanical loading are as effective as dexamethasone at inducing matrix production by human bone marrow mesenchymal stem cell.* Eur Cell Mater 2010, **20**, 45-57.

89. L Fassina, E Saino, MS Sbarra, L Visai, MG Cusella De Angelis, G Mazzini, F Benazzo, and G Magenes, *Ultrasonic and electromagnetic enhancement of a culture of human SAOS-2 osteoblasts seeded onto a titanium plasma-spray surface.* Tissue Eng Part C Methods 2009, **15**, 233-242.

90. L Fassina, E Saino, L Visai, and G Magenes, *Electromagnetically enhanced coating of a sintered titanium grid with human SAOS-2 osteoblasts and extracellular matrix.* Conf Proc IEEE Eng Med Biol Soc 2008, 3582-3585.

91. L Fassina, E Saino, L Visai, G Silvani, MG Cusella De Angelis, G Mazzini, F Benazzo, and G Magenes, *Electromagnetic enhancement of a culture of human SAOS-2 osteoblasts seeded onto titanium fiber-mesh scaffolds.* J Biomed Mater Res A 2008, **87**, 750-759.

92. L Fassina, L Visai, F Benazzo, L Benedetti, A Calligaro, MG De Angelis, A Farina, V Maliardi, and G Magenes, *Effects of electromagnetic stimulation on calcified matrix production by SAOS-2 cells over a polyurethane porous scaffold.* Tissue Eng 2006, **12**, 1985-1999.

93. E Saino, L Fassina, S Van Vlierberghe, MA Avanzini, P Dubruel, G Magenes, L Visai, and F Benazzo, *Effects of electromagnetic stimulation on osteogenic differentiation of human mesenchymal stromal cells seeded onto gelatin cryogel.* Int J Immunopathol Pharmacol 2011, **24**, 1-6.

94. A Sittichockechaiwut, AM Scutt, AJ Ryan, LF Bonewald, and GC Reilly, *Use of rapidly mineralising osteoblasts and short periods of mechanical loading to accelerate matrix maturation in 3D scaffolds.* Bone 2009, **44**, 822-829.

95. E Engvall and P Perlmann, *Enzyme-linked immunosorbent assay (ELISA). Quantitative assay of immunoglobulin G.* Immunochemistry 1971, **8**, 871-874.

96. H Towbin, T Staehelin, and J Gordon, *Electrophoretic transfer of proteins from polyacrylamide gels to nitrocellulose sheets: procedure and some applications.* Proc Natl Acad Sci U S A 1979, **76**, 4350-4354.

97. DN Perkins, DJ Pappin, DM Creasy, and JS Cottrell, *Probability-based protein identification by searching sequence databases using mass spectrometry data.* Electrophoresis 1999, **20**, 3551-3567.

98. Y Ishihama, Y Oda, T Tabata, T Sato, T Nagasu, J Rappsilber, and M Mann, *Exponentially modified protein abundance index (emPAI) for estimation of absolute protein amount in proteomics by the number of sequenced peptides per protein.* Mol Cell Proteomics 2005, **4**, 1265-1272.

99. RL Goldberg and LM Kolibas, *An improved method for determining proteoglycans synthesized by chondrocytes in culture.* Connect Tissue Res 1990, **24**, 265-275.

100. PK Smith, RI Krohn, GT Hermanson, AK Mallia, FH Gartner, MD Provenzano, EK Fujimoto, NM Goeke, BJ Olson, and DC Klenk, *Measurement of protein using bicinchoninic acid.* Anal Biochem 1985, **150**, 76-85.

101. G Szymanowicz and G Laurain, *An automatic method of 4-hydroxyproline determination convenient for large series.* Anal Biochem 1981, **113**, 58-61.

102. D Kang, Y Gho, M Suh, and C Kang, *Highly Sensitive and Fast Protein Detection with Coomassie Brilliant Blue in Sodium Dodecyl Sulfate-Polyacrylamide Gel Electrophoresis.* Bull Korean Chem Soc 2002, **23**, 1511-1512.

103. DM Rissin, CW Kan, TG Campbell, SC Howes, DR Fournier, L Song, T Piech, PP Patel, L Chang, AJ Rivnak, EP Ferrell, JD Randall, GK Provuncher, DR Walt, and DC Duffy, *Single-molecule enzyme-linked immunosorbent assay detects serum proteins at subfemtomolar concentrations.* Nat Biotechnol 2010, **28**, 595-599.

104. M Li, Y Alnouti, R Leverence, H Bi, and AI Gusev, *Increase of the LC-MS/MS sensitivity and detection limits using on-line sample preparation with large volume plasma injection.* J Chromatogr B Analyt Technol Biomed Life Sci 2005, **825**, 152-160.

105. JM Walker, ed. *Protein Protocols Handbook (Methods in Molecular Biology)*. 2nd ed., ed. JM Walker. Vol. 1. 2002, Humana Press Inc.: Totowa, NJ. 57.

106. F Yang, JGC Wolke, and JA Jansen, *Biomimetic calcium phosphate coating on electrospun poly(ε-caprolactone) scaffolds for bone tissue engineering.* Chem Eng J 2008, **137**, 154-161.

107. K Schladitz, *Quantitative micro-CT.* J Microsc 2011, **243**, 111-117.

108. ST Ho and DW Hutmacher, *A comparison of micro CT with other techniques used in the characterization of scaffolds.* Biomaterials 2006, **27**, 1362-1376.

109. C Vater, P Kasten, and M Stiehler, *Culture media for the differentiation of mesenchymal stromal cells.* Acta Biomater 2010, **7**, 463-477.

110. PV Hauschka, JB Lian, DE Cole, and CM Gundberg, *Osteocalcin and matrix Gla protein: vitamin K-dependent proteins in bone.* Physiol Rev 1989, **69**, 990-1047.

111. DN Haylock and SK Nilsson, *Osteopontin: a bridge between bone and blood.* Br J Haematol 2006, **134**, 467-474.

112. GS Stein, JB Lian, and TA Owen, *Relationship of cell growth to the regulation of tissue-specific gene expression during osteoblast differentiation.* FASEB J 1990, **4**, 3111-3123.

113. SD McCullen, AG Chow, and MM Stevens, *In vivo tissue engineering of musculoskeletal tissues.* Curr Opin Biotechnol 2011, **22**, 715-720.

114. PM Conn, ed. *Sourcebook of models for biomedical research*. ed. PM Conn. Vol. 1. 2008, Humana Press: Totowa, NJ, USA. 6.

115. MT Rodrigues, ME Gomes, CA Viegas, JT Azevedo, IR Dias, FM Guzon, and RL Reis, *Tissue-engineered constructs based on SPCL scaffolds cultured with goat marrow cells: functionality in femoral defects.* J Tissue Eng Regen Med 2011, **5**, 41-49.

116. VI Sikavitsas, J van den Dolder, GN Bancroft, JA Jansen, and AG Mikos, *Influence of the in vitro culture period on the in vivo performance of*

*cell/titanium bone tissue-engineered constructs using a rat cranial critical size defect model.* J Biomed Mater Res A 2003, **67**, 944-951.

117. K Ruan, S Bao, and G Ouyang, *The multifaceted role of periostin in tumorigenesis.* Cell Mol Life Sci 2009, **66**, 2219-2230.

118. TW Bauer and GF Muschler, *Bone graft materials. An overview of the basic science.* Clin Orthop Relat Res 2000, **371**, 10-27.

119. WG De Long, Jr, TA Einhorn, K Koval, M McKee, W Smith, R Sanders, and T Watson, *Bone grafts and bone graft substitutes in orthopaedic trauma surgery. A critical analysis.* J Bone Joint Surg Am 2007, **89**, 649-658.

120. CG Finkemeier, *Bone-grafting and bone-graft substitutes.* J Bone Joint Surg Am 2002, **84-A**, 454-464.

121. WE Huffer, JJ Benedict, AS Turner, A Briest, R Rettenmaier, M Springer, and XF Walboomers, *Repair of sheep long bone cortical defects filled with COLLOSS, COLLOSS E, OSSAPLAST, and fresh iliac crest autograft.* J Biomed Mater Res B Appl Biomater 2007, **82**, 460-470.

122. JB Mulliken, J Glowacki, LB Kaban, J Folkman, and JE Murray, *Use of demineralized allogeneic bone implants for the correction of maxillocraniofacial deformities.* Ann Surg 1981, **194**, 366-372.

123. E Ahlmann, M Patzakis, N Roidis, L Shepherd, and P Holtom, *Comparison of anterior and posterior iliac crest bone grafts in terms of harvest-site morbidity and functional outcomes.* J Bone Joint Surg Am 2002, **84-A**, 716-720.

124. RC Sasso, JI Williams, N Dimasi, and PR Meyer, Jr, *Postoperative drains at the donor sites of iliac-crest bone grafts. A prospective, randomized study of morbidity at the donor site in patients who had a traumatic injury of the spine.* J Bone Joint Surg Am 1998, **80**, 631-635.

125. DJ Hak, *The use of osteoconductive bone graft substitutes in orthopaedic trauma.* J Am Acad Orthop Surg 2007, **15**, 525-536.

126. P Arpornmaeklong, P Pripatnanont, and N Suwatwirote, *Properties of chitosan-collagen sponges and osteogenic differentiation of rat-bone-marrow stromal cells.* Int J Oral Maxillofac Surg 2008, **37**, 357-366.

127. NL Leong, J Jiang, and HH Lu, *Polymer-ceramic composite scaffold induces osteogenic differentiation of human mesenchymal stem cells.* Conf Proc IEEE Eng Med Biol Soc 2006, **1**, 2651-2654.

128. T Takamoto, Y Hiraoka, and Y Tabata, *Enhanced proliferation and osteogenic differentiation of rat mesenchymal stem cells in collagen sponge reinforced with different poly(ethylene terephthalate) fibers.* J Biomater Sci Polym Ed 2007, **18**, 865-881.

129. I Wall, N Donos, K Carlqvist, F Jones, and P Brett, *Modified titanium surfaces promote accelerated osteogenic differentiation of mesenchymal stromal cells in vitro.* Bone 2009, **45**, 17-26.

130. F Arai, A Hirao, M Ohmura, H Sato, S Matsuoka, K Takubo, K Ito, GY Koh, and T Suda, *Tie2/angiopoietin-1 signaling regulates hematopoietic stem cell quiescence in the bone marrow niche.* Cell 2004, **118**, 149-161.

131. LM Calvi, GB Adams, KW Weibrecht, JM Weber, DP Olson, MC Knight, RP Martin, E Schipani, P Divieti, FR Bringhurst, LA Milner, HM Kronenberg, and DT Scadden, *Osteoblastic cells regulate the haematopoietic stem cell niche.* Nature 2003, **425**, 841-846.

132. E Fuchs, T Tumbar, and G Guasch, *Socializing with the neighbors: stem cells and their niche.* Cell 2004, **116**, 769-778.

133. CM Kolf, E Cho, and RS Tuan, *Mesenchymal stromal cells. Biology of adult mesenchymal stem cells: regulation of niche, self-renewal and differentiation.* Arthritis Res Ther 2007, **9**, 204-213.

134. SG Ball, AC Shuttleworth, and CM Kielty, *Direct cell contact influences bone marrow mesenchymal stem cell fate.* Int J Biochem Cell Biol 2004, **36**, 714-727.

135. C Csaki, U Matis, A Mobasheri, and M Shakibaei, *Co-culture of canine mesenchymal stem cells with primary bone-derived osteoblasts promotes osteogenic differentiation.* Histochem Cell Biol 2009, **131**, 251-266.

136. H Sun, Z Qu, Y Guo, G Zang, and B Yang, *In vitro and in vivo effects of rat kidney vascular endothelial cells on osteogenesis of rat bone marrow mesenchymal stem cells growing on polylactide-glycoli acid (PLGA) scaffolds.* Biomed Eng Online 2007, **6**, 41-47.

137. W Wagner, F Wein, C Roderburg, R Saffrich, A Faber, U Krause, M Schubert, V Benes, V Eckstein, H Maul, and AD Ho, *Adhesion of hematopoietic progenitor cells to human mesenchymal stem cells as a model for cell-cell interaction.* Exp Hematol 2007, **35**, 314-325.

138. A De Ranieri, AS Virdi, S Kuroda, S Shott, Y Dai, and DR Sumner, *Local application of rhTGF-beta2 modulates dynamic gene expression in a rat implant model.* Bone 2005, **36**, 931-940.

139. JA Jansen, JW Vehof, PQ Ruhe, H Kroeze-Deutman, Y Kuboki, H Takita, EL Hedberg, and AG Mikos, *Growth factor-loaded scaffolds for bone engineering.* J Control Release 2005, **101**, 127-136.

140. AH Reddi, *Morphogenesis and tissue engineering of bone and cartilage: inductive signals, stem cells, and biomimetic biomaterials.* Tissue Eng 2000, **6**, 351-359.

141. FN Syed-Picard, LM Larkin, CM Shaw, and EM Arruda, *Three-dimensional engineered bone from bone marrow stromal cells and their autogenous extracellular matrix.* Tissue Eng Part A 2009, **15**, 187-195.

142. M Jager, T Feser, H Denck, and R Krauspe, *Proliferation and osteogenic differentiation of mesenchymal stem cells cultured onto three different polymers in vitro.* Ann Biomed Eng 2005, **33**, 1319-1332.

143. QP Pham, U Sharma, and AG Mikos, *Electrospun poly(epsilon-caprolactone) microfiber and multilayer nanofiber/microfiber scaffolds: characterization of scaffolds and measurement of cellular infiltration.* Biomacromolecules 2006, **7**, 2796-2805.

144. DJ Prockop, *Marrow stromal cells as stem cells for nonhematopoietic tissues.* Science 1997, **276**, 71-74.

145. KH Larsen, CM Frederiksen, JS Burns, BM Abdallah, and M Kassem, *Identifying A Molecular Phenotype for Bone Marrow Stromal Cells With In Vivo Bone Forming Capacity.* J Bone Miner Res 2010, **25**, 796-808.

146. SJ Peter, CR Liang, DJ Kim, MS Widmer, and AG Mikos, *Osteoblastic phenotype of rat marrow stromal cells cultured in the presence of dexamethasone, beta-glycerolphosphate, and L-ascorbic acid.* J Cell Biochem 1998, **71**, 55-62.

147. HJ Prins, H Rozemuller, S Vonk-Griffioen, VG Verweij, W Dhert, I Slaper-Cortenbach, and AC Martens, *Bone Forming Capacity of Mesenchymal Stromal Cells when Cultured in the Presence of Human Platelet Lysate as Substitute for Fetal Bovine Serum.* Tissue Eng Part A 2009, **15**, 3741-3751.

148. IW Li, S Cheifetz, CA McCulloch, KT Sampath, and J Sodek, *Effects of osteogenic protein-1 (OP-1, BMP-7) on bone matrix protein expression by*

*fetal rat calvarial cells are differentiation stage specific.* J Cell Physiol 1996, **169**, 115-125.

149. JB Lian and GS Stein, *The developmental stages of osteoblast growth and differentiation exhibit selective responses of genes to growth factors (TGF beta 1) and hormones (vitamin D and glucocorticoids).* J Oral Implantol 1993, **19**, 95-105.

150. H Castano-Izquierdo, J Alvarez-Barreto, J van den Dolder, JA Jansen, AG Mikos, and VI Sikavitsas, *Pre-culture period of mesenchymal stem cells in osteogenic media influences their in vivo bone forming potential.* J Biomed Mater Res A 2007, **82**, 129-138.

151. O Fromigue, Z Hamidouche, S Chateauvieux, P Charbord, and PJ Marie, *Distinct osteoblastic differentiation potential of murine fetal liver and bone marrow stroma-derived mesenchymal stem cells.* J Cell Biochem 2008, 104, 620-628.

152. N Maegawa, K Kawamura, M Hirose, H Yajima, Y Takakura, and H Ohgushi, *Enhancement of osteoblastic differentiation of mesenchymal stromal cells cultured by selective combination of bone morphogenetic protein-2 (BMP-2) and fibroblast growth factor-2 (FGF-2).* J Tissue Eng Regen Med 2007, **1**, 306-313.

153. C Maniatopoulos, J Sodek, and AH Melcher, *Bone formation in vitro by stromal cells obtained from bone marrow of young adult rats.* Cell Tissue Res 1988, **254**, 317-330.

154. M Taira, H Nakao, J Takahashi, and Y Araki, *Effects of two vitamins, two growth factors and dexamethasone on the proliferation of rat bone marrow stromal cells and osteoblastic MC3T3-E1 cells.* J Oral Rehabil 2003, **30**, 697-701.

155. TM Dexter, TD Allen, and LG Lajtha, *Conditions controlling the proliferation of haemopoietic stem cells in vitro.* J Cell Physiol 1977, **91**, 335-344.

156. G Balciunaite, R Ceredig, S Massa, and AG Rolink, *A B220+ CD117+ CD19- hematopoietic progenitor with potent lymphoid and myeloid developmental potential.* Eur J Immunol 2005, **35**, 2019-2030.

157. B Dai and P Wang, *In vitro differentiation of adult bone marrow progenitors into antigen-specific CD4 helper T cells using engineered stromal cells expressing a notch ligand and a major histocompatibility complex class II protein.* Stem Cells Dev 2009, **18**, 235-245.

158. SM Lehar and MJ Bevan, *T cell development in culture.* Immunity 2002, **17**, 689-692.

159. H Schacke, WD Docke, and K Asadullah, *Mechanisms involved in the side effects of glucocorticoids.* Pharmacol Ther 2002, **96**, 23-43.

160. RM Stanbury and EM Graham, *Systemic corticosteroid therapy--side effects and their management.* Br J Ophthalmol 1998, **82**, 704-708.

161. FD Burstein, *Bone substitutes.* Cleft Palate Craniofac J 2000, **37**, 1-4.

162. JC Banwart, MA Asher, and RS Hassanein, *Iliac crest bone graft harvest donor site morbidity. A statistical evaluation.* Spine 1995, **20**, 1055-1060.

163. DL Skaggs, MA Samuelson, JM Hale, RM Kay, and VT Tolo, *Complications of posterior iliac crest bone grafting in spine surgery in children.* Spine 2000, **25**, 2400-2402.

164. G Chen, T Ushida, and T Tateishi, *Poly(DL-lactic-co-glycolic acid) sponge hybridized with collagen microsponges and deposited apatite particulates.* J Biomed Mater Res 2001, **57**, 8-14.

165. WJ Habraken, OC Boerman, JG Wolke, AG Mikos, and JA Jansen, *In vitro growth factor release from injectable calcium phosphate cements containing gelatin microspheres.* J Biomed Mater Res A 2009, **91**, 614-622.

166. ZS Patel, M Yamamoto, H Ueda, Y Tabata, and AG Mikos, *Biodegradable gelatin microparticles as delivery systems for the controlled release of bone morphogenetic protein-2.* Acta Biomater 2008, **4**, 1126-1138.

167. ZS Patel, S Young, Y Tabata, JA Jansen, ME Wong, and AG Mikos, *Dual delivery of an angiogenic and an osteogenic growth factor for bone regeneration in a critical size defect model.* Bone 2008, **43**, 931-940.

168. J Ratanavaraporn, H Furuya, H Kohara, and Y Tabata, *Synergistic effects of the dual release of stromal cell-derived factor-1 and bone morphogenetic protein-2 from hydrogels on bone regeneration.* Biomaterials 2011, **32**, 2797-2811.

169. J Liao, X Guo, D Nelson, FK Kasper, and AG Mikos, *Modulation of osteogenic properties of biodegradable polymer/extracellular matrix scaffolds generated with a flow perfusion bioreactor.* Acta Biomater 2010, **6**, 2386-2393.

170. WS Argraves, H Tran, WH Burgess, and K Dickerson, *Fibulin is an extracellular matrix and plasma glycoprotein with repeated domain structure.* J Cell Biol 1990, **111**, 3155-3164.

171. T Itoh, M Tanioka, H Yoshida, T Yoshioka, H Nishimoto, and S Itohara, *Reduced angiogenesis and tumor progression in gelatinase A-deficient mice.* Cancer Res 1998, **58**, 1048-1051.

172. T Maruhashi, I Kii, M Saito, and A Kudo, *Interaction between periostin and BMP-1 promotes proteolytic activation of lysyl oxidase.* J Biol Chem 2010, **285**, 13294-13303.

173. P Sabatelli, P Bonaldo, G Lattanzi, P Braghetta, N Bergamin, C Capanni, E Mattioli, M Columbaro, A Ognibene, G Pepe, E Bertini, L Merlini, NM Maraldi, and S Squarzoni, *Collagen VI deficiency affects the organization of fibronectin in the extracellular matrix of cultured fibroblasts.* Matrix Biol 2001, **20**, 475-486.

174. P Singh, C Carraher, and JE Schwarzbauer, *Assembly of fibronectin extracellular matrix.* Annu Rev Cell Dev Biol 2010, **26**, 397-419.

175. AE Canfield, KD Hadfield, CF Rock, EC Wylie, and FL Wilkinson, *HtrA1: a novel regulator of physiological and pathological matrix mineralization?* Biochem Soc Trans 2007, **35**, 669-671.

176. J Tombran-Tink and CJ Barnstable, *Osteoblasts and osteoclasts express PEDF, VEGF-A isoforms, and VEGF receptors: possible mediators of angiogenesis and matrix remodeling in the bone.* Biochem Biophys Res Commun 2004, **316**, 573-579.

177. X Zhang and J Lawler, *Thrombospondin-based antiangiogenic therapy.* Microvasc Res 2007, **74**, 90-99.

178. S Kazerounian, KO Yee, and J Lawler, *Thrombospondins in cancer.* Cell Mol Life Sci 2008, **65**, 700-712.

179. EJ Brochmann, K Behnam, and SS Murray, *Bone morphogenetic protein-2 activity is regulated by secreted phosphoprotein-24 kd, an extracellular pseudoreceptor, the gene for which maps to a region of the human genome important for bone quality.* Metabolism 2009, **58**, 644-650.

180. MD McKee and A Nanci, *Osteopontin at mineralized tissue interfaces in bone, teeth, and osseointegrated implants: ultrastructural distribution and implications for mineralized tissue formation, turnover, and repair.* Microsc Res Tech 1996, **33**, 141-164.

181. H Orimo, *The mechanism of mineralization and the role of alkaline phosphatase in health and disease.* J Nippon Med Sch 2010, **77**, 4-12.

182. KD Hankenson, MT Sweetwyne, H Shitaye, and KL Posey, *Thrombospondins and novel TSR-containing proteins, R-spondins, regulate bone formation and remodeling.* Curr Osteoporos Rep 2010, **8**, 68-76.

183. K Kozaki, O Miyaishi, O Koiwai, Y Yasui, A Kashiwai, Y Nishikawa, S Shimizu, and S Saga, *Isolation, purification, and characterization of a collagen-associated serpin, caspin, produced by murine colon adenocarcinoma cells.* J Biol Chem 1998, **273**, 15125-15130.

184. GM Quan, J Ojaimi, Y Li, V Kartsogiannis, H Zhou, and PF Choong, *Localization of pigment epithelium-derived factor in growing mouse bone.* Calcif Tissue Int 2005, **76**, 146-153.

185. J Dai and AB Rabie, *VEGF: an essential mediator of both angiogenesis and endochondral ossification.* J Dent Res 2007, **86**, 937-950.

186. HQ Miao, R Ishai-Michaeli, R Atzmon, T Peretz, and I Vlodavsky, *Sulfate moieties in the subendothelial extracellular matrix are involved in basic fibroblast growth factor sequestration, dimerization, and stimulation of cell proliferation.* J Biol Chem 1996, **271**, 4879-4886.

187. MS Park, SS Kim, SW Cho, CY Choi, and BS Kim, *Enhancement of the osteogenic efficacy of osteoblast transplantation by the sustained delivery of basic fibroblast growth factor.* J Biomed Mater Res B Appl Biomater 2006, **79**, 353-359.

188. ME Gomes, CM Bossano, CM Johnston, RL Reis, and AG Mikos, *In vitro localization of bone growth factors in constructs of biodegradable scaffolds seeded with marrow stromal cells and cultured in a flow perfusion bioreactor.* Tissue Eng 2006, **12**, 177-188.

189. RZ LeGeros, *Calcium phosphate-based osteoinductive materials.* Chem Rev 2008, **108**, 4742-4753.

190. AL Boskey, *Amorphous calcium phosphate: the contention of bone.* J Dent Res 1997, **76**, 1433-1436.

191. AL Boskey, *Bone mineral crystal size.* Osteoporos Int 2003, **14 Suppl 5**, S16-20.

192. LC Palmer, CJ Newcomb, SR Kaltz, ED Spoerke, and SI Stupp, *Biomimetic systems for hydroxyapatite mineralization inspired by bone and enamel.* Chem Rev 2008, **108**, 4754-4783.

193. S Weiner and HD Wagner, *The Material Bone: Structure-Mechanical Function Relations.* Ann Rev Mater Sci 1998, **28**, 271-298.

194. R Dimitriou, E Jones, D McGonagle, and PV Giannoudis, *Bone regeneration: current concepts and future directions.* BMC Med 2011, **9**, 66-76.

195. BL Eppley, WS Pietrzak, and MW Blanton, *Allograft and alloplastic bone substitutes: a review of science and technology for the craniomaxillofacial surgeon.* J Craniofac Surg 2005, **16**, 981-989.

196. A Piattelli, A Scarano, M Corigliano, and M Piattelli, *Comparison of bone regeneration with the use of mineralized and demineralized freeze-dried bone allografts: a histological and histochemical study in man.* Biomaterials 1996, **17**, 1127-1131.

197. G Zimmermann and A Moghaddam, *Allograft bone matrix versus synthetic bone graft substitutes.* Injury 2011, **42 Suppl 2**, S16-21.

198. SM Bowman, J Zeind, LJ Gibson, WC Hayes, and TA McMahon, *The tensile behavior of demineralized bovine cortical bone.* J Biomech 1996, **29**, 1497-1501.

199. PM Crapo, TW Gilbert, and SF Badylak, *An overview of tissue and whole organ decellularization processes.* Biomaterials 2011, **32**, 3233-3243.

200. SL Dahl, J Koh, V Prabhakar, and LE Niklason, *Decellularized native and engineered arterial scaffolds for transplantation.* Cell Transplant 2003, **12**, 659-666.

201. L Gui, SA Chan, CK Breuer, and LE Niklason, *Novel utilization of serum in tissue decellularization.* Tissue Eng Part C Methods 2010, **16**, 173-184.

202. MC Kruyt, JD de Bruijn, CE Wilson, FC Oner, CA van Blitterswijk, AJ Verbout, and WJ Dhert, *Viable osteogenic cells are obligatory for tissue-engineered ectopic bone formation in goats.* Tissue Eng 2003, **9**, 327-336.

203. H Lu, T Hoshiba, N Kawazoe, and G Chen, *Autologous extracellular matrix scaffolds for tissue engineering.* Biomaterials 2011, **32**, 2489-2499.

204. H Stegemann and K Stalder, *Determination of hydroxyproline.* Clin Chim Acta 1967, **18**, 267-273.

205. X Guo, H Park, G Liu, W Liu, Y Cao, Y Tabata, FK Kasper, and AG Mikos, *In vitro generation of an osteochondral construct using injectable hydrogel composites encapsulating rabbit marrow mesenchymal stem cells.* Biomaterials 2009, **30**, 2741-2752.

206. JE Aaron, PA Shore, RC Shore, M Beneton, and JA Kanis, *Trabecular architecture in women and men of similar bone mass with and without vertebral fracture: II. Three-dimensional histology.* Bone 2000, **27**, 277-282.

207. LC Junqueira, G Bignolas, and RR Brentani, *Picrosirius staining plus polarization microscopy, a specific method for collagen detection in tissue sections.* Histochem J 1979, **11**, 447-455.

208. I Kiviranta, J Jurvelin, M Tammi, AM Saamanen, and HJ Helminen, *Microspectrophotometric quantitation of glycosaminoglycans in articular cartilage sections stained with Safranin O.* Histochemistry 1985, **82**, 249-255.

209. Z Ferdous, VM Wei, R Iozzo, M Hook, and KJ Grande-Allen, *Decorin-transforming growth factor- interaction regulates matrix organization and mechanical characteristics of three-dimensional collagen matrices.* J Biol Chem 2007, **282**, 35887-35898.

210. A Bader, T Schilling, OE Teebken, G Brandes, T Herden, G Steinhoff, and A Haverich, *Tissue engineering of heart valves--human endothelial cell seeding of detergent acellularized porcine valves.* Eur J Cardiothorac Surg 1998, **14**, 279-284.

211. B Yang, Y Zhang, L Zhou, Z Sun, J Zheng, Y Chen, and Y Dai, *Development of a porcine bladder acellular matrix with well-preserved extracellular bioactive factors for tissue engineering.* Tissue Eng Part C Methods 2010, **16**, 1201-1211.

212. M Grunert, C Dombrowski, M Sadasivam, K Manton, SM Cool, and V Nurcombe, *Isolation of a native osteoblast matrix with a specific affinity for BMP2.* J Mol Histol 2007, **38**, 393-404.

213. HT Meryman, *Physical limitations of the rapid freezing method.* Proc R Soc Lond B Biol Sci 1957, **147**, 452-459.

214. A Helenius and K Simons, *The binding of detergents to lipophilic and hydrophilic proteins.* J Biol Chem 1972, **247**, 3656-3661.

215. P Maurer and E Hohenester, *Structural and functional aspects of calcium binding in extracellular matrix proteins.* Matrix Biol 1997, **15**, 569-580.

216. VI Sikavitsas, GN Bancroft, and AG Mikos, *Formation of three-dimensional cell/polymer constructs for bone tissue engineering in a spinner flask and a rotating wall vessel bioreactor.* J Biomed Mater Res 2002, **62**, 136-148.